Mechanochemical synthesis, reactions, and mass spectrometric characterization of glycated amino acids with fructose and glucose

Kayleigh Hayashi-Mahedy

Department of Food Science and Agricultural Chemistry

McGill University, Montreal

April 2024

A thesis submitted to McGill University in partial fulfilment of the requirements of the degree of Master of Science

Abstract

During thermal processing of food, excess sugars and amino acids relative to the initially formed Maillard reaction intermediates, such as Amadori or Heyns compounds, presents a statistically favourable environment for their further interaction, potentially leading to the formation of novel compounds that can serve as flavour precursors; a largely unexplored phenomenon in the Maillard reaction research. Furthermore, mechanochemical reactions, specifically the ball milling of amino acids and sugars at ambient temperatures, can generate mixtures rich in Amadori and Heyns rearrangement products (ARPs and HRPs). This easy access to important aroma and flavour precursors was exploited in this thesis to study their subsequent reactions with free amino acids, such as histidine, cysteine, phenylalanine, and sugars, such as fructose and glucose. Selected Amadori products were synthesized using mechanochemistry and characterized through their MS/MS and FTIR spectra. Subsequently, they were milled (30Hz/30min) with excess amino acids or reducing sugars to initiate their interaction and possible formation of the expected di-glycated amino acids or di-aminated sugars. Indeed, the ESI-qTOF-MS analysis of the milled reaction mixtures indicated the formation of diglycated amino acids in ARP/sugar mixtures and di-aminated sugars in ARP/amino acid mixtures as indicated by observation of their appropriate masses and accurate elemental composition. Furthermore, the proposed structures were confirmed through ESI-qTOF-MS/MS analysis, revealing characteristic fragmentation patterns under negative ionization mode. In addition, when Amadori products were either milled or heated in solution phase with an exogenous amino acid, the mass spectrometric analysis indicated the presence of Heyns product of the exogenous amino acid, in addition to the free amino acid of the original Amadori product. The formation of the new Heyns compound was rationalized through the reaction of the added amino acid with the carbonyl group of the Amadori product and the formation of an ene-diamine intermediate. Upon hydrolysis, this intermediate can generate the Heyns compound and the free amino acid. Moreover, the conversion parameters of the Amadori compounds to Heyns products in the presence of free amino acids and the release of the starting amino acid can be optimized to de-glycate food proteins. This approach may provide new avenues in reducing the potentially harmful effects of glycation and preserve the optimal functionality of proteins.

Résume

Pendant le traitement thermique des aliments, un excès de sucres et d'acides aminés par rapport aux intermédiaires formés initialement par la réaction de Maillard, tels que les composés d'Amadori ou de Heyns, présente un environnement statistiquement favorable à leur interaction ultérieure, conduisant potentiellement à la formation de nouveaux composés pouvant servir de précurseurs de saveur ; un phénomène largement inexploré dans la recherche sur la réaction de Maillard. De plus, les réactions mécano-chimiques, notamment le broyage à billes d'acides aminés et de sucres à température ambiante, peuvent générer des mélanges riches en produits de réarrangement d'Amadori et de Heyns (ARPs et HRPs). Cet accès facile à d'importants précurseurs d'arômes et de saveurs a été exploité dans cette thèse pour étudier leurs réactions ultérieures avec des acides aminés libres, tels que l'histidine, la cystéine, la phénylalanine, et des sucres, tels que le fructose et le glucose. Des produits d'Amadori sélectionnés ont été synthétisés par mécano-chimie et caractérisés par leurs spectres MS/MS et FTIR. Par la suite, ils ont été broyés (30 Hz/30 min) avec un excès d'acides aminés ou de sucres réducteurs pour initier leur interaction et la formation possible des acides aminés di-glyqués attendus ou des sucres di-aminés. En effet, l'analyse par ESI-qTOF-MS des mélanges réactionnels broyés a indiqué la formation d'acides aminés di-glyqués dans les mélanges ARP/sucre et de sucres di-aminés dans les mélanges ARP/acide aminé, comme indiqué par l'observation de leurs masses appropriées et de leur composition élémentaire précise. De plus, les structures proposées ont été confirmées par une analyse ESI-qTOF-MS/MS, révélant des motifs de fragmentation caractéristiques sous mode d'ionisation négative. De plus, lorsque les produits d'Amadori étaient soit broyés, soit chauffés en phase solution avec un acide aminé exogène, l'analyse spectrométrique de masse indiquait la présence de produits de Heyns de l'acide aminé exogène, en plus de l'acide aminé libre du produit d'Amadori d'origine. La formation du nouveau composé de Heyns a été rationalisée par la réaction de l'acide aminé ajouté avec le groupe carbonyle du produit d'Amadori et la formation d'un intermédiaire énédiamine. Lors de l'hydrolyse, cet intermédiaire peut générer le composé de Heyns et l'acide aminé libre. De plus, les paramètres de conversion des composés d'Amadori en produits de Heyns en présence d'acides aminés libres et la libération de l'acide aminé de départ peuvent être optimisés pour déglyquer les protéines alimentaires. Cette approche peut ouvrir de nouvelles voies pour réduire les effets potentiellement nocifs de la glycation et préserver la fonctionnalité optimale des protéines.

Acknowledgements

I am deeply grateful to my supervisor, Dr. Varoujan Yaylayan, whose guidance, encouragement, and academic direction were instrumental throughout the process of completing this thesis. His constant support, wisdom, patience, advice, and understanding have enriched my graduate studies experience; I am fortunate to have him as my advisor. Thank you for instilling confidence in my abilities and providing me with this opportunity to excel academically and cultivate a deeper appreciation for research.

I extend my sincere gratitude to Dr. Alexander Wahba for his assistance in obtaining mass spectroscopy data. Additionally, I am thankful to my friends and lab mates who provided companionship during my studies. Their support and encouragement provided moral support and helped me navigate academic and personal challenges. I am extremely grateful to you all.

To my parents and brother, I express my most heartfelt thanks for your unwavering encouragement, motivation, and continuous support, which have been the foundation of my success and achievements. Your endless sacrifices, selflessness, and unwavering faith in me not only propelled me forward but also enriched my character and shaped my path to this significant milestone. I am forever grateful for your love and unwavering presence in my life.

Table of Contents

List of Tables

List of Figures

Chapter 1. Introduction

1.1 Rationale of the Proposed Research

Food systems consist of various components, including carbohydrates, lipids, proteins, minerals, vitamins, etc. This innate composition undergoes profound transformations during thermal processing and storage due to chemical changes like the Maillard reaction, thereby amplifying the complexity inherent in these systems. Discovered by Louis C. Maillard in 1912, the Maillard reaction has captivated scientists across diverse disciplines, owing to its profound impact on the sensory properties of food, coupled with its implications for health and broader applications, underscoring the enduring relevance and significance of this fundamental chemical process.

Maillard reaction products contribute greatly to the flavour profile of various foods, generating desirable characteristics such as pleasing sensory attributes and the formation of biologically active molecules (1). However, the occurrence of this reaction in foods is not always desirable as advanced reaction products can yield unfavourable outcomes such as off-flavours and nutrient depletion (1) and can also have cytotoxic, genotoxic, and carcinogenic effects. Nonetheless, recent in vitro studies have highlighted potential positive attributes of Maillard reaction products (MRPs), particularly in their early reaction stages. In vivo, advanced glycation end products (AGEs) are believed to play a significant role in various pathologies and, more broadly, in the aging process (1). Thus, convenient methods for generating glycated amino acids are vital in advancing research, product development, analytical techniques, and biomedical understanding related to the Maillard reaction.

Understanding the reactivity of Amadori rearrangement products (ARPs) and the mechanisms of their further reactions is crucial to controlling the reaction in both food and physiological systems. Given its pivotal role in food systems, the Maillard Reaction yields crucial and distinct Maillard reaction products during food processing. Mechanochemistry offers a promising opportunity for producing reactive and otherwise difficult-to-obtain compounds under conventional thermochemistry conditions to promote the controlled synthesis of important Maillard reaction intermediates (2). Compared to Maillard reaction products which are volatile, and it is difficult to maintain the stability of flavoured end products for application, especially during heat treatment, cooking, and baking processes (3), intermediates have stable physiochemical properties. Notably,

ARPs, relatively stable Maillard reaction intermediates produced during the initial stage of Maillard reaction, are significant non-volatile flavour precursors, contributing substantially to flavour generation during thermal reactions (4). Mechanochemical reactions, specifically the ball milling of amino acids and sugars at ambient temperatures, generate mixtures rich in glycated amino acid isomers such as ARPs, Heyn's rearrangement products (HRPs), and their respective Schiff bases.

1.2 Objectives of Research

The overall objective of this thesis aims to elucidate the formation mechanisms of novel flavour-active compounds resulting from the interaction between excess sugars and amino acids relative to initial Maillard reaction adducts, such as ARPs, during thermal processing. Leveraging convenient methods for accessing key aroma and flavour precursors, our study seeks to provide insights into the intricate dynamics of ARPs and HRPs, and their subsequent reactions with free amino acids and sugars. Through this investigation, we aim to advance our understanding of the Maillard reaction and its role in flavour development, thereby contributing to the enhancement of food quality and sensory experience.

Specific objectives include **(1)** mechanochemical synthesis and mass spectral characterization of selected Amadori and Heyns compounds **(2)** investigation of their further reactions with selected amino acids (cysteine, histidine, phenylalanine) for the purpose of identification of di-aminated sugars, and study their MS/MS fragmentations **(3)** investigation of their further reactions with glucose and fructose, for the purpose of identification of di-glycated amino acids, and study their MS/MS fragmentations.

1.3 References

1. Laroque, D.; Inisan, C.; Berger, C.; Vouland, É.; Dufossé, L.; Guérard, F. Kinetic Study on the Maillard Reaction. Consideration of Sugar Reactivity. *Food Chem.* **2008**, *111*(4), 1032-1042. https://doi.org/10.1016/j.foodchem.2008.05.033
2. Xing, H.; Yaylayan, V. Insight into Isomeric Diversity of Glycated Amino Acids in Maillard Reaction Mixtures. *Int. J. Mol. Sci.* **2022**, *23*(7), 3430.
3. Cui, H.; Jia, C.; Hayat, K.; Yu, J.; Deng, S.; Karangwa, E.; Zhang, X. Controlled Formation of Flavor Compounds by Preparation and Application of Maillard Reaction Intermediate (MRI) Derived from Xylose and Phenylalanine. *RSC Adv.* **2017**, *7*(72), 45442-45451.
4. Harohally, N. V.; Srinivas, S. M.; Umesh, S. ZnCl2-Mediated Practical Protocol for the Synthesis of Amadori Ketoses. *Food Chem.* **2014**, *158*, 340-344.

Chapter 2. Literature Review

2.1 Importance of Glycated Amino Acids

In 1912, French scientist Lois-Camille Maillard first described the Maillard reaction (non-enzymatic glycation reaction) between amino acids and reducing sugars during heating, resulting in the browning of the reaction mixture with the formation of aroma and carbon dioxide (1). Following the initial reaction between the amino and carbonyl compounds, a complex network of reactions ensues, forming a diverse array of compounds known as Maillard reaction products (2). The Maillard reaction is omnipresent, proceeding at different extents, attributed to the widespread presence of the starting materials – i.e., amino acids and sugars –making it a common phenomenon leading to flavour formation and nutritional losses in heat-processed foods (3), abiotic generation of humic substances in soil (4), and protein modification in vivo in living organisms (glycation) (5).

In the food industry, the Maillard reaction naturally occurs during processing and storage, leading to a multitude of transformations. These encompass changes in aroma, colour, flavour, nutritional content, and the formation of both stabilizing and potentially mutagenic compounds (5). Therefore, controlling the Maillard reaction is crucial because it influences desirable features (i.e., pleasant sensory characteristics and the formation of biologically active molecules) and undesirable features (i.e., off-flavours, loss of nutritional value, and generation of toxic compounds) (6).
Initially proposed to explain alterations in colour, taste, and texture in heat-processed and stored foods, the concept of Maillard Reaction has evolved over the recent decades. A growing interest in the biomedical field has emerged, focusing on investigating the chemistry and biological activities associated with Maillard reaction products or AGEs. The discovery of the glycated form of hemoglobin (HbA1c) by Kunkel and Wallenius (7), subsequently confirmed by Rahbar (8), revealed elevated levels in red blood cells from diabetic patients, highlighting the *in vivo* occurrence of glycation reaction and its potential role in pathological conditions. Following these revelations, advances in this field have since accelerated, with a growing number of publications presenting experimental data on endogenous and exogenous AGE formation, emphasizing their participation in various physiological and pathological processes. Notably, established associations between MR-derived AGEs, α-dicarbonyl compounds, and several chronic and age-

related diseases, including diabetes, atherosclerosis, cataractogenesis, and Alzheimer's disease, further underscore the crucial role of AGEs as key precursors in these processes (9).

2.1.1 Chemistry of the Maillard Reaction

About 40 years after the discovery of the Maillard reaction, John E. Hodge was the first to summarize the complex network of reactions into three distinct stages, noted as the “Hodge Scheme” (3). It comprises the initial, intermediate, and final stages of browning. Hodge revealed multiple types of reactions within the proposed three stages (Figure 2.1). The initial stage begins with a sugar-amine condensation reaction, producing a reversible N-substituted glycosylamine (Schiff Base). The Schiff base is usually detected only in low levels in sugar-amine systems as it readily rearranges into the more stable Amadori product (from an aldose) or Heyn’s product (from a ketose), completing the final step of the initial stage (3, 10, 11). The Amadori rearrangement products (ARPs) and Heyns rearrangement products (HRPs) are considered early glycation products, and HbA1c belongs to the former class (12). The subsequent degradation of the ARPs and HRPs begins the intermediate stage, leading to the formation of sugar fragmentation products and release of the amino groups, as well as Strecker aldehydes and other intermediate compounds (3, 13). Subsequently, various complex and interconnected reactions, such as condensation, cyclization, dehydration, fragmentation, and polymerization, proceed with the participation of the amino groups and initiate the final stage where melanoidins are irreversibly formed having coloured fluorescent properties (3, 10, 14).

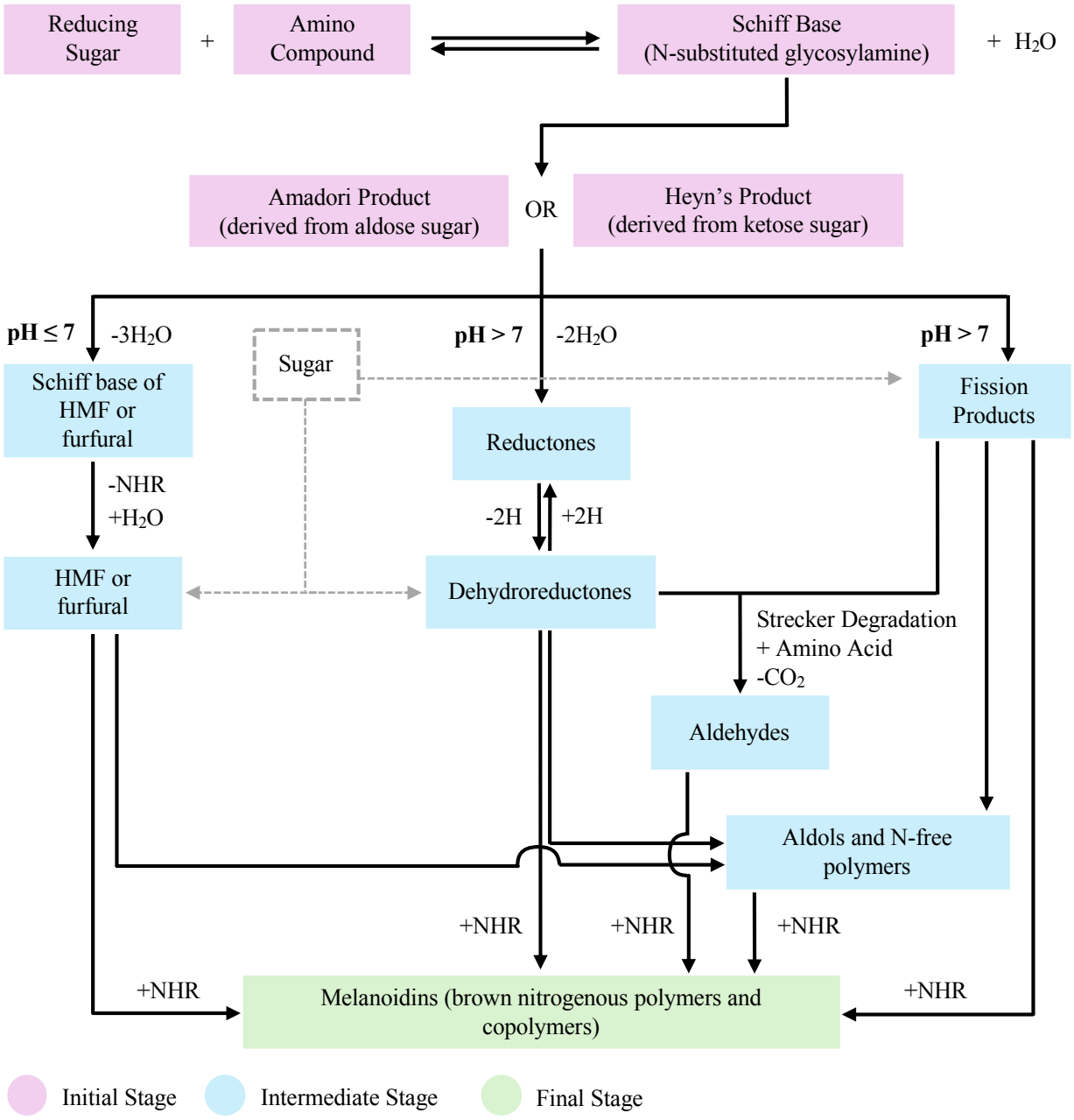

Figure 2.1. Scheme of the Maillard reaction organized into three stages adapted from Hodge (3)

An alternate view to understanding the complexity of the Maillard reaction was proposed by Yaylayan (15), introducing the concept of "chemical pools" (Figure 2.2). In the initial stage, the chemical pools are derived from the 'principal precursors' (amino acids, sugars, and Amadori or Heyn's products) and are described as the building blocks for Maillard reaction products (15). The term "pools" is defined as the collection of products that arise from a single precursor or multiple precursors (15). The primary fragmentation pool is formed from the decomposition of each of the

three principal precursors and determines the course of the reaction pathway. Subsequent reactions of the primary fragmentation pool include self-interaction pools (reactions involving components of a single pool), secondary interaction pools (reactions involving components of different fragmentation pools), and multiple-interaction pools (involving components of all the pools interacting with each other) (15). Therefore, compared to Hodge's scheme, Yaylayan's classification accounts for the independent degradations of the principal precursors and the interactions between the different pools produced in the reaction cascade.

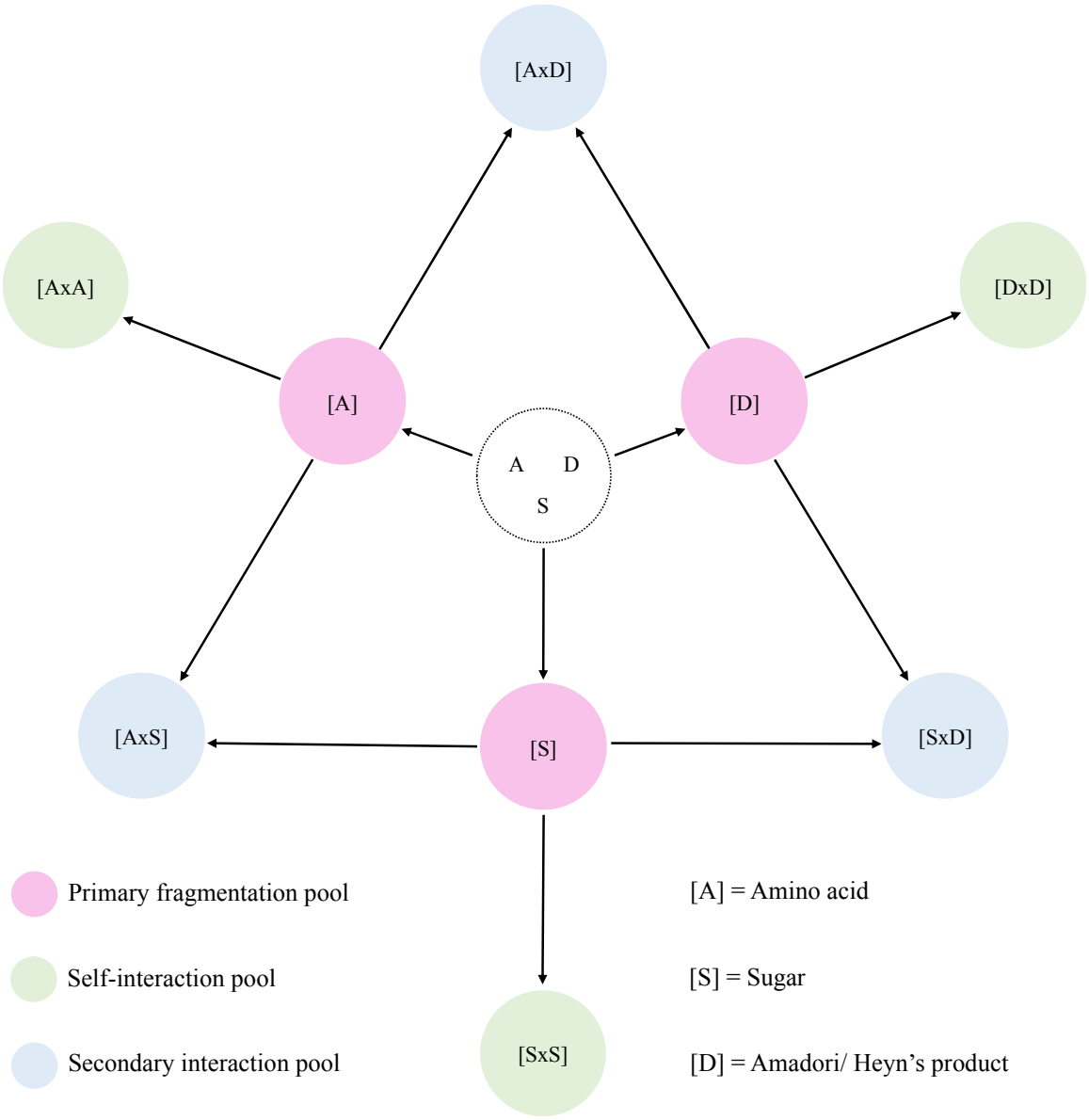

Figure 2.2 Yaylayan's classification of the Maillard reaction is described as proceeding by the formation and interaction of 'chemical pools' adapted from Yaylayan (15)

2.1.2 Complexities and Challenges in Investigating the Maillard Reaction

The chemical composition of raw food materials is well understood; however, significant chemical transformations occur during processing by thermal treatments, including cooking, frying, roasting, backing, and long-term storage, that completely alter the chemical composition of the food and generate a complex matrix, not all its components are completely identified till now. The primary precursors of the Maillard reaction (amino acid, sugar, and ARP/ HRPs) shown in Figure 2 can each produce distinct reaction products through participation in subsequent reaction cascades, contributing to the formation of highly intricate reaction mixtures (15). Adding to this complexity, other food components, such as lipids, vitamins, metals, and polyphenols, contribute to the intricate composition and dynamics of the overall reaction (16,17). Therefore, our current comprehension of the Maillard reaction predominantly relies on studying well-defined model systems. Model systems employ different amino acids and reducing sugars as simplified representations of the intricate food system, allowing for a more detailed and direct analysis and understanding of this complex reaction without interference from other components. Singular amino acids paired with reducing sugars, constituting model systems, have been extensively utilized and studied for their ability to establish a direct relationship between the resulting products and the specific amino acid under investigation. Furthermore, various peptides have been reported in numerous food systems, such as meat, hydrolyzed vegetable protein, and coffee beans (18,19). Consequently, studies have expanded to investigate Maillard reaction products formed from model systems with peptides having different chain lengths (20). Experiments involving the application of pure peptides in the Maillard reaction models have demonstrated their involvement in various pathways, such as bond cleavage, cyclization, and glycation (21).

The complexity of the Maillard reactions arises from its susceptibility to a multitude of reaction parameters, each specific combination leading to a unique case study. The factors that influence the chemical reactions involved include time, temperature, pH, presence or absence of solvent, concentration, and the ratio of reducing sugars to amino acids (22, 23). Furthermore, multiple fragmentation reactions of the sugar moiety constitute branch points in the reaction progress and establish many parallel reaction pathways (24). Each pathway yields distinct products with varying chemical properties, intensifying the challenge of predicting and controlling the outcomes. The different reactivity of amino acids towards carbohydrates further compounds the overall

complexity of the process. Hemmler et al. (25) conducted a study monitoring the thermal formation of early glycated amino acids contributing to the intricate web of the Maillard reaction cascade. Although the ARP breakdown is considered the main Maillard reaction pathway, other reactive intermediates, often of higher molecular weight than the ARP, contribute largely to the multitude of intermediates observed (25). The continuous generation of reactive intermediates feeds the reaction pool, resulting in an exponential increase in the production of Maillard reaction products (15). Therefore, despite many structural studies on the Maillard reaction, a comprehensive picture of the composition of the reaction system and interconnections between intermediates remains elusive (25). Furthermore, studies employing non-targeted analysis and data visualization, such as the one conducted by Hemmler et al., have delivered more insight into the overall chemical changes in the Maillard reaction of a single sugar heated with a single amino acid, identifying many compounds generated. However, the mechanism of formation of many of these products remains unknown.

2.2 Glycated Amino Acids

2.2.1 Formation of Glycated Amino Acids

The formation of ARP or HRP has been extensively reviewed in the literature (26). It involves a series of equilibrium reactions initiated by the nucleophilic addition reaction between an amino acid and reducing sugar. While hexoses and pentoses predominantly adopt a ring structure, a small fraction exists in an acyclic form known for its heightened reactivity in the Maillard reaction (27, 28). Therefore, thermal equilibrium-driven ring opening of the reducing sugars is considered a critical step in ARP or HRP formation (28). Following the ring opening of the sugar moiety, subsequent dehydration produces a glycosylamine - a cyclized Schiff base (26). The p bond (-C=N) of the Schiff base can then migrate towards the carbonyl group of the sugar moiety, generating a 1,2-enol that isomerizes, leading to early glycation products called Amadori or Heyns rearrangement products depicted in Figure 2.3.

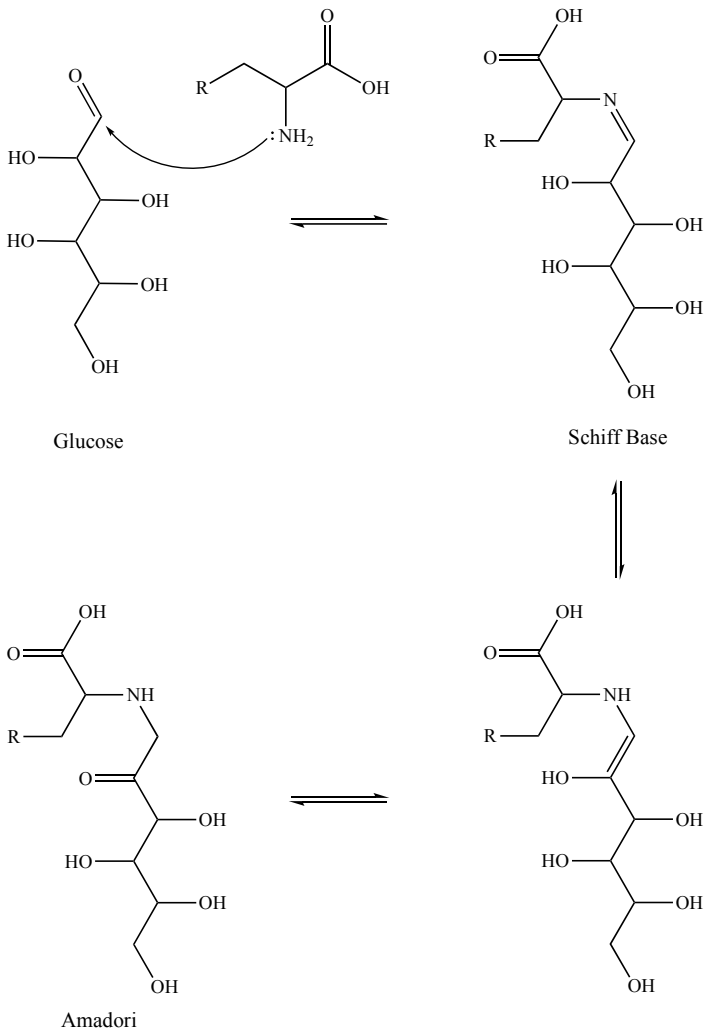

Figure 2.3 Mechanism of formation of Amadori product

2.2.2 Degradation of Glycated Amino Acids

The equilibrium mixture of ARPs or HRPs comprises cyclic and acyclic structures alongside anomeric conformations (27). Notably, the acyclic form of an ARP exhibits heightened reactivity compared to its cyclic counterparts due to its tendency to convert into enol isomers. Keto-enolization is the basis for the breakdown of the ARPs (or HRPs), where pH directs which keto-enol tautomer is produced in greater amounts, dictating which aroma compounds are formed (29). At low pH values, ARPs are prone to undergo 1,2-enolization, depicted in Figure 2.4. This pathway leads the 1,2-enaminol form of ARP to undergo β-elimination of its C-3 hydroxyl group, yielding 3-deoxy-2-hexosuloses, a highly reactive α-dicarbonyl intermediate (26, 29, 31). Conversely, at high pH values, 2,3-enolization is favoured because the electron-rich β-carbon of the 1,2-enol is

adjacent to an electron-rich amine, which produces an enediol that can generate two different reactive α-dicarbonyls through elimination reactions (29, 31). The first is through the elimination of the C-4 hydroxyl group to produce 1-amino-1,4,-dideoxy-2,3-hexodiulose, whereas the elimination of the C-1 amino group produces 1-deoxy-2,3-hexodiulose (26, 30).

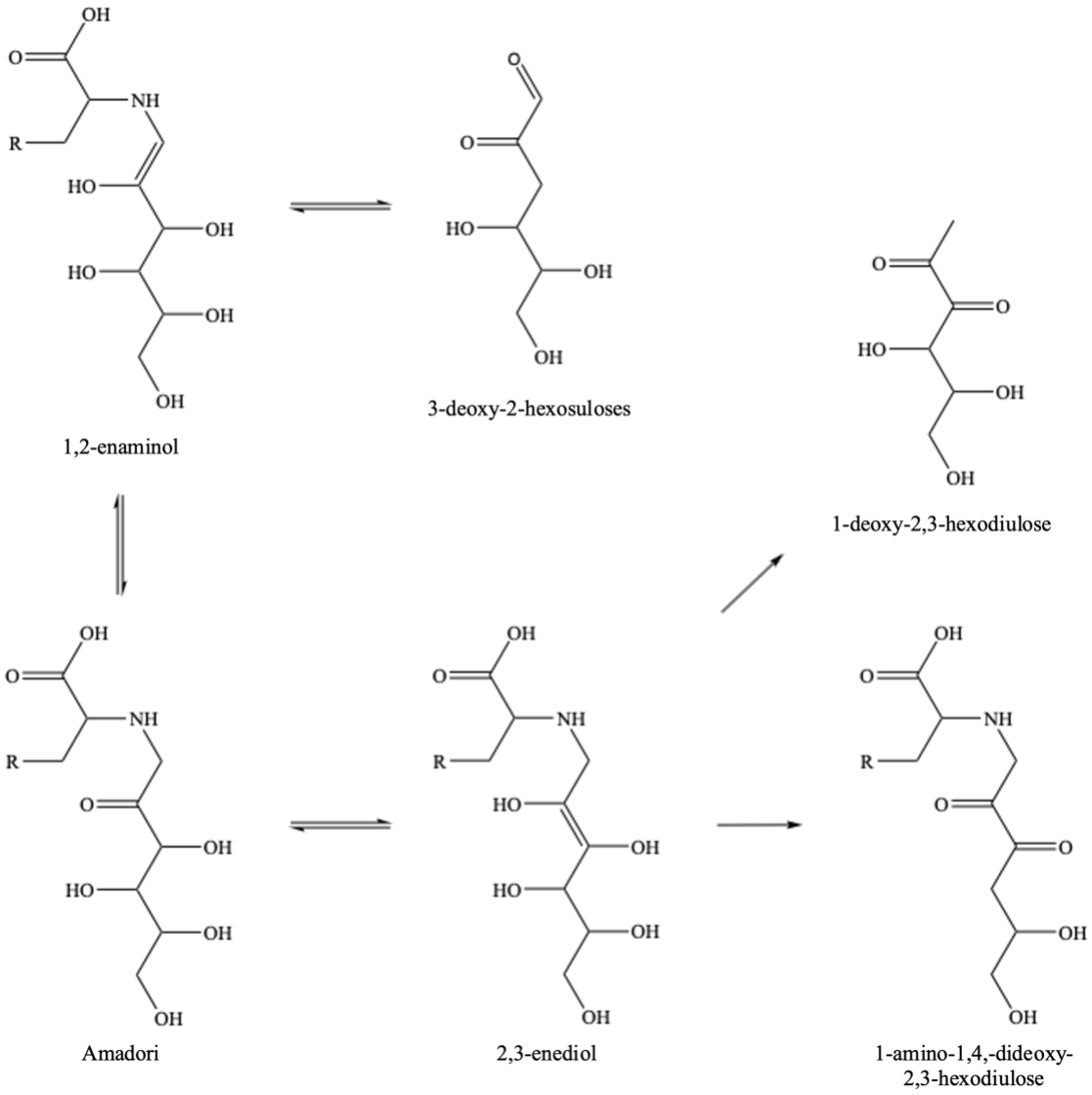

Figure 2.4 1,2- and 2,3-enolization and β-elimination of Amadori rearrangement products

Most of the identified Maillard reaction products are rationalized by the enolization of the open chain forms, although they only represent a low percentage of the total concentration. Yaylayan (32) proposed an alternative decomposition pathway for ARPs. This pathway involves direct

dehydration from the most abundant cyclic forms, like other deoxy sugars (32). For example, a 3-deoxyglucosone is converted into hydroxymethylfurfural (HMF) by dehydration of cyclic forms through the formation of furylium ions (26). In addition to enolization reactions, ARPs can undergo retro-aldol reactions, especially under basic conditions, which can lead to the production of more reactive C2, C3, C4, and C5 sugar fragments containing α-hydroxy carbonyl and α-dicarbonyls moieties such as hydroxyacetone derivative, glyceraldehyde, diketones, and hydroxy-ketoaldehydes that can oxidize and dehydrate (26, 33). These resulting short-chain α-hydroxy carbonyl and α-dicarbonyls are important flavour and melanoidin precursors in foods (26, 27). Furthermore, in addition to enolization, dehydration, and fragmentation, the secondary amino group of an ARP or HRP can further react with another reducing sugar to generate a disubstituted ARP or HRP (27). This compound has been proposed to degrade readily, leading to the generation of superoxide and 5-hydroxymethylfurfural (27, 34, 35).

2.3 Synthesis Methods of Glycated Amino Acids

There are two general approaches for the synthesis of glycated amino acids: solvent-free using mechanochemistry and in-solvent thermochemical reactions.

2.3.1 Introduction to Mechanochemistry

Activation energy is a fundamental requirement for almost all chemical transformations regardless of the source of energy. Chemical reactions can be classified based on different energy sources utilized to carry out the chemical transformation - including thermochemistry, photochemistry, electrochemistry, sonochemistry, and mechanochemistry (36). Traditionally, thermal energy (thermochemistry) has been the predominant source of energy used to perform chemical reactions. However, due to heightened environmental awareness, alternative methods have garnered attention, such as ultrasonication (37), pulsed electric field (PEF) (38), photochemical reactions induced by irradiation of UV or visible light (39), and direct absorption of mechanical energy supplied by ball milling (40). Mechanochemistry has emerged as a significant approach capable of efficiently facilitating rapid chemical transformations through milling or grinding, eliminating the need for bulk dissolution of reactants in harmful solvents (41, 42). The International Union of Pure and Applied Chemistry (IUPAC) Compendium of Chemical Terminology defines a mechanochemical reaction as a chemical reaction induced by the direct absorption of mechanical

energy (43). Several technical variables influence mechanochemical organic synthesis, including milling frequency or revolutions per minute, milling time, size and number of milling balls, and the material of the milling balls and jars (44). The absence of a solvent in mechanochemical reactions enhances the interaction between the two reactive groups, resulting in higher product yield (45), improved selectivity, shorter reaction time, and simpler work-up procedure (44).

2.3.2 Thermochemistry in Synthesis of Glycated Amino Acids

Analyzing the Maillard reaction within the intricate matrix of food that has been subject to diverse processing conditions is a challenging proposition. Model reactions are crucial for exploring food systems' aroma, flavour, and antioxidant properties. Hydrothermal reactions in the solution phase remain the prevailing method for producing Maillard reaction products. However, this method is time-consuming, and its reliance on solvents presents inefficiencies associated with containment, recovery, and reuse (46).

Glycated amino acids (ARPs/HRPs) present challenges in purification and isolation, often yielding mixtures containing unreacted starting materials, isomeric glycosyl amine precursors and various degradation products alongside the desired rearrangement products, making their separation challenging. Moreover, this reaction is highly sensitive to hydrolytic conditions, potentially leading to competition between the rearrangement reaction and the hydrolysis of the initially formed Schiff base, the latter reverting to the starting materials (47). Additionally, the resulting products are not very stable under the reaction and storage conditions, rendering them susceptible to decomposition.

Generally, glycated amino acids are prepared by refluxing an amino acid with excess glucose in methanol for several hours (26). Using an anhydrous organic medium like methanol favours the formation of the ARP because the degradation rate is minimized (27). The product is then isolated and purified by repeated column chromatography. However, limitations to this method include poor yields due to air oxidation and additional side reactions of glucose and ARPs (26). While aqueous medium is preferred to avoid contamination in the Maillard reaction, high water content during heating promotes hydrolysis, yielding free sugars and amino acids, significantly reducing

ARP yields (4, 48). Additionally, the removal of the water is energy-intensive and may lead to degradation or loss of aroma-active compounds (42).

A successful approach to increase ARP yield combined a thermal reaction with vacuum dehydration (49, 50). The simultaneous dehydration reaction removes water through thermal treatment, diminishing the negative effect of water activity and content on the stability of the ARP (50). Despite the ease of operation and time efficiency of thermal reaction coupled with vacuum dehydration, it poses challenges for large-scale production due to inherent drawbacks. The improved degree of ARP conversion depends on the removal of water in the reaction system; therefore, when water in the concentrator is removed, wall sticking is inevitable, resulting in difficulty for further dehydration and ARP conversion (51). Consequently, vacuum evaporation is limited to laboratory-scale ARP preparation due to difficulties in achieving stable and uniform products.

While studies on ARP synthesis and subsequent degradation reactions have predominantly occurred in aqueous mediums, using solvents in ARP synthesis presents challenges in the removal of the solvent used, subsequent purification, and crystallization steps. Accordingly, the development of solvent-free approaches has the potential to offer higher yields, ensure time efficiency, minimize waste, and cultivate environmentally friendly processes for synthesizing glycated amino acids.

2.3.3 Mechanochemistry in Synthesis of Glycated Amino Acids

While mechanochemistry has gained popularity in the scientific community, its application to generate Maillard reaction mixtures remains limited. The first reported use of mechanochemistry by ball-milling to produce Maillard reaction flavours from amino acids and sugars appeared in patent literature (40). It demonstrated the ability of solid-state mechanical processing to form solid flavour precursors into extremely well-pre-organized systems, allowing better control of flavour generation and analysis. Subsequently, Xing and Yaylayan (42) employed high-energy ball milling to investigate its role and the underlying mechanisms in aroma enhancement. Their findings revealed that ball milling glucose with various amino acids generates mixtures rich in reactive intermediates and hard-to-obtain intermediates like Schiff bases, ARPs, and HRPs, with minimal

degradation through decarboxylation, dehydration, and retro-aldol reactions relative to non-milled samples (42, 52). The amino acids side chain influenced the mixture's composition, with acidic side chains favouring more Amadori products and basic side chains yielding more Schiff bases (42, 52).

The formation of an ARP results from removing one molecule of water from N-glycosamine (Schiff Base). According to Le Chatelier's principle, this water removal alters the reaction equilibrium, leading to the accumulation of ARP or HRP (53). Low water content stabilizes the early Maillard reaction and accelerates glycation by increasing reactant concentrations and eliminating water's hindering effects, particularly in reactions that generate water as a by-product (54, 55). Consequently, the solvent-free nature of mechanochemistry via ball milling emerges as a promising approach to produce crucial precursors required for aroma and antioxidant generation - specifically, Amadori products and Schiff bases - in high yields to study their further reactions. This method allows for in-depth exploration of their complexity within the Maillard reaction, a task that would otherwise demand extensive synthetic procedures or pose challenges in obtaining commercial standards.

2.4 Glycated Amino Acids in Food

2.4.1 Glycated Amino Acids Occurrence in Food

Glycated amino acids (ARPs) have captured significant attention, prompting extensive studies focusing on their analysis in various food products. Pioneering work by Ingles and Reynolds in 1958 highlighted the presence of ARPs in browned freeze-dried apricots, employing ion exchange chromatography (56). Despite the complexity of the results, characterized by numerous overlapping peaks, their research effectively confirmed the existence of ARPs in this context. Since then, various ARPs have been successfully identified in various types of foods and beverages, such as fruit and vegetable products (57), dairy products (58), and nuts (59). The composition and content of glycated amino acids in different foods vary, and it is widely accepted that ARPs are consumed in significant quantities as part of the human diet (97, 158) (60, 61). While recognized for their antioxidant properties, potentially contributing to positive health effects in humans (62-65), under certain conditions, ARPs can also metabolize into potentially toxic compounds (66). Consequently, understanding the fate of ARPs during the thermal processing of food is crucial in

ensuring their presence in the human diet positively impacts overall health. Excessive glycation can lead to the degradation of essential amino acids, reduced digestibility, enzyme inactivation, hindered binding of regulatory molecules, and cross-linking of proteins (67). Diet is a significant source of pro-inflammatory AGEs. AGEs derived from digested food also contribute to AGE-related disorders (68), such as increased oxidative stress and inflammation, factors linked to diabetes and cardiovascular disease (69). The quantity of AGEs in foods depends on the type of protein, sugar, fat, and other components present.

2.4.2 The Role of Glycated Amino Acids in the Generation of Flavours, Aromas, and Antioxidants

The flavour and aroma of food are some of the most important factors in captivating consumers and optimizing food quality, and the MR plays a pivotal role in their creation. However, Maillard reaction products are hindered by a substantial drawback – their susceptibility to degradation when exposed to thermal treatments and storage conditions, which can lead to the loss of desirable flavours (31, 70). Preserving flavour quality and preventing deterioration present substantial challenges in food processing and storage, particularly when temperatures exceed room temperature (31). Specifically, consumers strongly prefer the development of fresh flavours during cooking or food consumption. To address these concerns, Maillard reaction intermediates, specifically ARPs, have recently become a focal point of research, significantly contributing to improving stability and flavour enhancement. ARPs, a flavourless intermediate, offer a significant advantage of improved stability during storage and the ability to produce fresh and desirable flavours simultaneously during thermal treatment (70). These characteristics make them promising flavour enhancers and potential food additives. According to Luo et al. (70), adding ARPs as seasoning is a promising way to extend shelf life for low water reactivity and storage under low or room temperature. However, using ARPs in different food matrices still needs to be considered, for example, in an acidic environment.

The complexity of food flavour arises from its intricate composition, involving a large number of molecules. Determining this complexity is challenging, given that not every component contributes equally to the overall perception, and various interactions can bind flavour compounds (71). Some ARPs are important non-volatile taste active molecules. Recent research conducted by

Wang et al. (72) has revealed that proline-glucose-ARP can enhance umami while also providing a salty taste. The study utilized an electronic tongue and sensory evaluation to demonstrate that the addition of just 0.4% of ARP can reduce salt intake by 20% without compromising the level of saltiness (72). These promising results suggest that ARP has the potential for use in healthy food products and seasonings, as it enables a reduction in the amount of sodium chloride and glutamate to achieve a healthier level of salt intake.

While ARPs lack volatility and distinct aroma characteristics, their degradation products readily generate numerous volatile aroma compounds during the MR. These compounds, usually characterized by low molecular weight and relatively low olfactory thresholds, include aldehydes, ketones, furans, pyrazines, thiophenes, thiazoles, oxazoles, and disulfides (27). Additionally, the degradation of ARPs can result in the formation of deoxyosones, contributing to the production of carbonyl compounds with varying chain lengths. Under the induction of carbonyls, amino acids can undergo Strecker degradation with α-dicarbonyl compounds, leading to decarboxylation and deamination to generate α-amino ketones, Strecker aldehydes, and carbon dioxide (73). These dicarbonyls are integral to the Strecker degradation process, forming crucial flavour compounds and initiating a cascade of reactions that leads to a diverse range of flavours (27). For example, Hartmann and Schieberle (74) explored the role of ARPs as precursors of aroma-active Strecker aldehydes in cocoa. Their research revealed that ARPs in unfermented cocoa are precursors of cocoa odorants through the roasting process, leading to the generation of Strecker aldehydes like 3- or 2-methylbutanal, 3-(methylthio)propanal, and phenylacetaldehyde (74).

2.5 Enzymatic deglycation by fructosamine-3-kinase (FN3K)

Enzymatic deglycation, a pivotal process in mitigating the adverse effects of glycation, involves the removal of sugar moieties from amino acids, proteins, and other biomolecules. Initially, non-enzymatic glycation was thought to be entirely non-enzymatic and irreversible (75). However, Szwergold et al. (76) discovered that the kinase fructosamine-3-kinases (FN3K) can act as a deglycating enzyme, challenging the conventional belief of irreversibility in glycation reactions. Subsequently, other enzymes, such as Amadoriases (77) and fructosamine-6-kinases (FN6K) (78), have been identified as facilitators of deglycation. This discovery opens new therapeutic interventions for combating the deleterious effects of diabetic complications.

The significance of the glycation mechanism in cellular maintenance and aging mechanisms was underscored by Emel'yanov (79), who highlighted the roles of glycation, antiglycation, and deglycation in aging processes and potential geroprotective effects. Protective enzymes within cells play crucial role in preventing glycation or repairing glycated proteins. Antiglycation enzymes metabolize highly active carbonyl products to polyols or acids, constituting the first line of defence against glycation. Whereas the second line of defence is represented by deglycation enzymes (79). An alternative FN3K-independent deglycation system involving removal, by transglycation, of sugar moieties from Schiff bases by a variety of biological nucleophiles, including free amino acids, thiols, and peptides, was highlighted by Szwergold (75). The effectiveness of these scavenging compounds depends on their nucleophilicity, which is a function of the pKa's of their primary or secondary amines. Building upon enzymatic deglycation, thermal deglycation in the presence of free amino acids offers an alternative mechanism to mitigate glycation-induced damage.

2.6 References

1. Maillard, L. C. Action of amino acids on sugars. Formation of melanoidins in a methodical way. Compte-rendu de l'academie des sciences **1912**, 154, 66-68.
2. Xu, H.; Zhang, X.; Karangwa, E. Inhibition Effects of Maillard Reaction Products Derived from l-Cysteine and Glucose on Enzymatic Browning Catalyzed by Mushroom Tyrosinase and Characterization of Active Compounds by Partial Least Squares Regression Analysis. *RSC Adv.* **2016**, *6* (7), 65825–65836. DOI: 10.1039/c6ra15769f.
3. Hodge, J. E. Dehydrated Foods, Chemistry of Browning Reactions in Model Systems. *J. Agric. Food Chem.***1953**, *1*(15), 928-943.
4. Nursten, H. Recent Advances. The Maillard Reaction: Chemistry, Biochemistry and Implications. *Royal Society of Chemistry* **2005**, 31−50.
5. Fay, L.B.; Brevard, H. Contribution of Mass Spectrometry to the Study of the Maillard Reaction in Food. *Mass Spectrom. Rev*. **2005**, *24*, 487-507. DOI: 10.1002/mas.20028
6. Laroque, D.; Inisan, C.; Berger, C.; Vouland, É.; Dufossé, L.; Guérard, F. Kinetic Study on the Maillard Reaction: Consideration of Sugar Reactivity. *Food Chem*. **2008**, *111*(4), 1032-1042. DOI: 10.1016/j.foodchem.2008.05.033
7. Kunkel, H. G.; Wallenius, G. New Hemoglobin in Normal Adult Blood. *Science* **1955**, *122*(3163), 288-288.
8. Rahbar, S. An Abnormal Hemoglobin in Red Cells of Diabetics. *Clinica Chimica Acta* **1968**, *22*(2), 296-298.
9. Henning, C.; Glomb, M.A. Pathways of the Maillard Reaction under Physiological Conditions. *Glycoconj J*. **2016**, *33*, 499–512. DOI: 10.1007/s10719-016-9694-y
10. Van Boekel, M. A. J. S. Formation of Flavour Compounds in the Maillard Reaction. *Biotechnol. Adv*. **2006**, *24*(2), 230-233. DOI: 10.1016/j.biotechadv.2005.11.004
11. Ames, J. M. The Maillard Reaction. In: Hudson, B. J. F. (Ed.) *Biochem. Food Proteins* **1992** pp 99-153. DOI: 10.1007/978-1-4684-9895-0_4
12. Twarda-Clapa, A.; Olczak, A.; Białkowska, A. M.; Koziołkiewicz, M. Advanced Glycation End-Products (AGEs): Formation, Chemistry, Classification, Receptors, and Diseases Related to AGEs. *Cells* **2022**, *11*(8). DOI: 10.3390/cells11081312

13. Diez-Simon, C.; Mumm, R.; Hall, R. D. Mass Spectrometry-Based Metabolomics of Volatiles as a New Tool for Understanding Aroma and Flavour Chemistry in Processed Food Products. *Metabolomics* **2019**, *15*(3), 1-20. DOI: 10.1007/s11306-019-1493-6
14. Ames, J. M. Applications of the Maillard reaction in the food industry. *Food Chemistry* **1998**, *62*(4), 431-439. DOI: 10.1016/S0308-8146(98)00078-8
15. Yaylayan, V. A. Classification of the Maillard reaction: A conceptual approach. *Trends in Food Sci. Technol.* **1997**, *8*(1), 13-18. DOI: 10.1016/S0924-2244(96)20013-5
16. Chao, P.; Hsu, C.; Yin, M. Analysis of Glycative Products in Sauces and Sauce-Treated Foods. *Food Chem.* **2009**, *113* (1), 262-266. DOI: 10.1016/j.foodchem.2008.06.076
17. Yu, J.; Renard, C. M.; Zhang, L.; Gleize, B. Fate of Amadori Compounds in Processing and Digestion of Multi-Ingredients Tomato-Based Sauces and Their Effect on Other Microconstituents. *Food Res. Int.* **2023**, *173*, 113381. DOI: 10.1016/j.foodres.2023.113381
18. Borthwick, A. D.; Da Costa, N. C. 2,5-Diketopiperazines in Food and Beverages: Taste and Bioactivity. *Crit. Rev. Food Sci. Nutr.* **2017**, *57*(4), 718-742. DOI: 10.1080/10408398.2014.911142.
19. Ludwig, E.; Lipke, U.; Raczek, U.; Jäger, A. Investigations of Peptides and Proteases in Green Coffee Beans. *Eur. Food Res. Technol.* **2000**, *211*, 111-116.
20. Fu, Y.; Zhang, Y.; Soladoye, O. P.; Aluko, R. E. Maillard Reaction Products Derived from Food Protein-Derived Peptides: Insights into Flavor and Bioactivity. *Crit. Rev. Food Sci. Nutr.* **2020**, *60*(20), 3429-3442. DOI: 10.1080/10408398.2019.1691500.
21. Yang, C.; Wang, R.; Song, H. The Mechanism of Peptide Bonds Cleavage and Volatile Compounds Generated from Pentapeptide to Heptapeptide via Maillard Reaction. *Food Chem.* **2012**, *133*(2), 373-382.
22. Wolfrom, M. L.; Kolb, D. K.; Langer, A. W., Jr. Chemical Interactions of Amino Compounds and Sugars. VII. pH Dependency. *J. Am. Chem. Soc.* **1953**, *75*, 3471−3573.
23. Ames, J. M. Control of the Maillard Reaction in Food Systems. *Trends in Food Sci. Technol.* **1990**, *1*, 150-154.
24. Golon, A.; Kropf, C.; Vockenroth, I.; Kuhnert, N. An Investigation of the Complexity of Maillard Reaction Product Profiles from the Thermal Reaction of Amino Acids with Sucrose Using High Resolution Mass Spectrometry. *Foods* **2014**, *3*, 461-475. https://doi.org/10.3390/foods3030461

25. Hemmler, D., Roullier-Gall, C., Marshall, J.W. et al. Evolution of Complex Maillard Chemical Reactions, Resolved in Time. *Sci Rep* **2017**, *7*, 3227. https://doi.org/10.1038/s41598-017-03691-z
26. Yaylayan, V. A.; Huyghues-Despointes, A.; Feather, M.S. Chemistry of Amadori Rearrangement Products: Analysis, Synthesis, Kinetics, Reactions, and Spectroscopic Properties. *Crit. Rev. Food Sci. Nutr.* **1994**, *34*(4), 321-369. DOI: 10.1080/10408399409527667
27. Cui, H.; Yu, J.; Zhai, Y.; Feng, L.; Chen, P.; Hayat, K.; Xu, Y.; Zhang, X.; Ho, C. Formation and Fate of Amadori Rearrangement Products in Maillard Reaction. *Trends Food Sci. Technol.* **2021**, *115*, 391-408. DOI: 10.1016/j.tifs.2021.06.055
28. Chanda, D.; Harohally, N. V. Revisiting Amadori and Heyns Synthesis: Critical Percentage of Acyclic Form Play the Trick in Addition to Catalyst. *Tetrahedron Lett.* **2018**, *59*(31), 2983-2988. DOI: 10.1016/j.tetlet.2018.06.050
29. Parker, J. Thermal Generation of Aroma. *Flavour Development, Analysis and Perception in Food and Beverages* **2015**, 151-185. DOI: 10.1016/B978-1-78242-103-0.00008-4
30. Martins, S. I.; Marcelis, A. T.; van Boekel, M. A. Kinetic Modelling of Amadori N-(1-Deoxy-d-fructos-1-yl)-glycine Degradation Pathways. Part I—Reaction Mechanism. *Carbohydr. Res.* **2003**, *338*(16), 1651-1663. DOI: 10.1016/S0008-6215(03)00173-3
31. Liu, S.; Sun, H.; Ma, G.; Zhang, T.; Wang, L.; Pei, H.; Li, X.; Gao, L. Insights into Flavor and Key Influencing Factors of Maillard Reaction Products: A Recent Update. *Front. Nutr.* **2022**, *9*. DOI: 10.3389/fnut.2022.973677
32. Yaylayan, V. In Search of Alternative Mechanisms for the Maillard Reaction. *Trends Food Sci. Technol.* **1990**, *1*, 20-22. DOI: 10.1016/0924-2244(90)90006-K
33. Huyghues-Despointes, A.; Yaylayan, V. Retro-Aldol and Redox Reactions of Amadori Compounds: Mechanistic Studies with Variously Labeled D-[13C] Glucose. *J. Agric. Food Chem.* **1996**, *44*(3), 672-681.
34. Burton, H. S.; McWeeny, D. J. Non-enzymatic browning - routes to the production of melanoidins from aldoses and amino-compounds. *Chem. Ind.* **1964**, (11), 462-463.
35. Feather, M. S.; Mossine, V. V. Correlations Between Structure and Reactivity of Amadori Compounds: The Reactivity of Acyclic Forms. Maillard Reaction Foods Med. **2005**, 37-42.

36. Fernández-Bertran, J. Mechanochemistry: An Overview. *Pure and Applied Chemistry* **1999**, *71*(4), 581-586. DOI: 10.1351/pac199971040581
37. Qu, W. X.; Zhang, W.; Chen, Z.; Wang, R.; He, H.; Ma, Y. H. Effects of Ultrasonic and Graft Treatments on Grafting Degree, Structure, Functionality, and Digestibility of Rapeseed Protein Isolate-Dextran Conjugates. *Ultrasonics Sonochemistry* **2018**, 42, 250–259. DOI: 10.1016/j.ult- sonch.2017.11.021.
38. Guan, J. J.; Qiu, A. Y.; Liu, X. Y.; Hua, Y. F.; Ma, Y. H. Microwave Improvement of Soy Protein Isolate–Saccharide Graft Reactions. *Food Chemistry* **2006**, 97(4), 577–585. DOI: 10.1016/j.foodchem.2005.05.035.
39. Hemmler, D.; Gonsior, M.; Powers, L. C.; Marshall, J. W.; Rychlik, M.; Taylor, A. J.; Schmitt-Kopplin, P. Simulated Sunlight Selectively Modifies Maillard Reaction Products in a Wide Array of Chemical Reactions. *Chem.–Eur. J.* **2019**, 25(57), 13208-13217.
40. Viton, F.; Oertling, H.R.; Fumeaux, R. Mechanical Generation of Flavour Compositions. Patent No. US20170079316A1, **2017**.
41. James, S. L.; Adams, C. J.; Bolm, C.; Braga, D.; Collier, P.; Friščić, T.; Waddell, D. C. Mechanochemistry: Opportunities for New and Cleaner Synthesis. *Chem. Soc. Rev.* **2012**, *41*(1), 413-447.
42. Xing, H.; Yaylayan, V. Investigation of Thermo-Chemical Properties of Mechanochemically Generated Glucose–Histidine Maillard Reaction Mixtures. Eur. *Food Res. Technol*. **2021**, *247*(1), 111-120.
43. IUPAC Compendium of Chemical Terminology, Ed. M. Nič, J. Jirát, B. Košata, A. Jenkins, A. McNaught; IUPAC, 2009.
44. Wang, G. W. Mechanochemical Organic Synthesis. *Chem. Soc. Rev.* **2013**, *42* (18), 7668–7700.
45. Xing, H.; Yaylayan, V. Insight into Isomeric Diversity of Glycated Amino Acids in Maillard Reaction Mixtures. *Int. J. Mol. Sci.* **2022**, *23* (7), 3430. DOI: 10.3390/ijms23073430
46. Sheldon, R. A. Green Solvents for Sustainable Organic Synthesis: State of the Art. *Green Chemistry* **2005**, *7* (5), 267-278.
47. Wrodnigg, T. M.; Eder, B. The Amadori and Heyns Rearrangements: Landmarks in the History of Carbohydrate Chemistry or Unrecognized Synthetic Opportunities?

Glycoscience, Ed. Stütz, A. E.; Springer: Berlin, Heidelberg, 2001; Vol 215, https://doi.org/10.1007/3-540-44422-X_6.

48. Kocadağlı, T.; Gökmen, V. Multiresponse Kinetic Modelling of Maillard Reaction and Caramelisation in a Heated Glucose/Wheat Flour System. *Food Chem.* **2016**, *211*, 892–902.
49. Cui, H.; Hayat, K.; Jia, C.; Duhoranimana, E.; Huang, Q.; Zhang, X.; Ho, C. T. Synergistic Effect of a Thermal Reaction and Vacuum Dehydration on Improving Xylose–Phenylalanine Conversion to N-(1-Deoxy-d-Xylulos-1-Yl)-Phenylalanine during an Aqueous Maillard Reaction. *J. Agric. Food Chem.* **2018**, *66*(38), 10077-10085.
50. Tang, W.; Cui, H.; Sun, F.; Yu, X.; Hayat, K.; Hussain, S.; Ho, C. T. N-(1-Deoxy-D-xylulos-1-yl)-glutathione: A Maillard Reaction Intermediate Predominating in Aqueous Glutathione-Xylose Systems by Simultaneous Dehydration-Reaction. *J. Agric. Food Chem.* **2019**, *67*(32), 8994-9001.
51. Wang, Y.; Cui, H.; Zhang, Q.; Hayat, K.; Yu, J.; Hussain, S.; Usman Tahir, M.; Zhang, X.; Ho, C. Proline-Glucose Amadori Compounds: Aqueous Preparation, Characterization and Saltiness Enhancement. *Food Res. Int.* **2021**, *144*, 110319. DOI: 10.1016/j.foodres.2021.110319.
52. Xing, H.; Yaylayan, V. Mechanochemical Generation of Schiff Bases and Amadori Products and Utilization of Diagnostic MS/MS Fragmentation Patterns in Negative Ionization Mode for Their Analysis. *Carbohydr. Res.* **2020**, *495*, 108091. DOI: 10.1016/j.carres.2020.108091.
53. Zhan, H.; Tang, W.; Cui, H.; Hayat, K.; Hussain, S.; Tahir, M. U.; Zhang, S.; Zhang, X.; Ho, C. T. Formation Kinetics of Maillard Reaction Intermediates from Glycine-Ribose System and Improving Amadori Rearrangement Product through Controlled Thermal Reaction and Vacuum Dehydration. Food Chem. 2020, 311, 125877.
54. Stanic-Vucinic, D.; Prodic, I.; Apostolovic, D.; Nikolic, M.; Cirkovic Velickovic, T. Structure and Antioxidant Activity of β-Lactoglobulin-Glycoconjugates Obtained by High-Intensity-Ultrasound-Induced Maillard Reaction in Aqueous Model Systems under Neutral Conditions. *Food Chem.* **2013**, *138*(1), 590-599. DOI: 10.1016/j.foodchem.2012.10.087

55. Xing, H.; Mossine, V. V.; Yaylayan, V. Mechanochemical Generation of N,N-Diglycated Glycine and MS/MS Characterization of Its Isomeric Composition. *Food Chem.* **2022**, *397*, 133757. DOI: 10.1016/j.foodchem.2022.133757
56. Ingles, D. L.; Reynolds, T. M. Chemistry of Non-enzymic Browning. IV. Determination of Amino Acids and Amino Acid-deoxyfructoses in Browned Freeze-dried Apricots. *Aust. J. Chem*. **1958**, *11*(4), 575-580.
57. Yang, C.; Zhang, S.; Shi, R.; Yu, J.; Li, S.; Tao, G.; Zhang, L. LC-MS/MS for Simultaneous Detection and Quantification of Amadori Compounds in Tomato Products and Dry Foods and Factors Affecting the Formation and Antioxidant Activities. *J. Food Sci.* **2020**, *85*(4), 1007-1017.
58. Schwietzke, U.; Malinowski, J.; Zerge, K.; Henle, T. Quantification of Amadori Products in Cheese. *Eur. Food Res. Technol.* **2011**, *233*(2), 243–251. doi:10.1007/s00217-011-1509-6.
59. Wellner, A.; Nußpickel, L.; Henle, T. Glycation Compounds in Peanuts. *Eur. Food Res. Technol.* **2012**, *234*(3), 423–429. doi:10.1007/s00217-011-1649-8.
60. Muir, D. D. The Maillard Reaction—Chemistry, Biochemistry and Implications. *Int. J. Dairy Technol.* **2007**, *60*(1), 59. https://doi.org/10.1111/j.1471-0307.2007.00233.
61. Cao, J., Yang, C., Zhang, J., Zhang, L., & Tsao, R. Amadori Compounds: Analysis, Composition in Food and Potential Health Beneficial Functions. *Crit. Rev. Food Sci. Nutr.* **2023**, 1-23.
62. Shakoor, A.; Zhang, C.; Xie, J.; Yang, X. Maillard Reaction Chemistry in Formation of Critical Intermediates and Flavor Compounds and Their Antioxidant Properties. *Food Chem.* **2022**, 393, 133416. DOI: 10.1016/j.foodchem.2022.133416
63. Cui, H.; Hayat, K.; Zhang, X. Antioxidant Activity In Vitro of N-(1-deoxy-α-d-xylulos-1-yl)-Phenylalanine: Comparison Among Maillard Reaction Intermediate, End-Products and Xylose-Phenylalanine. *J. Food Sci.* **2019**, 84(5), 1060-1067.
64. Bersuder, P.; Hole, M.; Smith, G. Antioxidants from a Heated Histidine-Glucose Model System. Investigation of the Copper(II) Binding Ability. *J. Am. Oil Chem. Soc.* **2001**, 78(11), 1079-1082.
65. Yang, C., Zhang, S., Shi, R., Yu, J., Li, S., Tao, G., ... & Zhang, L. LC-MS/MS for Simultaneous Detection and Quantification of Amadori Compounds in Tomato Products

and Dry Foods and Factors Affecting the Formation and Antioxidant Activities. *J. Food Sci.* **2020**, 85(4), 1007-1017.

66. Mottram, D. S.; Wedzicha, B. L.; Dodson, A. T. Acrylamide Is Formed in the Maillard Reaction. *Nature* **2002**, 419 (6906), 448–449. DOI: 10.1038/419448a.
67. Brownlee, M.; Vlassara, H.; Cerami, A. Nonenzymatic Glycosylation and the Pathogenesis of Diabetic Complications. *Ann. Intern. Med.* **1984**, 101 (4), 527–537.
68. Yamagishi, S.; Matsui, T.; Nakamura, K. Possible Link of Food-Derived Advanced Glycation End Products (AGEs) to the Development of Diabetes. *Med. Hypotheses* **2008**, 71 (6), 876–878. DOI: 10.1016/j.mehy.2008.07.034.
69. Uribarri, J.; Woodruff, S.; Goodman, S.; Cai, W.; Chen, X.; Pyzik, R.; Yong, A.; Striker, G. E.; Vlassara, H. Advanced Glycation End Products in Foods and a Practical Guide to Their Reduction in the Diet. *J. Am. Diet. Assoc.* **2010**, 110 (6), 911-916.e12. DOI: 10.1016/j.jada.2010.03.018.
70. Luo, Y.; Li, S.; Ho, T. Key Aspects of Amadori Rearrangement Products as Future Food Additives. Molecules 2021, 26 (14). DOI: 10.3390/molecules26144314.
71. Starowicz, M.; Zieliński, H. How Maillard Reaction Influences Sensorial Properties (Color, Flavor and Texture) of Food Products? Food Rev. Int. 2019, 35 (8), 707-725. DOI: 10.1080/87559129.2019.1600538.
72. Wang, Y.; Cui, H.; Zhang, Q.; Hayat, K.; Yu, J.; Hussain, S.; Usman Tahir, M.; Zhang, X.; Ho, C. Proline-Glucose Amadori Compounds: Aqueous Preparation, Characterization and Saltiness Enhancement. *Food Res. Int.* **2021**, *144*, 110319. DOI: 10.1016/j.foodres.2021.110319.
73. Cao, J.; Yang, C.; Zhang, J.; Zhang, L.; Tsao, R. Amadori Compounds: Analysis, Composition in Food and Potential Health Beneficial Functions. *Crit. Rev. Food Sci. Nutr.* **2023**, 1–23.
74. Hartmann, S.; Schieberle, P. On the Role of Amadori Rearrangement Products as Precursors of Aroma-Active Strecker Aldehydes in Cocoa. In Browned Flavors: Analysis, Formation, and Physiology. *ACS* **2016**, 1–13.
75. Szwergold, B. S. Carnosine and Anserine Act as Effective Transglycating Agents in Decomposition of Aldose-Derived Schiff Bases. *Biochem. Biophys. Res. Comm.* **2005**, *336*, 36-41.

76. Szwergold, B. S. et al. Identification of a Novel Protein Kinase Activity Specific for Amadori Adducts on Glycated Proteins. *Diabetes* **1997**, *46*, 108A.
77. Lin, Z.; Zheng, J. Occurrence, Characteristics, and Applications of Fructosyl Amine Oxidases (Amadoriases). *Appl. Microbiol. Biotechnol.* **2010**, *86*, 1613-1619.
78. Wiame, E.; Delpierre, G.; Collard, F.; Van Schaftingen, E. Identification of a Pathway for the Utilization of the Amadori Product Fructoselysine in *Escherichia coli*. *J. Biol. Chem.* **2002**, *277*(45), 42523-42529.
79. Emel'yanov, V. V. Glycation, Antiglycation, and Deglycation: Their Role in Aging Mechanisms and Geroprotective Effects. *Adv. Gerentol.* **2017**, *7*(1), 1-9.

Chapter 3. Methodology: Materials and Methods

3.1 Materials

D-glucose, L-histidine (98%), L-cysteine (97%), L-phenylalanine (≥98%), and N_{α}-(*tert*-Butoxycarbonyl)-L-lysine, N_{α}-Boc-L-lysine (>98 %) were obtained from Sigma-Aldrich Chemical Co. (Oakville, ON, Canada). All other chemicals and reagents were of analytical grade from Fisher Scientific. No further purification was conducted on any of the chemicals used in the experiments.

3.2 Preparation of Glycated Amino Acids by Mechanochemical Reactions

Samples (50mg) consisting of selected amino acid and sugar mixtures in a 1:1 molar ratio were mixed using a mortar and pestle to ensure homogeneity (~1 min) and then milled at ambient temperature. All mechanochemical reactions were conducted in a stainless-steel grinding jar (10 mL) with 2 steel balls (10 mm in diameter) for inner friction. The jars were seated in the Retsch Mixer Mill (MM 400, Newtown, PA, US) that performs radial oscillations in a horizontal position without coolant (the external jar temperature was ~25 °C) at a frequency of 30 Hz for 30 mins. Samples collected after milling were stored at −20°C for further analysis. Hydrothermal reactions were performed on milled samples by heating the mixture in water (~1 mL) at 120 °C for 1.5 hrs in sealed stainless-steel reactors. The mixture was then cooled to room temperature in the sealed stainless-steel reactors before transferring to an open vial and heated for at 120 °C in a sand bath for 0.5 h.

3.3 Preparation of Diglycated Amino Acids Using Mechanochemically Generated Glycated Amino Acid and Sugar Mixture

Selected mechanochemically generated glycated amino acid and sugar mixtures were mixed in a 1:1 molar ratio using a mortar and pestle to ensure homogeneity (~1 min) and then milled at ambient temperature. All mechanochemical reactions were conducted in a stainless-steel grinding jar (10 mL) with 2 steel balls (10 mm in diameter) for inner friction. The jars were seated in the Retsch Mixer Mill (MM 400, Newtown, PA, US) that performs radial oscillations in a horizontal position without coolant (the external jar temperature was ~25 °C) at a frequency of 30 Hz for 30 mins. Samples collected after milling were stored at −20°C for further analysis. Hydrothermal reactions were performed on milled samples by heating the mixture in distilled water (~1 mL) at

120 °C for 1.5 hrs in sealed stainless-steel reactors. The mixture was then cooled to room temperature in the sealed stainless-steel reactors before transferring to an open vial and heated for at 120 °C in a sand bath for 0.5 h.

3.4 Preparation of Di-aminated Sugars by Mixing a Mechanochemically Generated Glycated Amino Acid with a Second Amino Acid

Di-aminated sugar mixtures were prepared by mixing a select mechanochemically generated glycated amino acid with a second amino acid in a 1:1 molar ratio using a mortar and pestle to ensure homogeneity (~1 min) and then milled at ambient temperature. All mechanochemical reactions were conducted in a stainless-steel grinding jar (10 mL) with 2 steel balls (10 mm in diameter) for inner friction. The jars were seated in the Retsch Mixer Mill (MM 400, Newtown, PA, US) that performs radial oscillations in a horizontal position without coolant (the external jar temperature was ~25 °C) at a frequency of 30 Hz for 30 mins. Samples collected after milling were stored at −20°C for further analysis. Hydrothermal reactions were performed on milled samples by heating the mixture in distilled water (~1 mL) at 120 °C for 1.5 hrs in sealed stainless-steel reactors. The mixture was then cooled to room temperature in the sealed stainless-steel reactors before transferring to an open vial and heated at 120 °C in a sand bath for 0.5 h.

3.5 ATR-FTIR

FTIR spectra of the glycated amino acid samples were obtained using a Bruker Alpha-P FTIR spectrometer (Bruker Optic GmbH, Ettlingen, Germany). The spectrometer is equipped with a deuterated triglycine sulfate (DTGS) detector, a single-bounce diamond attenuated total reflectance (ATR) crystal, and a pressure application device for solid samples. A total of 32 scans at 4 cm^{-1} resolution were co-added. A spectrum of the background from a cleaned ATR crystal was obtained prior to the acquisition of a new set of spectra. The resulting data were recorded and processed using Bruker OPUS software.

3.6 Electrospray Ionization/Quadrupole Time of Flight/Mass Spectrometry (ESI/QqTOF/MS)

Samples were diluted (1 µL; 0.1 mg/mL) in 1:9 (v/v) water/methanol, and solutions were applied to the detector via a syringe. The analysis was performed on a Bruker Maxis Impact quadrupole

time-of-flight mass spectrometer (Bruker Daltonics, Bremen, Germany) operated in positive ion mode. Instrument calibration was performed using sodium formate clusters. The electrospray interphase settings were as follows: nebulizer pressure, 0.6 bar; drying gas, 4 L/min; temperature, 180 °C; and capillary voltage, 4500 V. The scan range was from *m/z* 50 to 1000. The data were analyzed using Bruker Compass Data Analysis software (version 4.2, Bremen, Germany). Tandem mass spectrometry (MS/MS) was carried out in MRM mode using various collision energy (eV) for selected ions. Molecular formulae were assigned to all the observed peaks based on their exact *m/z* values using the online software "ChemCalc" (Institute of Chemical Sciences and Engineering, Lausanne, Switzerland).

Chapter 4. Mechanochemical Synthesis of ARP/HRP and their MS/MS Characterization Under Negative Ionization Mode

ARPs and HRPs mechanochemical synthesis, structural intricacies, and chemical transformations were explored using Fourier transform infrared (FTIR) spectroscopy and advanced tandem mass spectrometry (MS/MS) characterization under negative ionization mode. Mechanochemical glycation, involving the milling of amino acids with reducing sugars, initiates the Maillard reaction, leading to the formation of ARPs and HRPs. FTIR spectroscopy serves as a tool to monitor these transformations by identifying characteristic infrared bands corresponding to various functional groups indicative of glycation. While FTIR spectroscopy offers valuable insights, integrating complementary analytical methods provides a comprehensive understanding of the structural changes, hence the inclusion of MS/MS data analysis. Elucidating the fragmentation patterns of ARPs and HRPs using MS/MS provides information into their structural diversity and allows for discrimination between isomeric compounds, further advancing our understanding of Maillard chemistry. The combination of FTIR spectroscopy and MS/MS characterization provides a robust analytical approach for interpreting the intricacies of mechanochemical synthesis and its role in the formation of ARP/HRP intermediates.

4.1. FTIR spectroscopy infrared band assignments

The effects of mechanochemical glycation were studied using FTIR spectroscopy, a prevalent technique for analyzing the structural characteristics of protein-carbohydrate interactions (11, 12). This technique offers valuable insight into the Maillard reaction by detecting chemical changes observable within the FTIR spectra, primarily arising from the emergence of additional functional groups such as the Amadori compound (CO) and Schiff base (C=N) (13). While attenuated total reflectance (ATR)-FTIR provides valuable information, its standalone capability for offering detailed structural information on Maillard reaction compounds is limited, often necessitating additional analytical techniques such as MS/MS data analysis.

ATR-FTIR spectra of the ARPs of cysteine, histidine, and phenylalanine milled with glucose were obtained under identical conditions described in the materials and methods section (see Figures 4.1 to 4.3). The presence of the carbonyl band in all spectra (1700 – 1600 cm^{-1}), mainly arising from the C=O stretching vibration (27), served as a marker for understanding milling-induced

changes. However, the imine of the isomeric Schiff base also has a vibration of ν(-C=N) at 1660 cm^{-1}; therefore, it is not possible to assign the vibrations of the new species with certainty. Broad absorption bands in the 3000-3500 cm^{-1} range in all spectra were attributed to overlapping absorption peaks of the O-H bond from the polyhydroxy structure of the Amadori products and the N-H bond stretching vibration, derived from the dehydration condensation of the carbonyl group and amino group on glucose. The strong absorption peaks in each model indicated successful amino acid reactions with glucose. Furthermore, the his-ARP model is unique as the overlapping absorption peak is also derived from the imidazole ring of histidine (26). Peaks around 2900 cm^{-1} are observed in each spectrum arising from the stretching vibrations of the C-H group in glucose and possibly also the N-H stretching vibrations of NH_3^+ groups in the free amino acids present in the model mixtures (14). Additionally, bands due to C-O stretching vibrations related to glucose were observed at 1020, 1024, and 1023 cm^{-1} for the cys-ARP, his-ARP, and phe-ARP, respectively.

Shifts in the frequency of the absorption band arising from C=O were observed after milling, indicating chemical changes (see Figures 4.1 to 4.3). Notably, his-ARP exhibited a downward shift (1631cm^{-1} to 1583cm^{-1}), suggesting imine formation due to a high content of Schiff base relative to ARP, aligning with Xing et al.'s (9) findings. Additionally, Wnorowski & Yaylayan (16) found that the Schiff base of alanine was observed at 1647 cm^{-1}, whereas the formation of the Amadori product was observed at 1700 cm^{-1}. In comparison, a shift to higher frequency was observed in both the cys-ARP (1582 cm^{-1} to 1620 cm^{-1}) and phe-ARP (1558 cm^{-1} to 1603 cm^{-1}) model systems. Ketone and aldehyde carbonyl groups typically exhibit strong absorption bands in the 1740 - 1710 cm^{-1} region. The position of the absorption frequency provides valuable insights into the electronic and steric effects resulting from the substituents attached to the carbonyl group, offering significant information. Unique peaks were observed in each spectrum due to side-chain absorptions of the amino acid present in the sample. For example, in the cys-ARP sample, the thiol signal (S-H) was detected around 2550 cm^{-1}, consistent with the findings of Pawlukojc et al. (17). Due to the apolar character of the side chain of phenylalanine, the side-chain absorptions are weak (18); thus, only a weak band at 1495cm^{-1} was detected in the spectrum, corresponding to a ring vibration of the phenyl group (18, 24). In contrast, the ring vibration at 1583cm-1 was observed in the his-ARP spectrum due to the imidazole moiety (24). When milled with glucose, the FTIR spectra of cysteine, histidine, and phenylalanine exhibited characteristic bands indicative of successful

glycation reactions. To further validate these findings, additional mass spectrometry measurements were conducted, affirming the conclusions drawn from the FTIR observations. Table 4.1 summarizes the characteristic bands of the Amadori products.

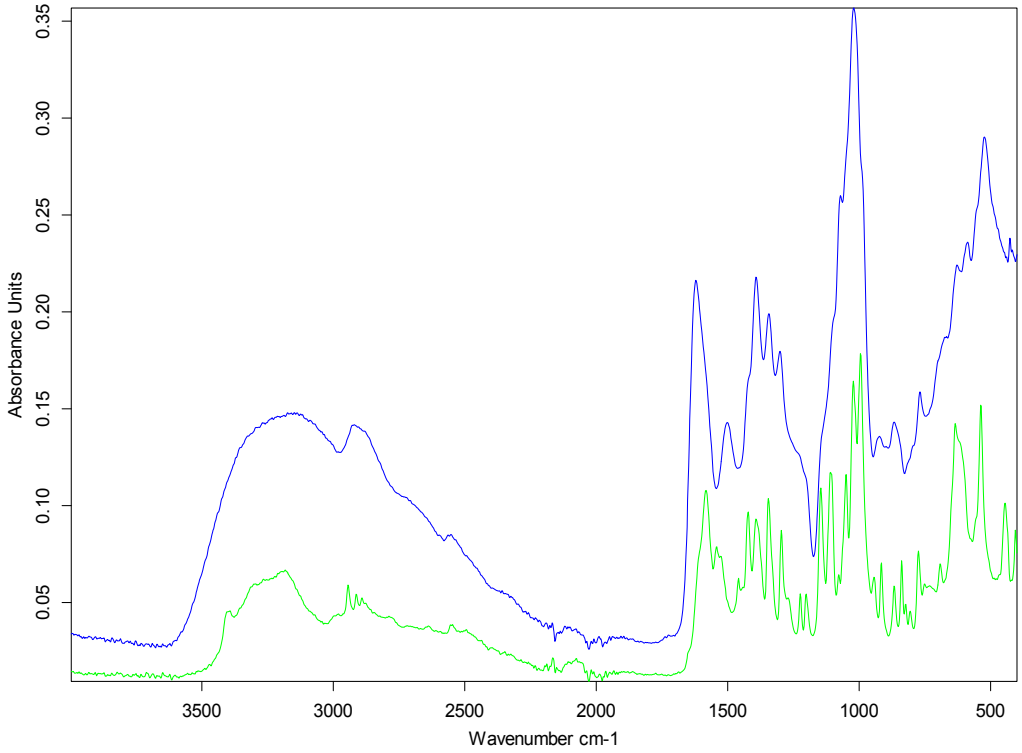

Figure 4.1 Superimposed FTIR spectrum of cysteine-glucose milled (blue) vs. not milled (green). See Table 4.1 for band assignments.

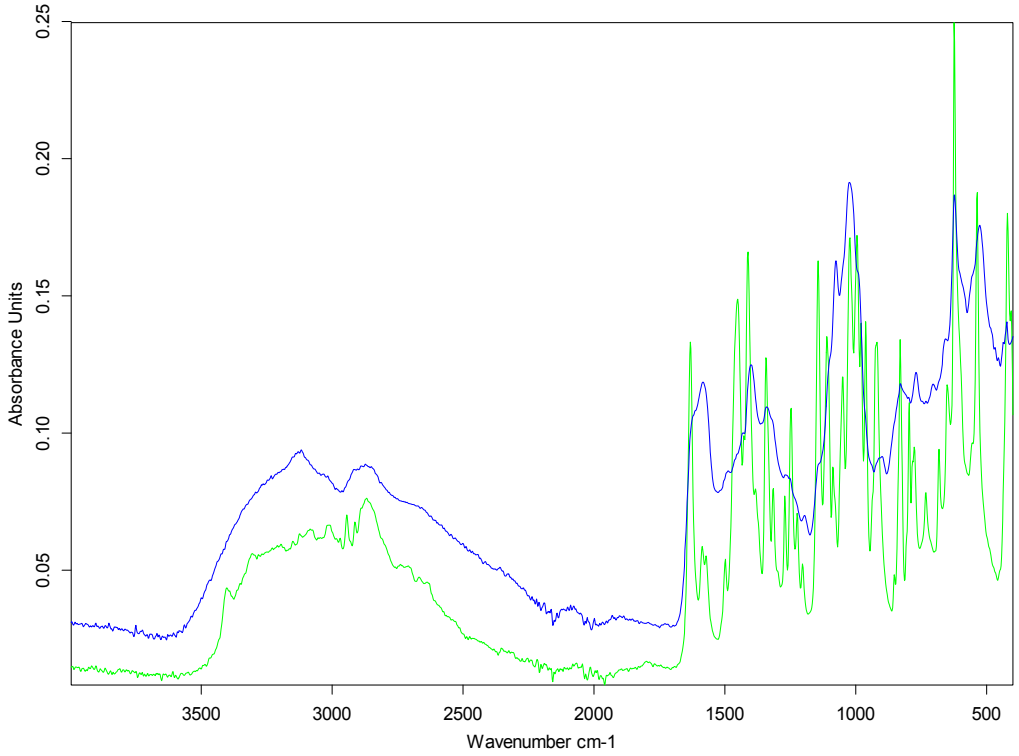

Figure 4.2 Superimposed FTIR spectrum of histidine-glucose milled (blue) vs. not milled (green). See Table 4.1 for band assignments.

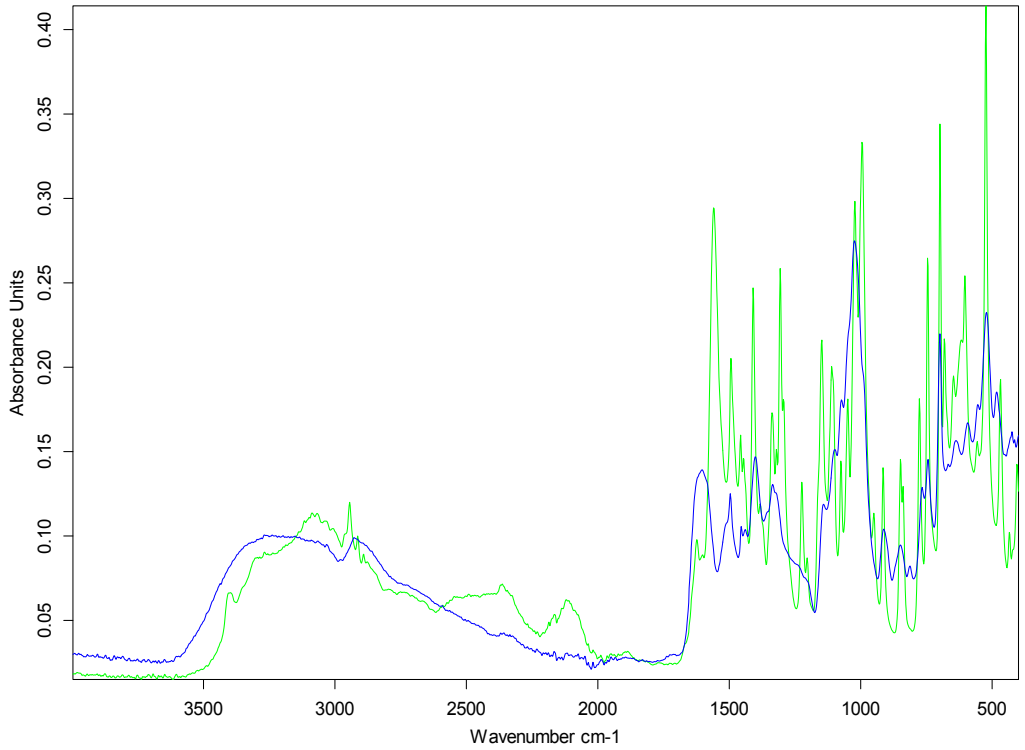

Figure 4.3 Superimposed FTIR spectrum of phenylalanine-glucose milled (blue) vs. not milled (green) See Table 4.1 for band assignments.

Table 4.1 ATR-FTIR spectral data of Amadori compounds

Compound	Assignment	Band position in cm^{-1}	References
Cys-ARP	ν(OH) & ν(NH)	3148	(21), (23), (26)
	ν(SH)	2554	(19)
	$\delta_{as}(NH_3^+)$	1620	(19)
	$\delta_s(NH_3^+)$	1501	(19)
	$\delta(CH_2)$	1391	(19)
	ν(CO)	1020	(23)
	$\delta(COO^-)$	536	(19)
His-ARP	ν(OH) & ν(NH)	3117	(21), (23), (26)
	ν(CH)	2873	(21), (23)
	ν(CC ring)	1583	(22), (24)
	ν(CN)	1451	(22)
	$\delta_s(CH_3)$	1399	(22)
	ν(CN)	1341	(22),
	ν(CO), ν(CN)	1075	(23), (26)
	ν(CO)	1024	(23)
Phe-ARP	ν(OH) & ν(NH)	3280	(21), (23), (26)
	ν(CH)	2895	(21), (23)
	ν(CC ring)	1603	(20)
	ν(CC ring)	1495	(20), (24)
	$\delta_{as}(CH_3)$	1400	(20)
	δ(CCH), δ(OCH)	1334	(23)
	ν(CO)	1023	(23)
	ν(CC ring)	698	(20)

ν = stretching vibration; δ = in-plane bending vibration; δ_{as} = antisymmetric in-plane bending vibration; δ_s = symmetric in-plane bending

4.2 MS/MS characterization under negative ionization mode

Mass spectrometry (MS) is a qualitative analytical technique known for its high selectivity, enabling the identification of various organic molecules based on their distinct mass-to-charge (*m/z*) ratios and characteristic MS/MS fragmentation patterns (1). In the pursuit of comprehending the intricacies of the Maillard reaction, MS serves as a valuable tool, offering rapid and highly sensitive detection of both early and advanced glycation products in food and biological systems (2-4). Furthermore, advanced tandem mass spectrometry (MS/MS) and MS^3 techniques

significantly improve selectivity and aid in structural identification by fragmentating each ion generated from the molecular ion (5). The fragmentation patterns of ARPs in MS/MS have been extensively documented and comprehensively understood through analyzing analytical standards and Maillard reaction model systems (6-8). However, there is a lack of MS/MS data to distinguish Amadori from Heyns compounds, especially in negative ionization mode.

4.2.1 ARP & HRP characteristic fragmentation patterns under negative ionization mode

The chemical composition of ball-milled glucose and various amino acids, such as cysteine, histidine, and phenylalanine, was explored using high-resolution mass spectrometry and MS/MS analysis under negative ionization mode. Electrospray ionization (ESI) of mechanochemically generated glycated amino acids yielded abundant $[M-H]^-$ ions (Cys-ARP *m/z* 282; His-ARP *m/z* 316; Phe-ARP *m/z* 326), with minimal degradation products commonly observed under hydrothermal reaction conditions. Furthermore, the elemental composition of the fragmentation ions was consistent with the proposed structure of their corresponding Amadori or Heyns product. Fragmentation ions of the deprotonated molecular ion $[M-H]^-$ are summarized in Table 4.2, along with the elemental composition of significant product ions provided in Table 4.3.

Table 4.2 MS/MS spectral data of Amadori and Heyns compounds and their significant and diagnostic ions.

#	Compound	Precursor ion $[M-H]^-$ (*m/z*)	CID voltage (eV)	Conditions	Significant fragment ions in MS/MS spectra $[M-X]^-$, *m/z* (rel. int.)
1	Cysteine Amadori	$[M-H]^-$ 282	10	Milled	282 (46.7), 204 (27), 162 (31.1), 119 (100), 114 (45.5)
			12	Milled	282 (57), 238 (28.4), 204 (41.5), 162 (100), 119 (41.4), 114 (41)
			12	Milled + Heated	282 (86.6), 248 (26.1), 238 (34.9), 204 (53.3), 162 (100), 120 (52.2), 119 (51), 114 (38.8)
2	Cysteine Heyn's	$[M-H]^-$ 282	8	Milled	282 (100), 238 (15.6), 204 (33.6), 192 (26.6), 174 (11.5), 126 (9.2), 114 (10)
			10	Milled	282 (100), 238 (27), 204 (51.8), 192 (44), 174 (23.7), 126 (15.5), 114 (17.2)
3	Histidine Amadori	$[M-H]^-$ 316	12	Milled	316 (16.7), 196 (100), 154 (8.8)
			12	Milled	316 (19.3), 226 (68.4), 196 (46.4), 154 (100)
			12	Milled + Heated	316 (17.7), 226 (72.5), 196 (5.8) 154 (100)
4	Histidine Heyn's	$[M-H]^-$ 316	12	Milled	316 (25.1), 226 (12.5), 196 (100), 164 (17.9), 154 (27.9)
			15	Milled	316 (10.3), 226 (22.4), 196 (100), 194 (14.8), 164 (35.4), 154 (49.2)
5	Phenylalanine Amadori	$[M-H]^-$ 326	12	Milled	326 (2.9), 236 (65.1), 164 (100)
			12	Milled + Heated	326 (6.5), 236 (58.7), 164 (100)

6	Phenylalanine Heyn's	$[M-H]^-$ 326	12	Milled	326 (5.3), 236 (5.6), 206 (100), 164 (15.7)
			12	Milled + Heated	326 (8.4), 236 (7), 206 (100), 164 (17)

Table 4.3 Elemental composition of significant product ions of glycated amino acids (ARPs & HRPs) during MS/MS with cysteine, histidine, and phenylalanine.

Amadori Compounds				**Heyns Compounds**			
#	***m/z***	**MF**	**Error (ppm)**	**#**	***m/z***	**MF**	**Error (ppm)**
	Cysteine				**Cysteine**		
1	282.0642	$C_9H_{16}NO_7S$	3.89	1	282.0651	$C_9H_{16}NO_7S$	0.7
2	238.0727	$C_8H_{16}NO_5S$	11.62	2	238.0746	$C_8H_{16}NO_5S$	3.64
3	248.0765	$C_9H_{14}NO_7$	4.33	3	204.0868	$C_8H_{14}NO_5$	4.64
4	204.0866	$C_8H_{14}NO_5$	5.62	4	192.0323	$C_6H_{10}NO_4S$	6.78
5	162.0222	$C_5H_8NO_3S$	5.17	5	174.0763	$C_7H_{12}NO_4$	5.06
6	119.0348	$C_4H_7O_4$	1.53	6	126.0558	$C_6H_8NO_2$	2.00
7	114.0558	$C_5H_8NO_2$	2.21	7	114.0556	$C_5H_8NO_2$	3.96
	Histidine				**Histidine**		
1	316.1139	$C_{12}H_{18}N_3O_7$	3.55	1	316.1148	$C_{12}H_{18}N_3O_7$	0.71
2	272.1245	$C_{11}H_{18}N_3O_5$	2.55	2	226.0828	$C_9H_{12}N_3O_4$	2.34
3	226.0825	$C_9H_{12}N_3O_4$	3.67	3	196.073	$C_8H_{10}N_3O_3$	1.2
4	196.072	$C_8H_{10}N_3O_3$	3.90	4	164.0828	$C_8H_{10}N_3O$	0.83
	Phenylalanine				**Phenylalanine**		
1	326.1255	$C_{15}H_{20}NO_7$	2.99	1	326.1214	$C_{15}H_{20}NO_7$	1.37
2	236.0939	$C_{12}H_{14}NO_4$	4.53	2	236.0893	$C_{12}H_{14}NO_4$	14.96
				3	206.0804	$C_{11}H_{12}NO_3$	9.06

The presence of a mixture of both Schiff bases and ARPs in a model sample can be attributed to the dynamic nature of the Maillard reaction and the interplay of various factors influencing reaction

kinetics and product formation. Schiff bases, the immediate precursors to ARPs, are generally considered less stable due to their susceptibility to hydrolysis and other degradation pathways. The stability of ARPs allows them to persist within the reaction mixture alongside Schiff bases, thereby giving rise to a heterogeneous blend of intermediates. The relative abundance of Schiff bases and ARPs can vary significantly depending on the specific conditions of the Maillard reaction, including factors such as pH, temperature, moisture content, and the chemical composition of the reactants. Xing et al. (9) provided an illustrative example of this variability, noting a prevalence of Schiff bases over ARPs when conducting experiments involving the milling of basic amino acids like histidine with glucose. Such observations underscore the nuanced interplay between the properties of the amino acids and their interactions with the reducing sugars, ultimately influencing the distribution of reaction intermediates. To differentiate between Schiff bases and ARPs within the reaction mixture, one can identify the presence of specific diagnostic ions corresponding to Schiff bases and ARPs through the analysis of mass spectral data obtained from mechanochemically reacted products. Specifically, the presence of a diose attached to the amino acid residue in the MS/MS spectrum serves as a diagnostic marker for Schiff bases, whereas a triose fragment suggests the formation of Amadori compounds (9). The proposed mechanism of MS/MS fragmentation of the molecular ion $[M-H]^-$ ions of glycated cysteine, histidine, and phenylalanine consistent with the proposed structures are shown in Figures 4.4 to 4.6.

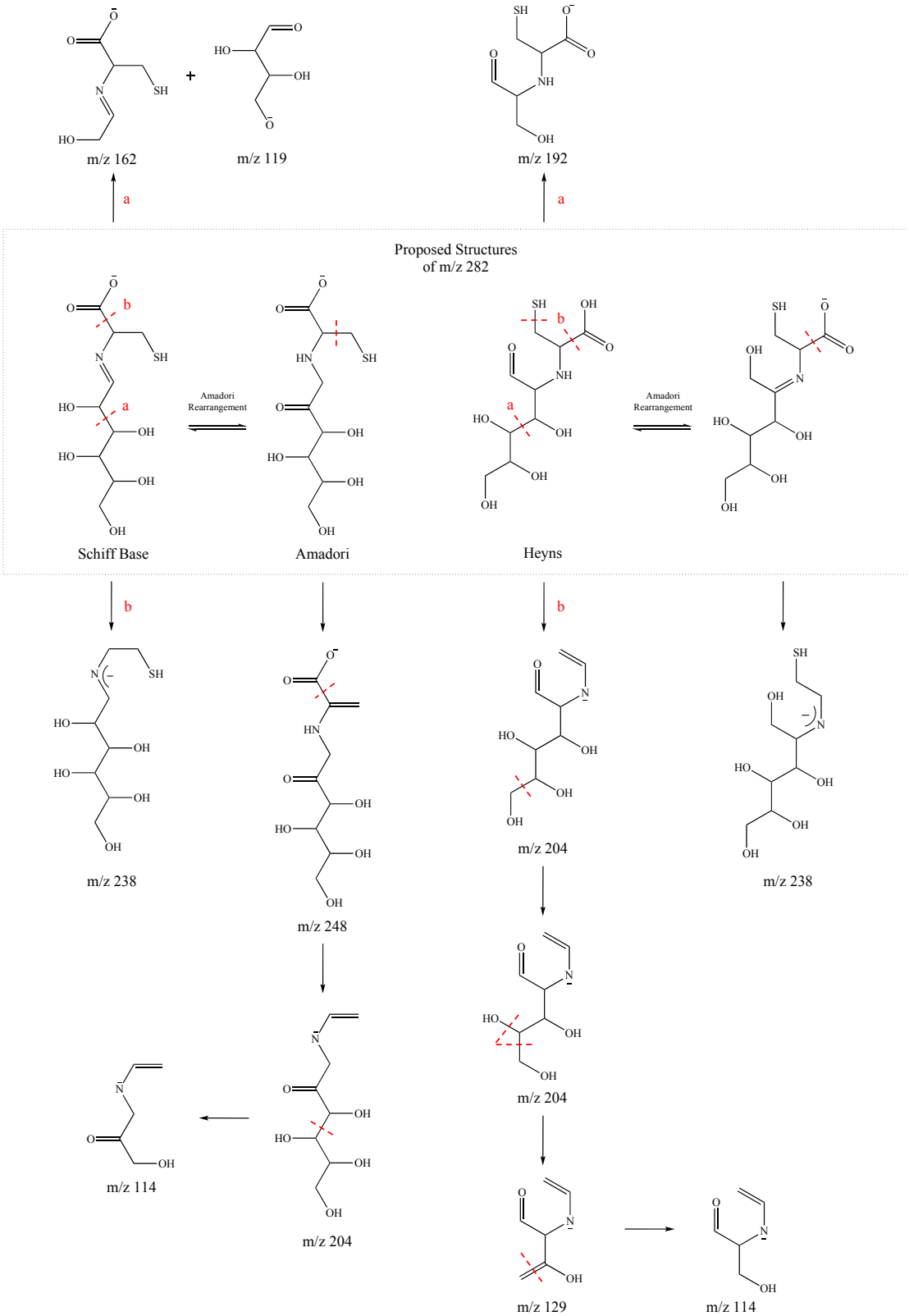

Figure 4.4 Proposed mechanism of MS/MS fragmentation of the molecular ion ($[M-H]^-$, *m/z* 282) of cysteine-ARP and cysteine-HRP, consistent with the proposed structures.

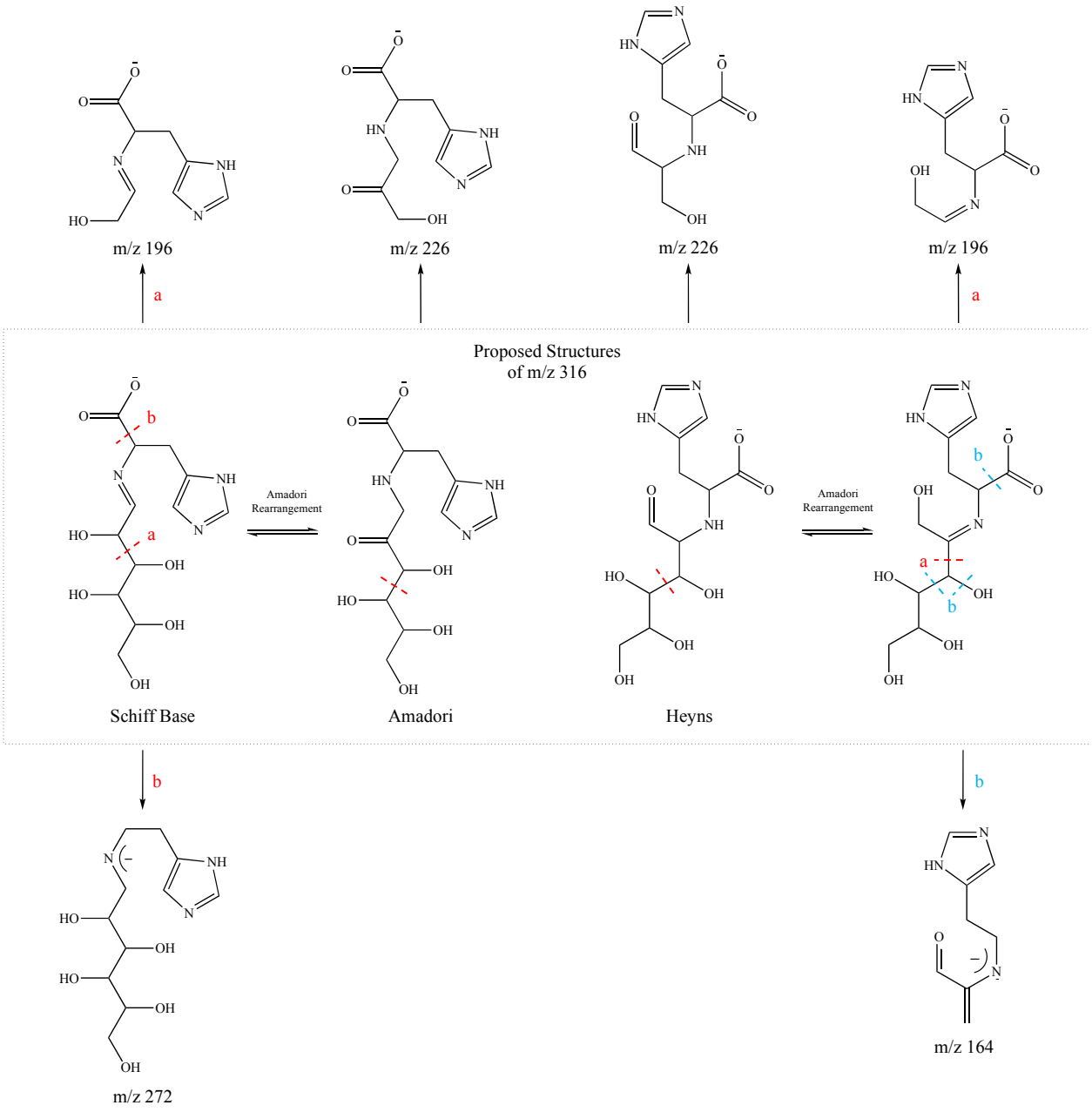

Figure 4.5 Proposed mechanism of MS/MS fragmentation of the molecular ion ($[M-H]^-$, *m/z* 282) of histidine-ARP and histidine-HRP, consistent with the proposed structures.

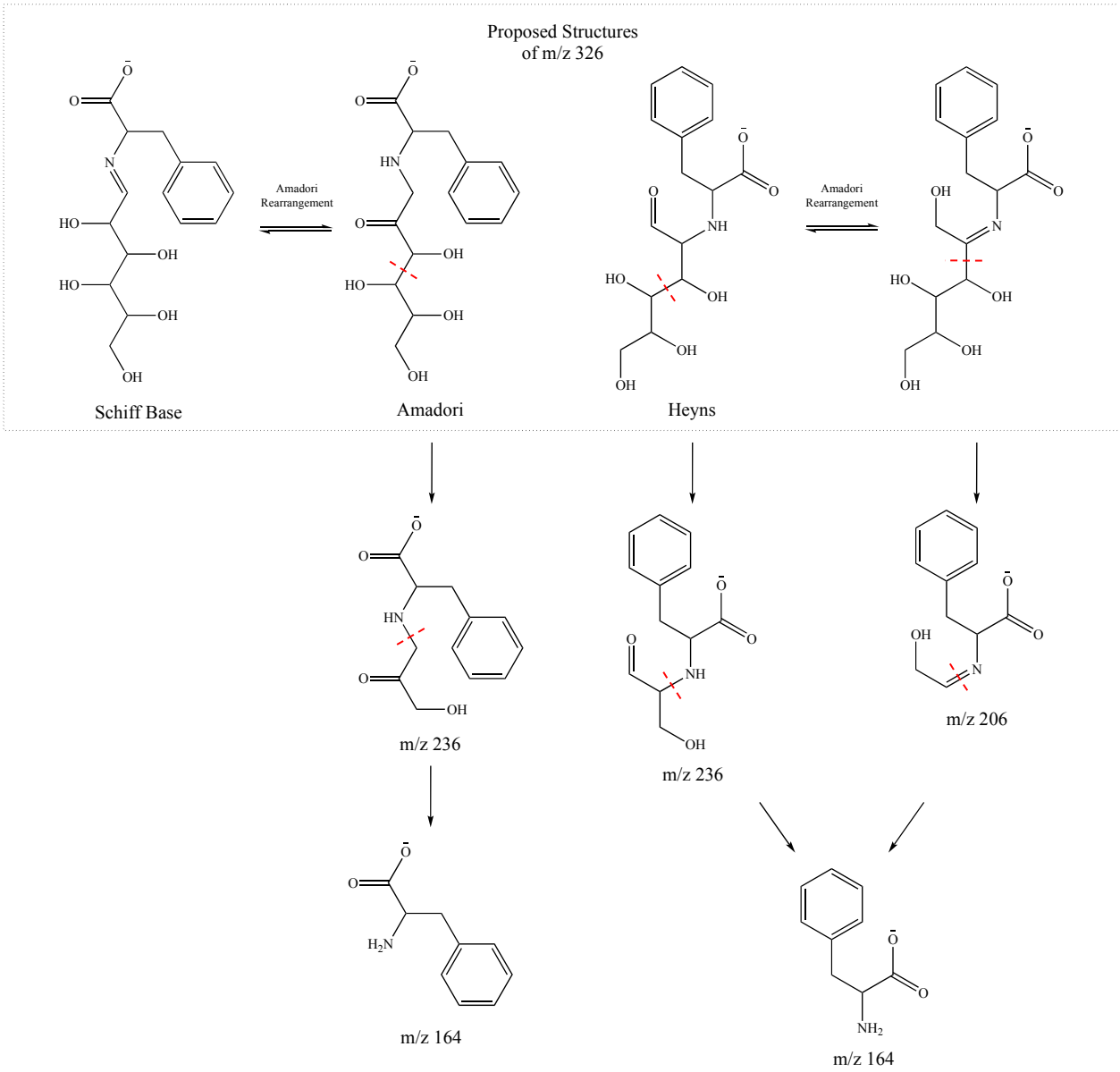

Figure 4.6 Proposed mechanism of MS/MS fragmentation of the molecular ion ($[M-H]^-$, *m/z* 282) of phenylalanine-ARP and phenylalanine-HRP, consistent with the proposed structures.

In the exploration of these intermediates, the formation of a 2-azaallyl anion generated through decarboxylation was observed across cys-ARP (*m/z* 238), cys-HRP (*m/z* 238), and his-ARP (*m/z* 272) model systems. This phenomenon, elucidated by Xing et al. (9), serves as a diagnostic ion for Schiff bases, indicating the presence or formation of these intermediates within the systems under study. Furthermore, the MS/MS spectra revealed the presence of fragmentation ions representing a triose attached to the amino acid moiety in cys-HRP, his-ARP, his-HRP, phe-ARP, and phe-HRP

spectra. This fragment results from the retro aldolization of the C3-C4 sugar chain. Conversely, another fragmentation ion representing a diose attached to the amino acid moiety was observed in the cys-ARP, his-ARP, his-HRP, and phe-HRP spectra, resulting from the retro aldolization of the C2-C3 sugar chain. Analysis of the mass spectral data generated under negative ionization mode of the fragmented characteristic ion $[M-H]^-$ of mechanochemically reacted glucose-histidine indicated the diagnostic ion of Schiff base at *m/z* 226 and ARP at *m/z* 196. This comprehensive characterization elucidates the coexistence of both intermediates within the reaction mixture, providing valuable insights into the intricate dynamics of the Maillard reaction under mechanochemical conditions.

Maillard reaction samples containing cysteine exhibit distinct behaviour characterized by reduced browning compared to other amino acids. This uniqueness stems from the inhibitory effect of cysteine on the Maillard reaction, attributed to the formation of 2-threityl-thiazolidine-4-carboxylic acid (TTCA). TTCA is formed through the intramolecular cyclization of the Schiff base, the dehydrated product of N-glucosyl cysteine (see Figure 4.7). The presence of TTCA limits or prevents the formation of cysteine Amadori compounds and their subsequent degradation into reactive α-dicarbonyls. Due to identical chemical compositions, MS techniques cannot differentiate these compounds alone. For instance, in a comparative study, Zhai et al. (10) analyzed the MS/MS spectra of purified cysteine-xylose ARP alongside its isomer TTCA, revealing identical fragmentation patterns. However, a unique fragment ion was observed in the MS/MS spectra of both cysteine Amadori and Heyns compounds. The fragment ion $[M-H-SH-COO]^-$ (*m/z* 204) signifies the formation of the cys-ARP (or cys-HRP) due to the specific decarboxylation and desulfurization of glycated cysteine involved in the generation of the ion. Furthermore, the additional retro-aldolization reaction of the C3-C4 sugar chain of the ion at *m/z* 204 results in the formation of $[M-H-SH-COO-C_3H_6O_3]^-$ (*m/z* 114), aiding in the identification of cysteine ARP.

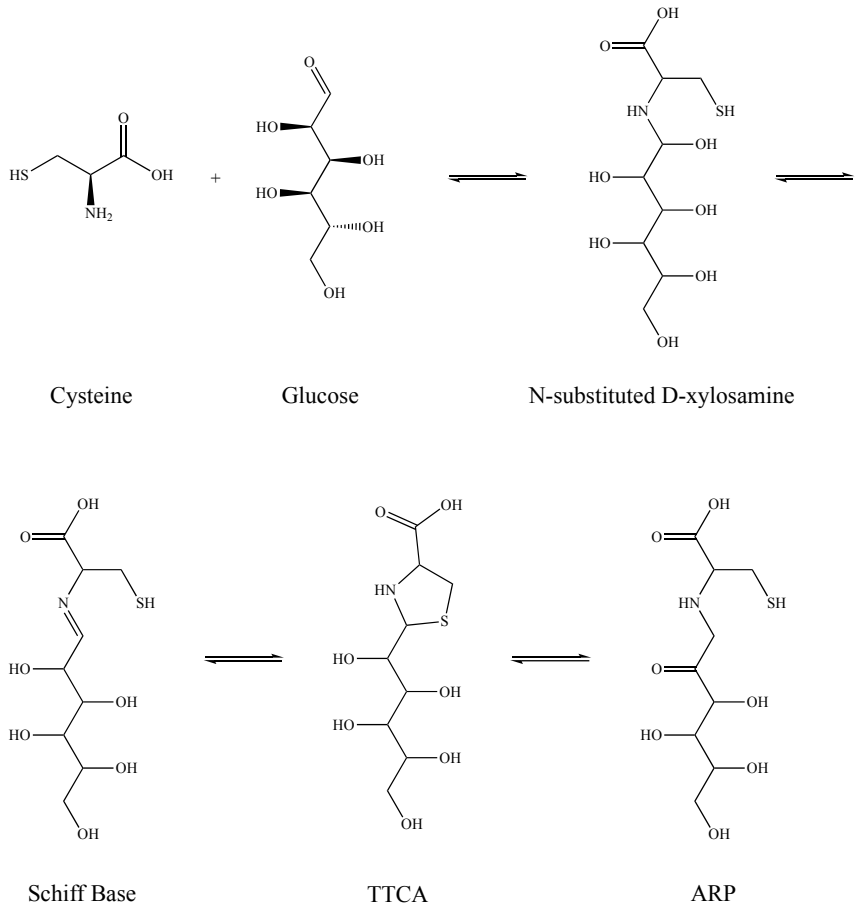

Figure 4.7 Schematic diagram of the Maillard reaction intermediate isomeric compounds (Schiff base, TTCA, and ARP) derived from cysteine-glucose systems

To mimic food conditions and observe degradation products, the mechanochemically generated ARPs were dissolved in water and heated in a closed vial in an oven at 120˚C for 1.5 hrs and then heated in an open vial to evaporate some water at 120˚C for 30 mins. The his-ARP and phe-ARP models had similar MS/MS fragmentation patterns when comparing the milled samples to the milled and heated samples (Table 4.2).

4.2.2 Comparison between ARP and HRP characteristic fragmentation patterns under negative ionization mode

Analytical discrimination between early Maillard reaction (MR) intermediates, such as the isomeric Schiff base, Amadori rearrangement product (ARP), and Heyns rearrangement product (HRP), poses a significant challenge despite extensive exploration of ARP fragmentation patterns

under both positive and negative ionization modes (6-8). While ARPs and HRPs share the same molecular formula, their distinct structural characteristics result in unique fragmentation patterns in MS/MS. To better understand the differences in the MS/MS spectra between ARPs and HRPs, their structural characteristics and specific fragmentation patterns were compared in Figure 4.8.

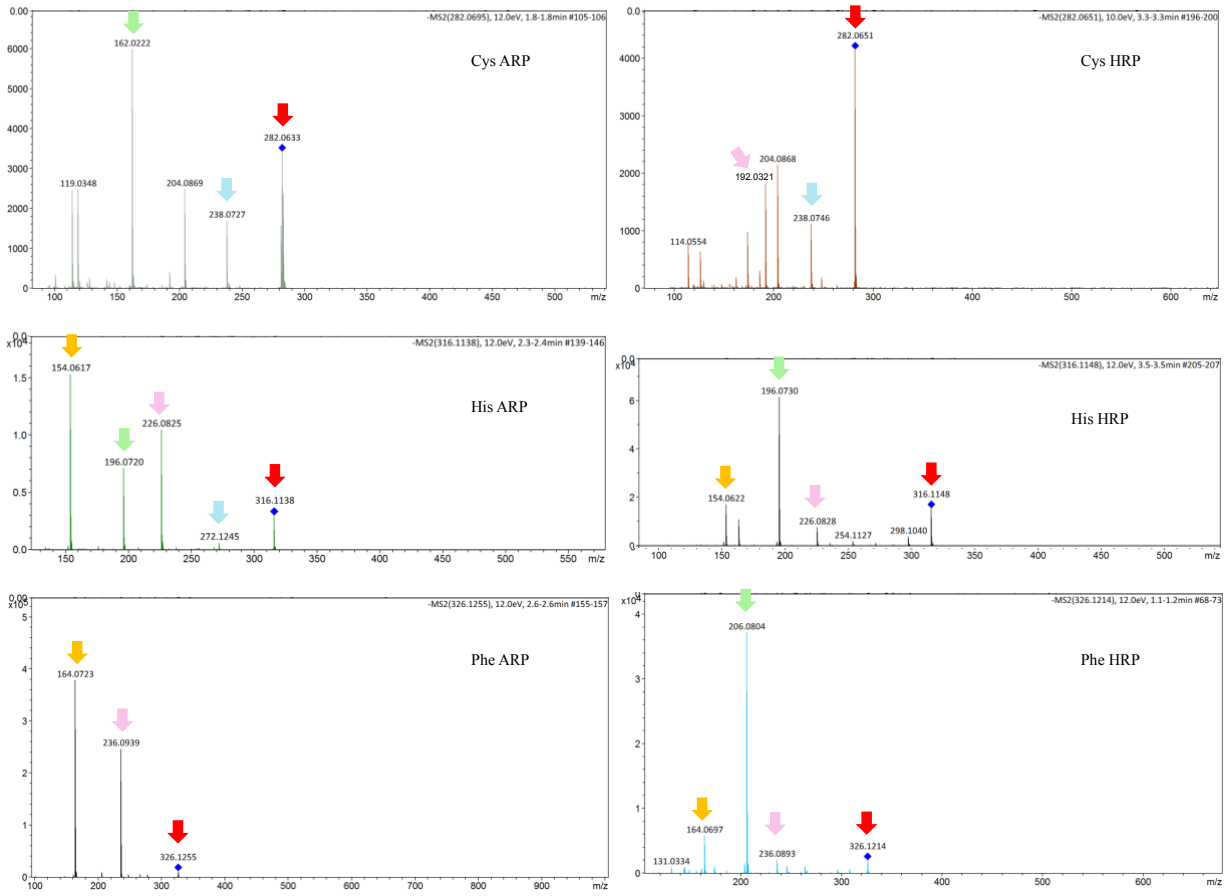

Figure 4.8 MS/MS fragmentation under ESI negative ionization mode of mechanochemically generated ARPs and HRPs. All the mechanochemical mixtures were prepared by ball mill glucose or fructose with the amino acid at a 1:1 M ratio for 30 min at 30 Hz. Diagnostic ions are identified with arrows, where the red arrows indicate the precursor ion; light blue arrows indicate the decarboxylated ARP or HRP; pink arrows indicate the amino acid with a triose; green arrows indicate the amino acid with a diose; and orange arrows indicate the amino acid. Proposed structures are based on elemental composition.

The MS/MS fragmentation pattern of ARPs reported in the literature observed cleavage of the sugar moiety between C1-C2 of the sugar, leaving a CH_2 unit attached to the amino acid (15, 25). However, the investigated conditions reported in the literature were in positive ionization mode. In contrast, under negative ionization mode, the most abundant peak in the his-ARP and phe-ARP models generated through β-elimination of the sugar moiety were the ions at *m/z* 154 and *m/z* 164, respectively. Furthermore, as previously mentioned, Xing et al. (9) proposed a diagnostic ion of ARPs to be a triose attached to the amino acid residue. The histidine and phenylalanine equivalents were the next abundant ions in their ARP MS/MS spectra at *m/z* 226 and *m/z* 236, respectively. The ions were present in the HRPs MS/MS spectra; however, they were present at significantly lower relative abundances. Therefore, it is a good candidate as a diagnostic ion for ARP.

Despite its structural differences from the Amadori rearrangement product (ARP), the Heyns rearrangement product (HRP) exhibits an MS/MS fragmentation pattern that is partially similar to ARP, evident in the presence of dehydration peaks and partially similar to the Schiff base (25). For example, its resemblance to the Schiff base was indicated by the detection of the ion at *m/z* 208 ($C_9H_{10}N_3O_3^-$) in the his-HRP MS/MS spectrum, although at a low relative intensity of 2%. It incorporates intact histidine with three carbon unit originating from the sugar. This structure is generated through retro-aldol cleavage of the Schiff base of fructose with histidine at the C3–C4 position. However, the base peak in the his-HRP MS/MS spectrum was observed to be the ion at *m/z* 196, signifying its stability and, consequently, its tendency to accumulate relative to the other fragments. It is generated through C2–C3 retro aldolization of the open form of the Heyns product. Thus, its presence indicates the predominance of the open form of the Heyns product under MS/MS analytical conditions.

The MS/MS fragmentation pattern of his-HRP was in accordance with those reported in the literature (26). The ion fragments at *m/z* 298 and 254 were formed by $[M-H]^-$ ion (*m/z* 316) removing a molecule of water and decarboxylation ($-COO^-$) in succession under ion bombardment. The ion *m/z* 254 could continue to lose $C_2H_4O_2$ and then CH_2O sequentially to form *m/z* 194 and *m/z* 164. Interestingly, Xing et al. (25) reported a characteristic fragment ion from MS/MS of glycine-HRP at *m/z* 84 formed by the loss of a three-carbon sugar moiety, a water molecule, and a carboxylic acid $[M-H-C_3H_6O_3-H_2O-COOH]^-$, which was absent from the MS/MS of its ARP and

can be considered a diagnostic ion for HRPs. The histidine-HRP equivalent of this ion was identified at *m/z* 164 ($C_8H_{10}N_3O^-$). This ion was not observed in the his-ARP spectrum, which confirms its potential as a diagnostic ion for HRPs. The phenylalanine-HRP equivalent of this ion was also observed in its spectrum at *m/z* 174 ($C_{11}H_{12}NO^-$), although at a low relative intensity of 3.1%. Furthermore, the cysteine equivalent of this ion was also present in the model system of cys-HRP at *m/z* 130 ($C_5H_8NOS^-$) at a relative intensity of 3.2%. The ions were not present in the ARP spectra.

The molecular ions obtained from mechanochemically generated Amadori and Heyns products of cysteine, histidine, and phenylalanine under ESI negative ionization mode generated some consistent MS/MS fragmentation ions (see Figure 4.8). The histidine and phenylalanine glycated models behaved similarly, whereas the cysteine glycated model exhibited distinct behaviour. In both the his-HRP and phe-HRP models, ion corresponding to a diose attached to the amino acid residue, was the most abundant peak. In the cys-HRP model, the molecular ion peak was the most abundant. In contrast, the most abundant peaks for the his-ARP and phe-ARP models corresponded to the amino acid peaks. In the cys-ARP model, the most abundant peak corresponded to the diose attached to the amino acid residue (*m/z* 162); its complementary four-carbon sugar fragment at *m/z* 119 was also observed. Both ions were absent in the cys-HRP model spectra. As mentioned, the base peak in the phe-HRP MS/MS spectrum was observed to be the ion at *m/z* 206, signifying its stability and, consequently, its tendency to accumulate relative to the other fragments. It can be generated through C2–C3 retroaldolization of the open form of the Heyns product. It is proposed as a diagnostic ion for phe-HRP as it is also not present in the ARP spectrum.

The MS/MS fragmentation patterns of the various glycated amino acids helped confirm that the corresponding ARPs and HRPs were generated in the reaction mixtures. While certain diagnostic ions were produced through ESI negative ionization mode, their value resided in their notably different relative intensities. The characteristic ions proposed are either uniquely present in a sample or significantly differ in their relative abundances.

4.3 References

1. Urban, P. L. Quantitative Mass Spectrometry: An Overview. *Philos. Trans. R. Soc. A* **2016**, *374*(2079), 20150382. DOI: 10.1098/rsta.2015.0382
2. Yeboah, F. K.; Yaylayan, V. A. Analysis of Glycated Proteins by Mass Spectrometric Techniques: Qualitative and Quantitative Aspects. *Food/Nahrung* **2001**, 45(3), 164–171.
3. Yaylayan, V.; Sporns, P. Electron Impact Spectra of 1-(Amino Acid)-1-Deoxy-D-Fructoses. *Org. Mass Spectrom.* **1988**, *23*, 849-850. DOI: 10.1002/oms.1210231211
4. Kislinger, T.; Humeny, A.; Seeber, S.; Becker, C. M.; Pischetsrieder, M. Qualitative Determination of Early Maillard-Products by MALDI-TOF Mass Spectrometry Peptide Mapping. Eur. Food Res. Technol **2002**, *215*, 65-71.
5. Ruan, D.L.; Wang, H.; Cheng, F.L. MS Charaterization of ARPs. In *The Maillard Reaction in Food Chemistry Current Technology and Applications*; Parisi, S., Ed.; Springer: Berlin, Germany, **2018**.
6. Hau, J.; Devaud, S.; Blank, I. Detection of Amadori Compounds by Capillary Electrophoresis Coupled to Tandem Mass Spectrometry. *Electrophoresis* **2004**, *25*, 2077-2083. DOI: 10.1002/elps.200405958
7. Davidek, T.; Kraehenbuehl, K.; Devaud, S.; Robert, F.; Blank, I. Analysis of Amadori Compounds by High-Performance Cation Exchange Chromatography Coupled to Tandem Mass Spectrometry. *Anal. Chem*. **2005**, *77*(1), 140-147.
8. Wang, J.; Lu, Y. M.; Liu, B. Z.; He, H. Y. Electrospray Positive Ionization Tandem Mass Spectrometry of Amadori Compounds. *J. Mass Spectrom.* **2008**, *43*(2), 262-264.
9. Xing, H.; Yaylayan, V. Mechanochemical Generation of Schiff Bases and Amadori Products and Utilization of Diagnostic MS/MS Fragmentation Patterns in Negative Ionization Mode for their Analysis. *Carbohydr. Res*. **2020**, *495*, 108091. DOI: 10.1016/j.carres.2020.108091
10. Zhai, Y.; Cui, H.; Hayat, K.; Hussain, S.; Tahir, M. U.; Deng, S.; Zhang, Q.; Zhang, X.; Ho, C. T. Transformation between 2-Threityl-Thiazolidine-4-Carboxylic Acid and Xylose-Cysteine Amadori Rearrangement Product Regulated by pH Adjustment during High-Temperature Instantaneous Dehydration. *J. Agric. Food Chem*. **2020**, *68*(39), 10884–10892. DOI: 10.1021/acs.jafc.0c04287

11. Yang, Y.; Cui, S.W.; Gong, J.; Guo, Q.; Wang, Q.; Hua, Y. A Soy Protein-Polysaccharides Maillard Reaction Product Enhanced the Physical Stability of Oil-in-Water Emulsions Containing Citral. *Food Hydrocoll*. **2015**, *48*, 155–164.
12. Liu, Q.; Kong, B.; Han, J.; Sun, C.; Li, P. Structure and Antioxidant Activity of Whey Protein Isolate Conjugated with Glucose via the Maillard Reaction under Dry-Heating Conditions. *Food Struct*. **2014**, *1*, 145–154.
13. Wong, B. T.; Day, L.; McNaughton, D.; Augustin, M. A. The Effect of Maillard Conjugation of Deamidated Wheat Proteins with Low Molecular Weight Carbohydrates on the Secondary Structure of the Protein. *Food Biophys*. **2009**, *4*, 1-12.
14. Kędzierska-Matysek, M.; Matwijczuk, A.; Florek, M.; Barłowska, J.; Wolanciuk, A.; Matwijczuk, A.; Chruściel, E.; Walkowiak, R.; Karcz, D.; Gładyszewska, B. Application of FTIR Spectroscopy for Analysis of the Quality of Honey. In *BIO Web of Conferences* **2008**, *10*, 02008
15. Yuan, H.; Sun, L.; Chen, M.; Wang, J. The Comparison of the Contents of Sugar, Amadori, and Heyns Compounds in Fresh and Black garlic. *J. Food Sci.* **2016**, *81*(7), C1662-C1668.
16. Wnorowski, A.; Yaylayan, V. A. Monitoring Carbonyl-Amine Reaction between Pyruvic Acid and α-Amino Alcohols by FTIR Spectroscopy a Possible Route to Amadori Products. *J. Agric. Food Chem*. **2003**, *51*(22), 6537-6543.
17. Pawlukojc, S.; Leciejewicz, J.; Ramirez-Cuesta, A. J.; Nowicka-Scheibe, J. L-cysteine: Neutron Spectroscopy, Raman, IR and Ab Initio Study. *Spectrochim*. *Acta A* **2005**, *61* 2474–81
18. Barth, A. The Infrared Absorption of Amino Acid Side Chains. *Prog. Biophys. Mol. Biol.* **2000**, *74*(3-5), 141-173. DOI: 10.1016/S0079-6107(00)00021-3
19. Susi, H.; Byler, D.; Gerasimowicz, W. V. Vibrational Analysis of Amino Acids: Cysteine, Serine, β-Chloroalanine. *J. Mol. Struct.* **1983**, *102*(1-2), 63-79. DOI: 10.1016/0022-2860(83)80007-6
20. Colthup, N. B.; Daly, L. H.; Wiberley, S. E. Aromatic and Heteroaromatic Rings. *Introduction to Infrared and Raman Spectroscopy (Second Edition)*, 1975; pp 257-277. DOI: 10.1016/B978-0-12-182552-2.50011-5
21. López, M. G.; Gruenwedel, D. W. Synthesis of Aromatic Amadori Compounds. Carbohydrate Research **1991**, *212*, 37-45. DOI: 10.1016/0008-6215(91)84043-E

22. Hasegawa, K.; Ono, T. A.; Noguchi, T. Vibrational Spectra and Ab Initio DFT Calculations of 4-Methylimidazole and Its Different Protonation Forms: Infrared and Raman Markers of the Protonation State of a Histidine Side Chain. J. Phys. Chem. B **2000**, *104*(17), 4253-4265.
23. Ibrahim, M.; Alaam, M.; El-Haes, H.; Jalbout, A. F.; Leon, A. D. Analysis of the Structure and Vibrational Spectra of Glucose and Fructose. *Ecletica quimica* **2006**, *31*, 15-21.
24. Venyaminov, S.Y.; Kalnin, N.N. Quantitative IR spectrophotometry of Peptide Compounds in Water (H_2O) Solutions. I. Spectral Parameters of Amino Acid Residue Absorption Bands. *Biopolymers* **1990**, *30*,1243-1257. DOI: 10.1002/bip.360301309
25. Xing, H.; Mossine, V. V.; Yaylayan, V. Diagnostic MS/MS fragmentation patterns for the Discrimination Between Schiff bases and their Amadori or Heyns Rearrangement Products. *Carbohydrate Research* **2020**, *491*, 107985. DOI: 10.1016/j.carres.2020.107985
26. Li, K.; Wang, J.; Zhuang, Y.; Yuan, G.; Li, Y.; Zhu, X. Glucose-Histidine Heyns Compound: Preparation, Characterization and Fragrance Enhancement. *Carbohydrate Research* **2023**, *532*, 108922. DOI: 10.1016/j.carres.2023.108922
27. Ji, Y.; Yang, X.; Ji, Z.; Zhu, L.; Ma, N.; Chen, D.; Cao, Y. DFT-Calculated IR spectrum Amide I, II, and III Band Contributions of N-methylacetamide Fine Components. *ACS omega* **2020**, *5*(15), 8572-8578.

Chapter 5. Reaction of Glycated Amino Acids with Free Sugars: Formation of Diglycated Amino Acids

The formation and identification of diglycated amino acids through mechanochemistry coupled with MS/MS analysis were explored. The results are elucidated through detailed MS/MS analysis, focusing on the fragmentation patterns and diagnostic ions that distinguish between different isomeric forms of diglycated amino acids. The combination of mechanochemical synthesis and mass spectrometric analysis provides a robust system for studying these complex molecules, revealing their formation mechanisms and structural intricacies.

5.1 Generation and Identification of Diglycated Amino Acids Using Mechanochemistry and MS/MS

Amadori products derived from primary amines are known to react with a second reducing sugar to form diglycated amino acids due to the nucleophilicity of the secondary amino groups. Diglycated amino acids have been observed to undergo decomposition more readily in aqueous conditions compared to monoglycated amino acids, producing reactive intermediates (4). This phenomenon aligns with Xing and Yaylayan (1), who observed that under hydrothermal conditions in water (50% w/v) at 120˚C for one hour, the reaction mixture predominantly contained unreacted sugar, with minimal amounts of monoglycated glycine and no indication of any diglycated adducts. Mechanochemistry emerged as a valuable alternative, as reactions under ball-milling conditions retain reactive intermediates due to shorter timescales, near-room temperature, and solvent-free conditions. Solid-state reaction induced by ball-milling (30Hz/30mins) of an amino acid with glucose leads to significant formation of monoglycated amino acids, as detailed in Chapter 4. Furthermore, it was observed that the free sugar could react further during ball milling, although at reduced levels, to produce diglycated amino acids (Figures 5.1 and 5.2). To increase the yield of diglycated amino acids in a mixture, mechanochemically and thermochemically reacting free glucose with the mechanochemically generated ARP was explored (see Figures 5.3 to 5.5).

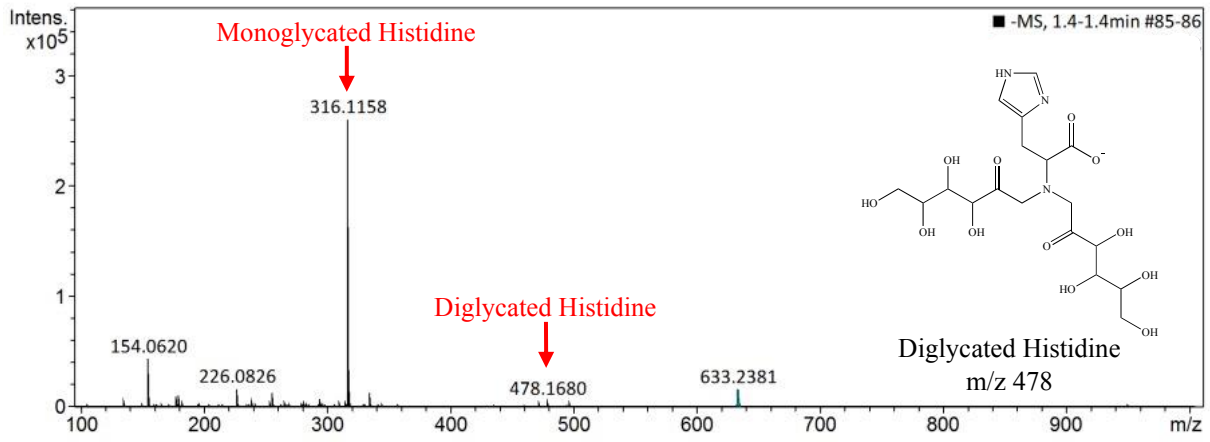

Figure 5.1 ESI (-ve) MS spectrum of ball milled (30mins/30Hz) histidine-glucose (1:1)

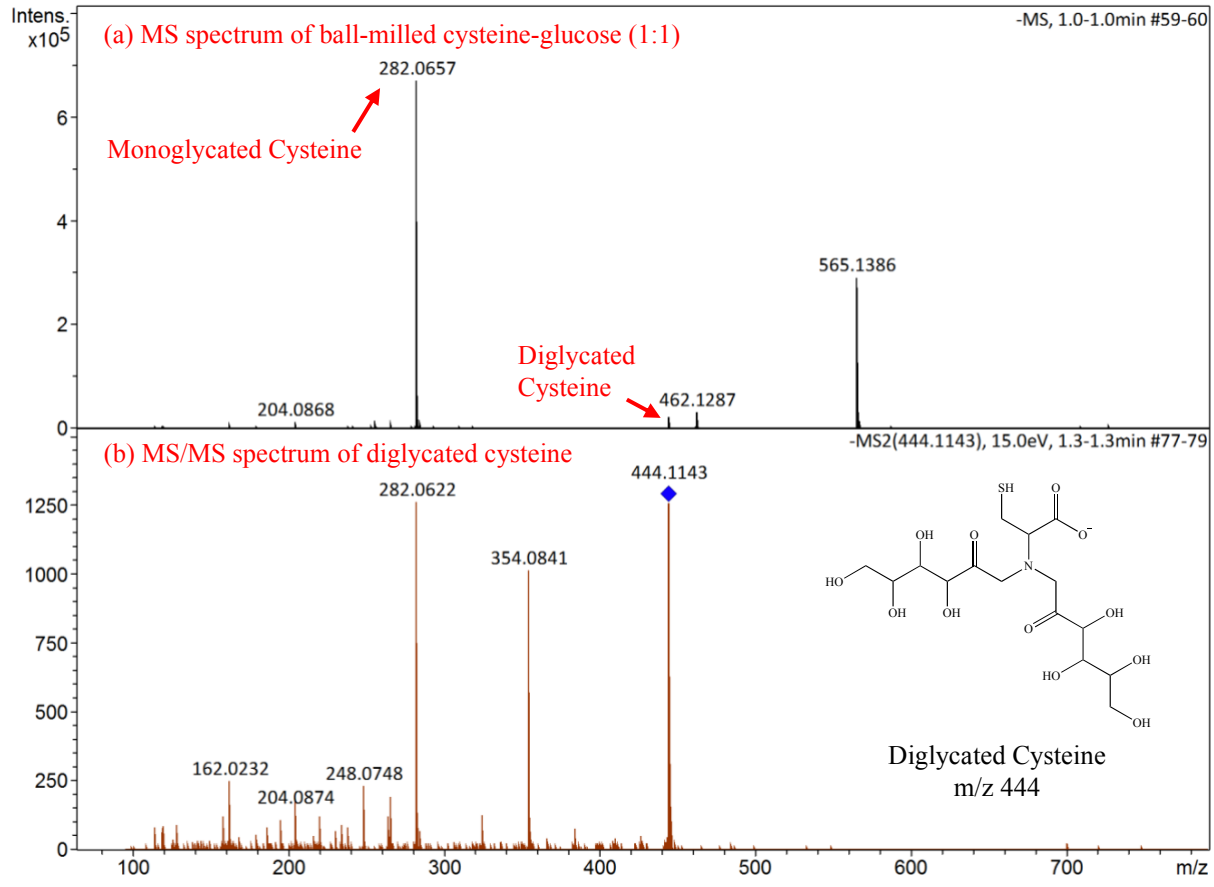

Figure 5.2 MS and MS/MS spectra in negative ionization mode of (a) heated ball-milled cysteine-glucose (1:1) and (b) diglycated cysteine at *m/z* 444. The reaction mixture was prepared at a 1:1 molar ratio and ball milled for 30 min at 30 Hz, followed by dissolution in H_2O. Subsequently, it

was heated in a closed vial in an oven for 1.5 hours at 120˚C and then for 30 minutes in an open vial in a sand bath at 120˚C.

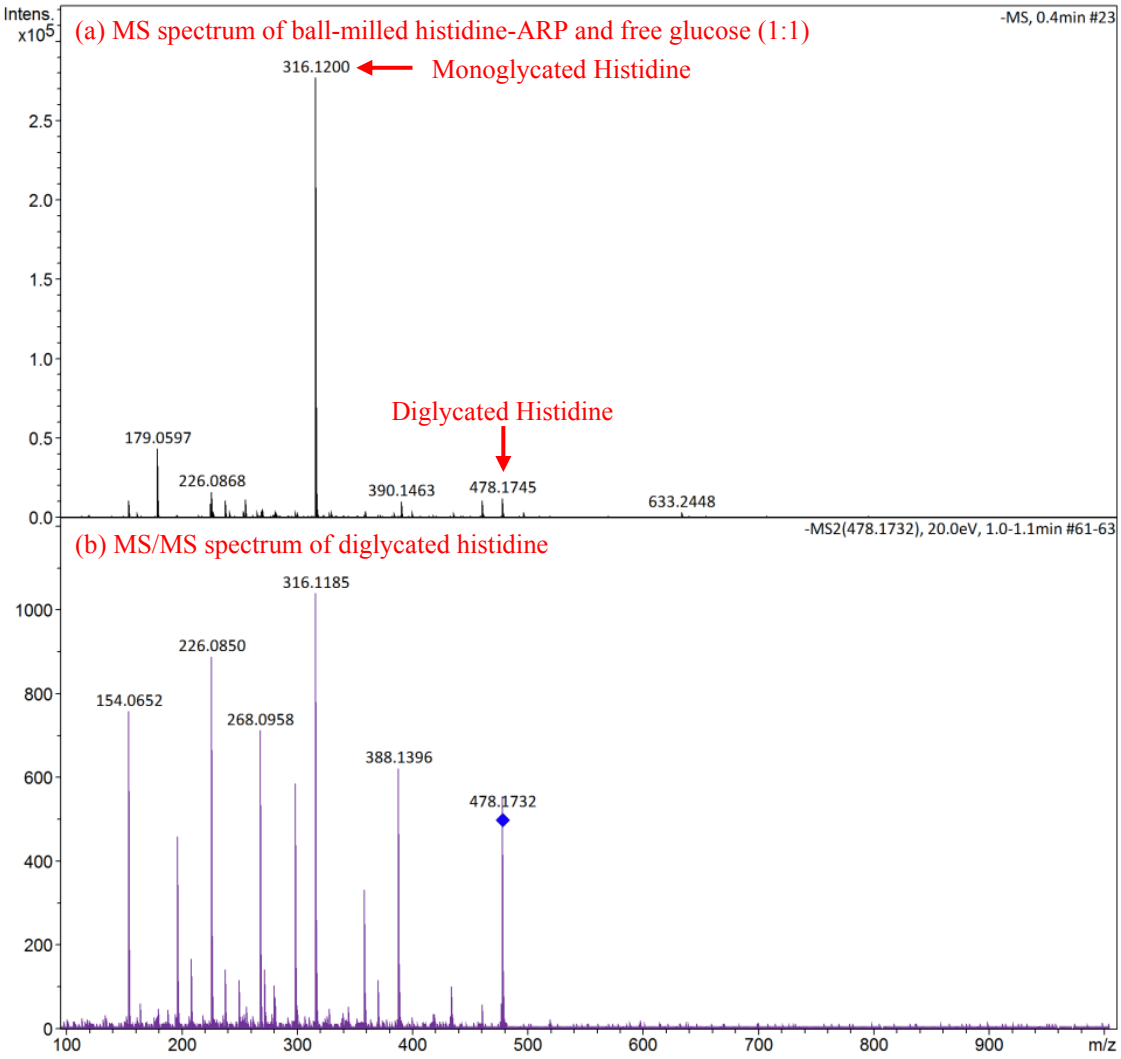

Figure 5.3 MS and MS/MS spectra in negative ionization mode of (a) ball-milled histidine-ARP and free glucose (1:1) and (b) diglycated histidine at *m/z* 478. The reaction mixture was prepared at a 1:1 molar ratio and ball-milled for 30 minutes at 30 Hz.

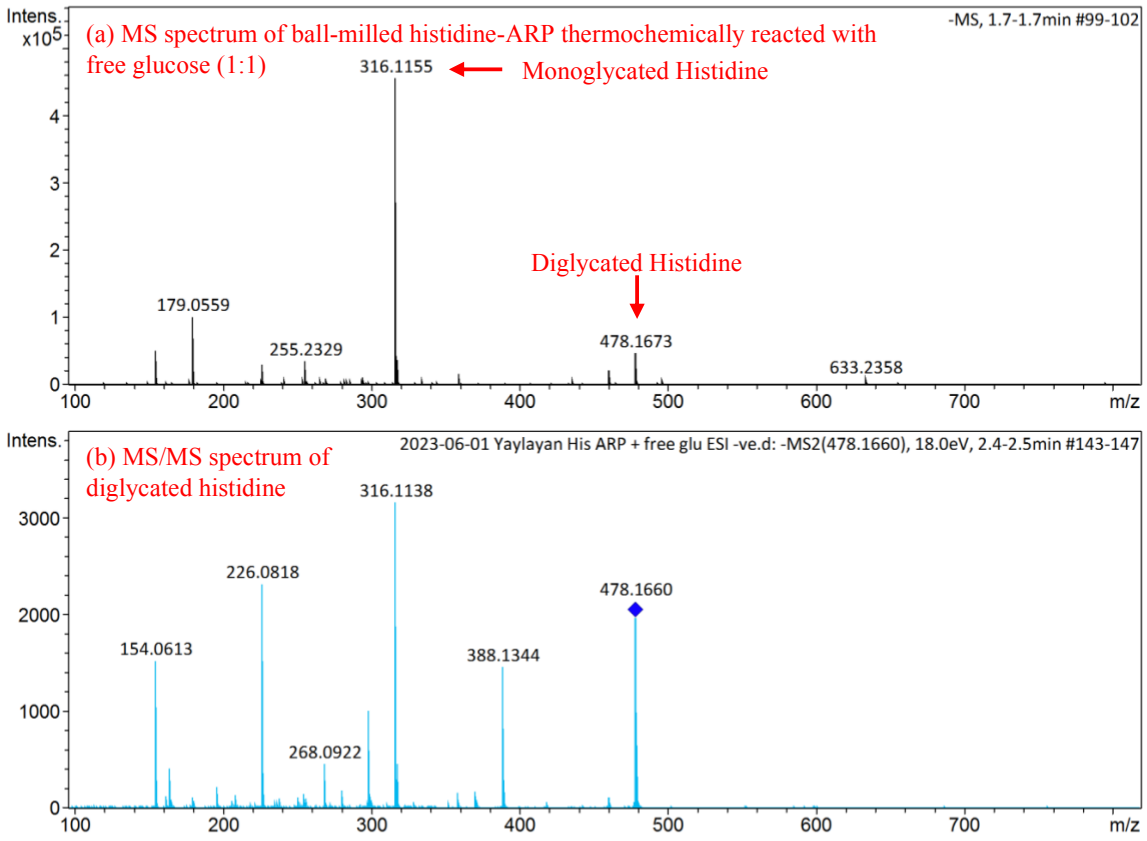

Figure 5.4 MS and MS/MS spectra in negative ionization mode of (a) histidine-ARP thermochemically reacted with free glucose (1:1) and (b) diglycated histidine at *m/z* 478. The reaction mixture was prepared at a 1:1 molar ratio and dissolved in H_2O. Subsequently, it was heated in a closed vial in an oven for 1.5 hours at 120˚C and then for 30 minutes in an open vial in a sand bath at 120˚C.

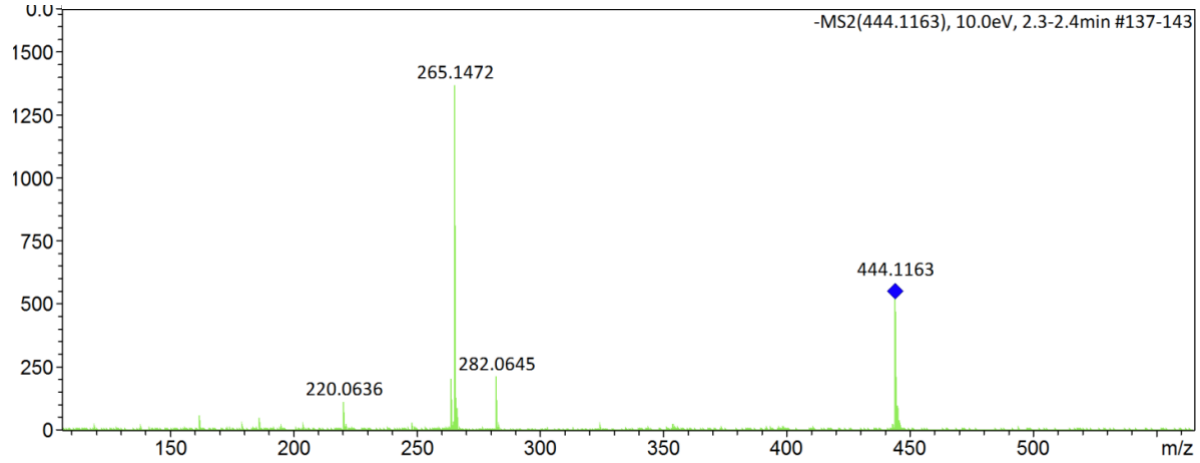

Figure 5.5 MS/MS spectrum in negative ionization mode of diglycated cysteine at *m/z* 444 formed during the thermochemical reaction of cys-ARP with free glucose. The reaction mixture was prepared at a 1:1 molar ratio and dissolved in H_2O. Subsequently, it was heated in a closed vial in an oven for 1.5 hours at 120˚C and then for 30 minutes in an open vial in a sand bath at 120˚C.

Maillard reaction mixtures generate diverse compounds, including numerous isomeric forms, notably of glycated amino acids. Excluding stereoisomers, regioisomers, anomers, and various conformations and open-chain structures, most amino acids can form two monoglycated (i.e., Schiff base and ARP) and three N, N-diglycated isomers (i.e., Schiff-Schiff, ARP-ARP, and ARP-Schiff) (1). In solutions, these isomers can undergo tautomeric isomerization, leading to diverse anomeric configurations, such as α- and β-furanoses and pyranoses, as well as unique spirobicyclic structures where one carbohydrate unit exists in acyclic form (5). Mossine et al. (12) provided comprehensive structural insights into N, N-difructosyl glycine in crystalline and aqueous states, determining that the major tautomeric form features at least one sugar moiety in an open chain conformation, accounting for its greater instability compared to mono-glycated glycine. The isomeric compositions of diglycated amino acids can be elucidated by analyzing their MS/MS fragmentation pattern, utilizing characteristic MS/MS fragmentations and diagnostic ions outlined in Chapter 4 for ARPs and Schiff bases. Specifically, an amino acid moiety linked to two-carbon atom residues from the sugar in the MS/MS spectrum serves as a diagnostic marker for Schiff bases (6, 9). In contrast, an amino acid moiety linked to three-carbon atom residues from the sugar suggests the formation of Amadori compounds (6, 9). These ions arise from either the sugar chain cleavage at C2–C3 in the Schiff bases or at C3–C4 in the ARP. Thus, through structural insights

and MS/MS fragmentation analysis, the presence and composition of diglycated amino acid isomers generated within Maillard reaction mixtures, including Schiff-Schiff, ARP-ARP, and ARP-Schiff, can be discerned, further enriching our understanding of the molecular intricacies underlying Maillard reactions. Fragmentation of the deprotonated molecular ion $[M-H]^-$ are summarized in Table 5.1, alongside the elemental composition of significant product ions outlined in Table 5.2.

Table 5.1 MS/MS spectral data of diglycated amino acids and their significant and diagnostic ions.

#	**Compound**	**Precursor ion $[M-H]^-$ (*m/z*)**	**CID voltage (eV)**	**Significant fragment ions in MS/MS spectra $[M-X]^-$, *m/z* (rel. int)**
1	Histidine ARP + Free Glucose	$[M-H]^-$ 478	20	478 (46.2), 434 (9.9), 388 (60), 358 (27.5), 316 (100), 298 (56.5), 272 (13.7), 268 (68.5), 238 (12.8), 226 (85.5), 196 (44.2), 154 (72.9)
			18	478 (62.2), 388 (46), 358 (5.1), 316 (100), 298 (31.7), 268 (14.4), 226 (73.3), 196 (7.1), 154 (48)
2	Cysteine ARP + Free Glucose	$[M-H]^-$ 444	15	444 (37.7), 282 (15.5), 265 (100), 264 (14.7), 220 (8.3)

Table 5.2 Elemental composition of significant product ions of diglycated amino acids during MS/MS in negative ionization mode with histidine and cysteine.

#	*m/z*	MF	Error (ppm)
	Histidine		
1	478.166	$C_{18}H_{28}N_3O_{12}$	3.86
2	434.1799	$C_{17}H_{28}N_3O_{10}$	4.34
3	388.1344	$C_{15}H_{22}N_3O_9$	4.52
4	358.1286	$C_{14}H_{20}N_3O_8$	8.41
5	316.1138	$C_{12}H_{18}N_3O_7$	3.87
6	298.1034	$C_{12}H_{16}N_3O_6$	3.55
7	272.128	$C_{11}H_{18}N_3O_5$	10.31
8	268.0922	$C_{11}H_{14}N_3O_5$	6.32
9	238.0849	$C_{10}H_{12}N_3O_4$	6.60
10	226.0818	$C_9H_{12}N_3O_4$	6.77
11	196.0727	$C_8H_{10}N_3O_3$	0.33
12	154.0613	$C_6H_8N_3O_2$	5.84
	Cysteine		
1	444.1163	$C_{15}H_{26}NO_{12}S$	1.07
2	282.0645	$C_9H_{16}NO_7S$	2.82
4	264.0526	$C_9H_{14}NO_6S$	8.07
5	220.0636	$C_8H_{14}NO_4S$	5.92

5.2 Characteristic MS/MS fragmentations of diglycated amino acids

The formation of diglycated histidine results in the detection of an ion $[M-H]^-$ at *m/z* 478, with its corresponding MS/MS fragmentation pathway illustrated in Figure 5.6. Notably, the ion observed at *m/z* 316 represents the base peak in the diglycated histidine MS/MS spectra shown in Figures 5.3 and 5.4. This fragmentation corresponds to the loss of a sugar moiety through β-elimination, which can occur in the ARP or Schiff base isomeric forms (Figure 5.6). Further analysis of the mass spectral data indicated the presence of diagnostic ions of Schiff base at *m/z* 226 [$C_9H_{12}N_3O_4$]

and of ARP at *m/z* 196 [$C_8H_{10}N_3O_3$], corresponding to the results reported by Xing et al. (9). The difference between the diagnostic ions of the two isomers arises from the specific cleavage pattern of the sugar chain in both structures. During the fragmentation of a diglycated amino acid, the sugar moiety can undergo cleavage at various positions, contingent upon whether the molecule exists in the Schiff base isomeric form or its ARP counterpart. This variation in cleavage positions leads to unique diagnostic ions, allowing for the discrimination between the two isomeric forms. According to findings by Xing et al. (10), in a diglycated amino acid model where both sugars are in Schiff base form (Schiff-Schiff), the diagnostic ion would correspond to a structure comprising the intact amino acid with two sugar carbons attached to the amino group. The diglycated histidine equivalent was observed at *m/z* 238 [$C_{10}H_{12}N_3O_4$] and was observed only under 20 eV fragmentation. The diagnostic ion of the ARP-ARP diglycated histidine isomer, consisting of histidine with two attached three-carbon chains, was observed at *m/z* 298 [$C_{12}H_{16}N_3O_6$]. Whereas the diagnostic ion consistent with the ARP-Schiff diglycated histidine isomer at *m/z* 268 [$C_{11}H_{14}N_3O_5$] corresponds to histidine decorated with three-carbon and two-carbon chains. According to Xing et al. (6), the ion at *m/z* 358 [$C_{14}H_{20}N_3O_8$] serves as a diagnostic ion for both Schiff-Schiff and ARP-Schiff isomers, which corresponds to a histidine moiety with an intact glucose and a two-carbon chain attached to the amino group. Conversely, the ion at *m/z* 388 [$C_{15}H_{22}N_3O_9$] can be a diagnostic ion for both ARP-ARP and ARP-Schiff base, corresponding to a histidine moiety with glucose and a three-carbon chain attached to the amino group. A 2-azaallyl anion generated through decarboxylation was formed only under 20 eV fragmentation at *m/z* 434 [$C_{17}H_{28}N_3O_{10}$], present at a relative intensity of 9.9. Xing et al. (9) suggested that this ion serves as a diagnostic ion for Schiff bases, indicating the presence or formation of these intermediates within the studied systems.

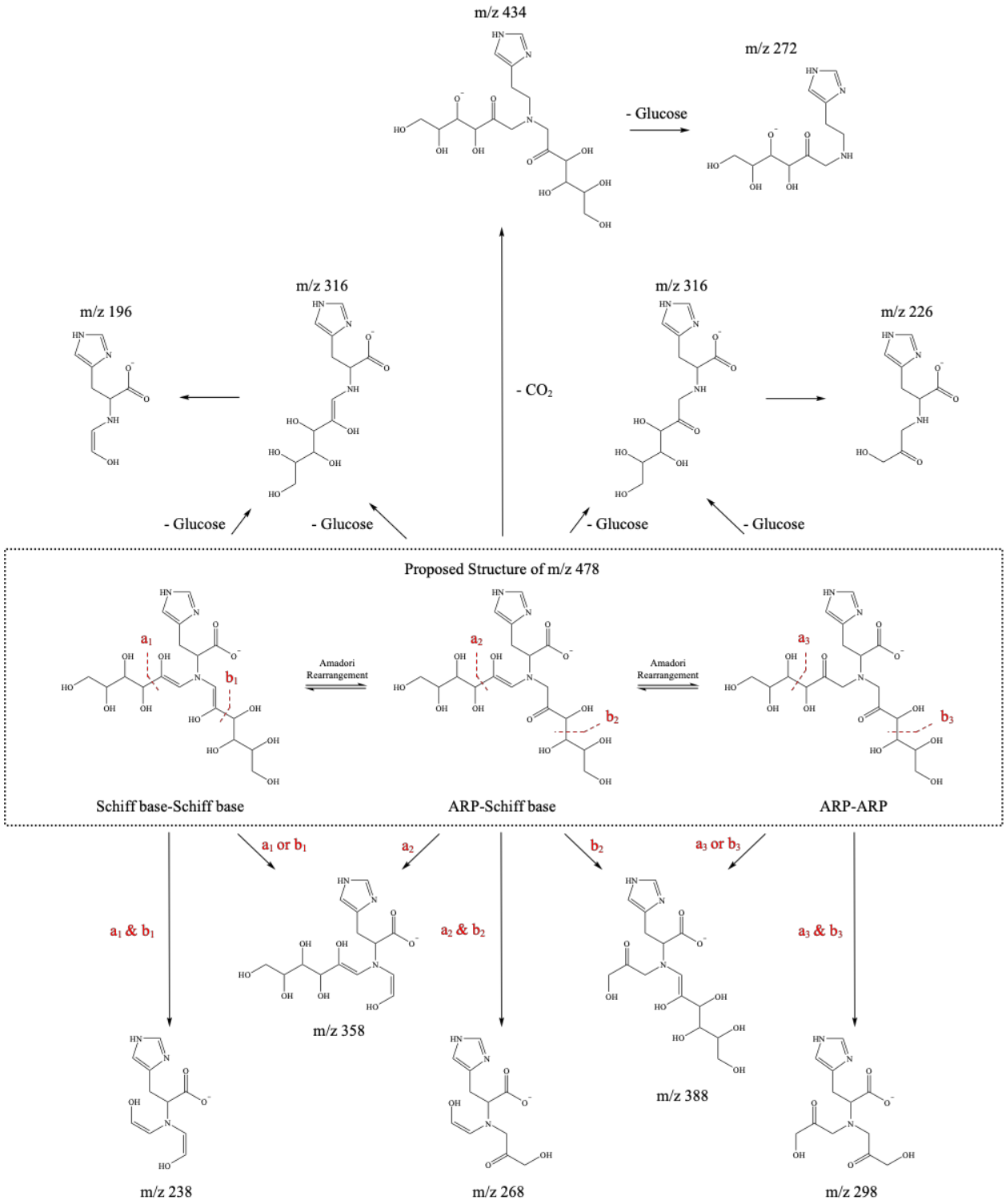

Figure 5.6 Proposed mechanism of MS/MS fragmentation of the molecular ion ($[M-H]^-$, *m/z* 478) of diglycated histidine, consistent with the proposed structure (see Table 5.1 for relative intensities and Table 5.2 for elemental compositions).

To emulate the Maillard reaction in food, the mechanochemically generated ARP was dissolved in water with excess glucose and heated. The thermal reaction to generate diglycated products generated more diglycated histidine than the mechanochemical reaction of his-ARP with excess glucose. In the milled sample, the intensity count for the diglycated histidine (*m/z* 478) was 12,408, compared to when his-ARP was heated with free glucose, which produced a diglycated histidine with an intensity count of 46,793 for the same amount of starting material. Furthermore, no significant degradation products were detected in either MS spectra of his-ARP mechanochemically (Figure 5.3a) or thermochemically (Figure 5.4a) reacted with glucose.

The formation of diglycated cysteine results in the detection of an ion $[M-H]^-$ at *m/z* 444, accompanied by its respective MS/MS fragmentation pathways depicted in Figure 5.7. In the analysis of monoglycated cysteine models discussed in Chapter 4, distinct behaviour was observed in the MS/MS fragmentation pattern, which was also evident in the study of the diglycated cysteine model. Sulphur compounds, particularly L-cysteine, exhibit a significant inhibitory effect on the Maillard reaction (8). This inhibition arises due to the presence of the free thiol group in cysteine, which has redox and nucleophilic characteristics owing to the large atomic radius of the sulphur atom and the low dissociation energy of the thiol S-H bond (7). Hence, an additional isomer, known as 2-threityl-thiazolidine-4-carboxylic acid (TTCA), can form through intramolecular cyclization of the Schiff base. In the context of diglycated amino acids, the TTCA isomer emerges due to the presence of a Schiff base, such as in the Schiff-Schiff or ARP-Schiff diglycated cysteine isomer. This occurs because the aldehyde group on a sugar molecule is attacked by the mercapto group on cysteine, forming a five-membered ring. Compared to ARPs, TTCA is generated from a Schiff base during the Maillard reaction of cysteine due to its enhanced structural stability relative to ARP (11).

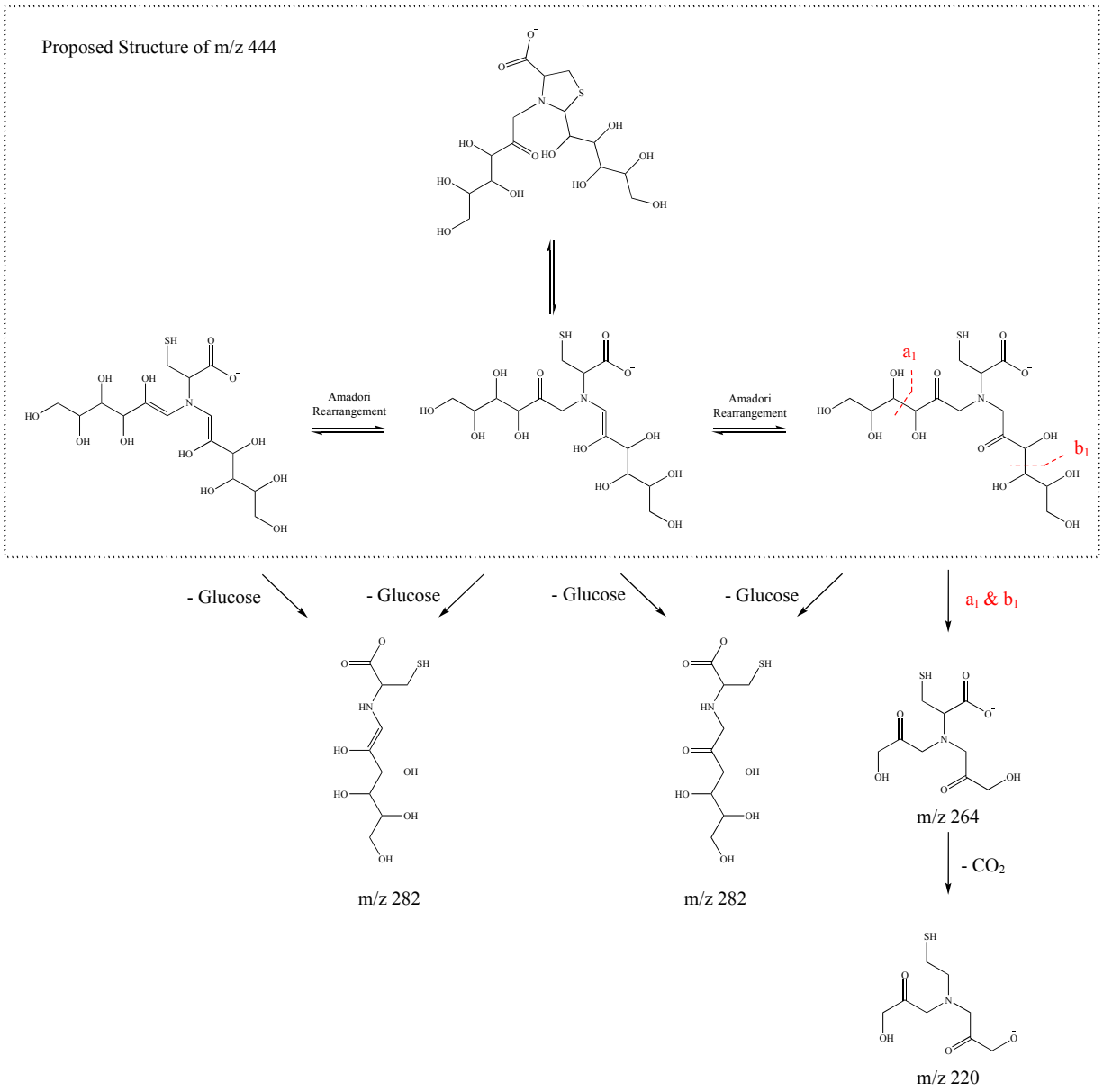

Figure 5.7 Proposed mechanism of MS/MS fragmentation of the molecular ion ($[M-H]^-$, *m/z* 444) of diglycated cysteine, consistent with the proposed structure.

Fewer fragment ions were observed in the MS/MS spectrum of the diglycated cysteine compared to the diglycated histidine model, which may be due to the increased stability of the TTCA isomer. The ion detected at *m/z* 282, can result from the loss of a sugar moiety through β-elimination. Additionally, the diagnostic ion of the ARP-ARP diglycated cysteine isomer, consisting of cysteine with two attached three-carbon chains, was observed at *m/z* 264 [$C_9H_{14}NO_6S$]. Subsequently, decarboxylation of the ion at *m/z* 264 led to the formation of the ion at *m/z* 220 [$C_8H_{14}NO_4S$]. Xing

et al. (9) revealed that the ratio of the Schiff bases to Amadori compounds is dependent on the nature of the side chain of the amino acid, where amino acids with basic side chains generate more Schiff bases, whereas those with acidic side chains produce more ARPs. Given that cysteine is an acidic amino acid, the findings from our MS/MS fragmentation analysis align with Xing et al.'s (9) findings. Notably, in the MS/MS fragmentation of diglycated cysteine, the sole fragmentation ion observed was the diagnostic ion of the ARP-ARP isomer (*m/z* 264), further corroborating the prevalence of this isomer in the reaction mixture.

5.3 Proposed mechanism of formation of diglycated amino acids

The study of diglycated amino acids in the Maillard reaction has attracted some attention, yet it remains relatively underexplored compared to the monoglycated counterparts. The disparity in research focus can be attributed to the transient nature of N, N-diglycated amino acids within the Maillard reaction, primarily due to the prevalence of open ring forms in their sugar moieties. Studies employing NMR and X-ray diffraction (12) have shown that in diglycated amino acids, at least one sugar moiety predominantly exists in the acyclic form. Notably, this acyclic configuration serves as the primary reactive intermediate in the oxidation and dehydration reactions of ARPs (13).

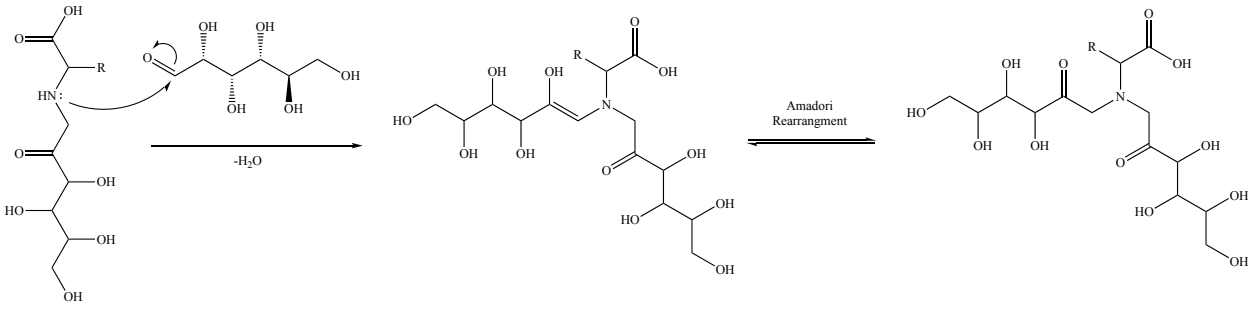

Figure 5.8 Proposed mechanism of formation of diglycated amino acids

The formation of diglycated amino acids in the reaction is facilitated by the nucleophilic properties of ARPs. Specifically, the secondary amino group of an ARP can further react with another reducing sugar and form a disubstituted ARP (Figure 5.8) (14, 15). Current research suggests that the resulting diglycated amino acid (a disubstituted ARP) can contain significant amounts of acyclic forms in solution, explaining their high reactivity (14). Additionally, with increasing

temperature, the mutarotation rates and the concentration of acyclic forms are expected to rise (3). Further insights on reversible enolization and superoxide generation have revealed that diglycated amino acids can readily degrade, forming superoxide much more rapidly than monosubstituted compounds (14). Although the conversion of diglucosyl derivatives into brown pigments is more difficult because of the absence of a secondary amine group, the relatively low reactivity is compensated by an increased browning rate induced by caramelization of glucose, catalyzed by ammonium ions present from the ARP (16). The adjacent sugar moieties on a single nitrogen atom (N, N-diglycated amino acids) form significant heterocyclic moieties in both solution and the solid state (13).

5.4 References

1. Xing, H.; Yaylayan, V. Insight into Isomeric Diversity of Glycated Amino Acids in Maillard Reaction Mixtures. *Int. J. Mol. Sci*. **2020**, *23*(7), 3430. DOI: 10.3390/ijms23073430
2. Yaylayan, V.; Forage, N. A Kinetic Model for the Reaction of Tryptophan with Glucose and Mannose—The Role of Diglycation in the Maillard Reaction. *Food Chem*. **1992**, *44*(3), 201-208. DOI: 10.1016/0308-8146(92)90188-8
3. Pigman, W.; Isbell, H. S. Mutarotation of Sugars in Solution: Part I: History, Basic Kinetics, and Composition of Sugar Solutions. *Adv. Carbohydr. Chem*. **1968**, *23*, 11-57.
4. Gottschalk, A. *Glycoproteins*, Vol. 5b, 2nd ed.; Elsevier: Amsterdam, 1972; pp 141-157.
5. Xing, H.; Mossine, V. V.; Yaylayan, V. Mechanochemical Generation of N, N-Diglycated Glycine and MS/MS characterization of its Isomeric Composition. *Food Chem.* **2022**, *397*, 133757. DOI: 10.1016/j.foodchem.2022.133757
6. Xing, H.; Mossine, V. V.; Yaylayan, V. Diagnostic MS/MS fragmentation patterns for the Discrimination Between Schiff bases and their Amadori or Heyns Rearrangement Products. *Carbohydrate Research* **2020**, *491*, 107985. DOI: 10.1016/j.carres.2020.107985
7. Bak, D. W.; Bechtel, T. J.; Falco, J. A.; Weerapana, E. Cysteine Reactivity Across the Sub-Cellular Universe. *Curr. Opin. Chem. Biol.* **2019**, *48*, 96. DOI: 10.1016/j.cbpa.2018.11.002
8. Cui, H.; Jia, C.; Hayat, K.; Yu, J.; Deng, S.; Karangwa, E.; Zhang, X. Controlled Formation of Flavor Compounds by Preparation and Application of Maillard Reaction Intermediate (MRI) Derived from Xylose and Phenylalanine. *RSC Adv*. **2017**, *7*(72), 45442-45451.
9. Xing, H.; Yaylayan, V. Mechanochemical Generation of Schiff Bases and Amadori Products and Utilization of Diagnostic MS/MS Fragmentation Patterns in Negative Ionization Mode for their Analysis. *Carbohydr. Res*. **2020**, *495*, 108091. DOI: 10.1016/j.carres.2020.108091
10. Xing, H.; Mossine, V. V.; Yaylayan, V. Identification of MS/MS Diagnostic Ions to Distinguish Schiff Bases of Nα- or Nε-Mono-Glycated and Nα, Nε-Di-Glycated Lysines from their Amadori Isomers. *Eur. Food Res. Technol*. **2022**, *248*(11), 2753-2763.

11. Zhai, Y.; Cui, H.; Hayat, K.; Hussain, S.; Tahir, M. U.; Deng, S.; Ho, C. T. Transformation between 2-Threityl-Thiazolidine-4-Carboxylic Acid and Xylose–Cysteine Amadori Rearrangement Product Regulated by pH Adjustment During High-Temperature Instantaneous Dehydration. J. Agric. Food Chem. **2020**, *68*(39), 10884-10892.
12. Mossine, V. V.; Glinsky, G. V.; Barnes, C. L.; Feather, M. S. Crystal Structure of an Amadori Compound, N-(1-Deoxy-β-d-Fructopyranos-1-yl)-Glycine ("D-Fructose-Glycine"). *Carbohydr. Res*. **1995**, *266*(1), 5-14. DOI: 10.1016/0008-6215(94)00256-F
13. Feather, M. S.; Mossine, V. V. Correlations between Structure and Reactivity of Amadori Compounds: The Reactivity of Acyclic Forms. In *The Maillard Reaction in Foods and Medicine*; Woodhead Publishing: 2005; pp. 37-42.
14. Cui, H.; Yu, J.; Zhai, Y.; Feng, L.; Chen, P.; Hayat, K.; Xu, Y.; Zhang, X.; Ho, C. Formation and Fate of Amadori Rearrangement Products in Maillard Reaction. *Trends Food Sci. Technol.* **2021**, *115*, 391-408. DOI: 10.1016/j.tifs.2021.06.055
15. Yaylayan, V. A.; Huyghues-Despointes, A.; Feather, M.S. Chemistry of Amadori Rearrangement Products: Analysis, Synthesis, Kinetics, Reactions, and Spectroscopic Properties, *Crit. Rev. Food Sci. Nutr.* **1994**, *34*(4), 321-369, DOI: 10.1080/10408399409527667
16. Pokorný, J.; Pilkova, L.; Davidek, J.; Valentova, H. Effect of Amadori Rearrangement Products on the Non-Enzymic Browning in Model Systems. *Food/Nahrung* **1988**, *32*(8), 767-776.

Chapter 6. Reaction of glycated amino acids with free amino acids: formation of diamino acid sugar derivatives.

In the thermal processing of food, the abundance of sugars and amino acids compared to the initial Maillard reaction intermediates, including Schiff bases, Amadori, and Heyns products, suggests a high likelihood of their interaction, leading to the creation of new precursors for flavour-active compounds. However, current literature lacks a comprehensive examination of this phenomenon. Chapter 6 aims to fill this gap by investigating the formation of diamino acid sugar derivatives through interactions between glycated amino acids and free amino acids.

6.1 Reactivity of glycated amino acids with free amino acids to demonstrate the formation of di-aminated sugar derivatives.

The reaction between glycated amino acids and excess sugars can produce N, N-diglycated amino acid derivatives, as evidenced in Chapter 5. Similarly, interactions between ARPs and amino acids can form di-aminated sugar derivatives. Amino acids, characterized by their polyfunctional nature, exhibit remarkable chemical reactivity, particularly towards carbonyl compounds (8). The formation of di-aminated sugar derivatives, as initially reported by Westphal and Kroh (10), involves the amino group of the exogenous amino acid reacting with the carbonyl group of the ARP. Subsequent investigations by Cremer et al. (9) revealed the formation of two Strecker aldehydes from the respective amino acids in low-moisture model systems, a process that bypasses the need for a dehydration step.

The involvement of exogenous amino acids has been proven to have many different benefits to the Maillard reaction. For example, Zhou et al. (3) discovered that exogenous alanine inhibits the generation of 2-furfural during the thermal degradation of the alanine-xylose ARP. Given that elevated concentrations of 2-furfural may pose health risks, encompassing hepatotoxic, neurotoxic, nephrotoxic, cytotoxic, and genotoxic effects (4), the inhibition of its formation through the addition of exogenous alanine presents a potential strategy for mitigating these adverse health effects while enhancing the quality and safety of food products subjected to thermal processing. Recent studies have also explored the use of exogenous amino acids and peptides, demonstrating their potential to promote pyrazine formation. The simultaneous promotion of furans and pyrazines, facilitating a balanced formation of flavour compounds, was observed in

models of glycyl-L-glutamine-glucose ARP (11), glutathione–ribose ARP (14), glutamic acid–galactose ARP (14), L-alanyl-l-glutamine-glucose ARP (15), and glutamic acid-xylose ARPs (16). To explore the mechanism by which the addition of amino acids/peptides facilitates pyrazine generation in ARP models, Chen et al. (12) investigated the role of exogenous threonine in promoting the generation of pyrazines in the threonine-glucose ARP model using isotope labelling techniques. The study revealed that exogenous threonine increased total threonine content and directly participated in Strecker degradation, forming pyrazines and an unstable adduct that releases endogenous threonine, generating Thr-HRP (12). This aligns with the proposal by Yaylayan and Huyghues-Despointes (2), suggesting the interconversion between Schiff bases of Amadori and Heyns products through a second amino acid molecule reacting with the ARPs in the equilibrium reaction. The dynamic interconversion between Schiff bases of ARPs and HRPs in di-aminated sugars with amino acids or proteins presents an opportunity for non-enzymatic deglycation of amino acids, particularly proteins, during food processing. This process aims to mitigate the detrimental effects of glycation and preserve functionality. The formation of the Schiff base is a critical stage in deglycation, facilitated by water through hydrolysis or by transglycation with other amino acids or nucleophiles (22, 23). However, the irreversible nature of ARPs once they form requires enzymatic intervention for deglycation, such as through the enzymes Amadoriases, fructosamine-3-kinases, and fructosamine-6-kinases (24). Notably, a thermal equivalent for deglycation has yet to be proposed until now. In thermal processing, due to the irreversibility of the Amadori rearrangement, the reaction of an ARP with a second amino acid at the C-2 atom provides an opportunity to regenerate the Schiff base at the C-1 atom, followed by hydrolysis. The interconversion of ARPs and HRPs is a complex and dynamic process that influences both flavour formation and deglycation in food systems, with implications for food quality and human health.

Understanding the interaction between ARPs and free amino acids is pivotal in elucidating the intricate pathways within the Maillard reaction in various biological systems, such as food processing and in vivo conditions. The interplay between Schiff bases from Amadori and Heyns products holds significant potential for non-enzymatic deglycation in food processing, aiming to mitigate glycation's adverse effects while preserving functionality. This chapter provides evidence

that adding free amino acids to selected Amadori products, including Nε-t-BOC-lysine, can de-glycate the Amadori compound or the associated protein.

6.2 Decomposition of di-aminated sugar derivatives: ARP to HRP interconversion

Excess amino acids are proposed to react with the carbonyl group of Amadori products to form di-aminated sugar derivatives, which can promote interconversion between Schiff bases of Amadori and Heyns products through the equilibrium reaction shown in Figure 6.1. To study the interconversion mechanism, excess amino acids were mechanochemically or thermochemically reacted with ARPs and the MS/MS spectra of the resulting ARP and HRP in the mixture were compared to their corresponding glycated amino acid standards established in Chapter 3 (refer to Figure 6.2). By comparing the ARP and HRP characteristic fragmentation patterns under negative ionization mode derived from different amino acids, it can be discerned which isomer was formed. The ARP MS/MS spectra is expected to correspond to the starting unreacted ARPs, and the HRP MS/MS spectra is expected to correspond to the newly formed amino acid-HRP. Due to the different reactivities of amino acids, various model systems were studied. In addition, mechanochemistry, by ball milling of amino acids and reducing sugars, is expected to generate isomeric mixtures of the glycated amino acids (21).

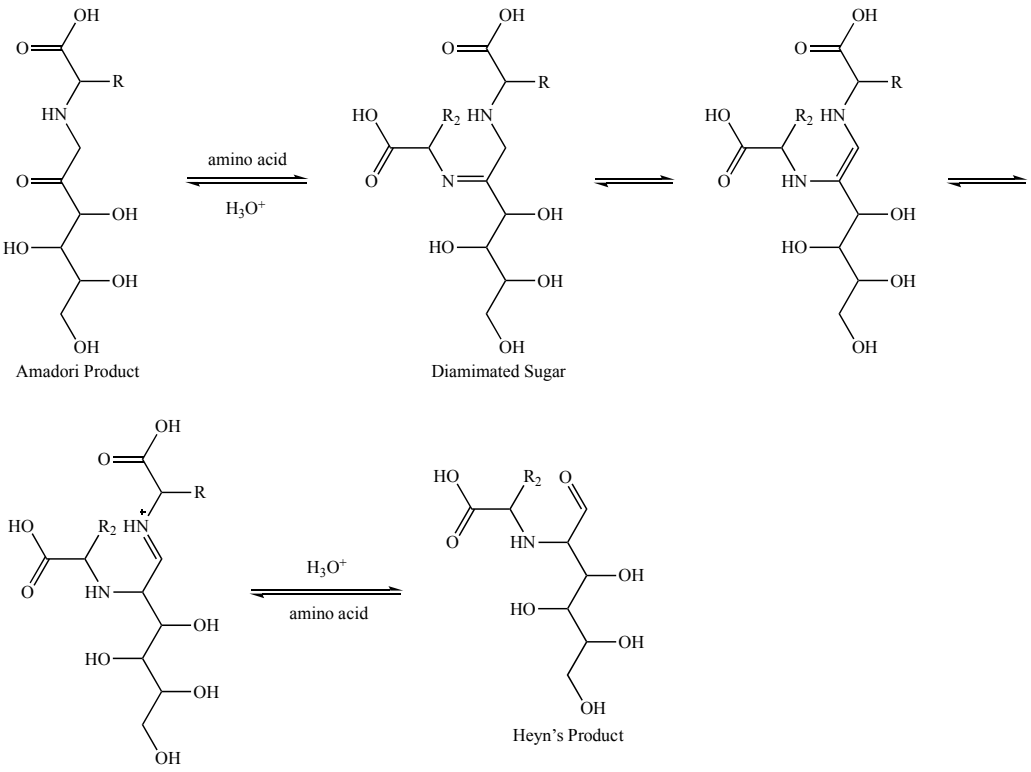

Figure 6.1 Interconversion of Amadori and Heyns Products

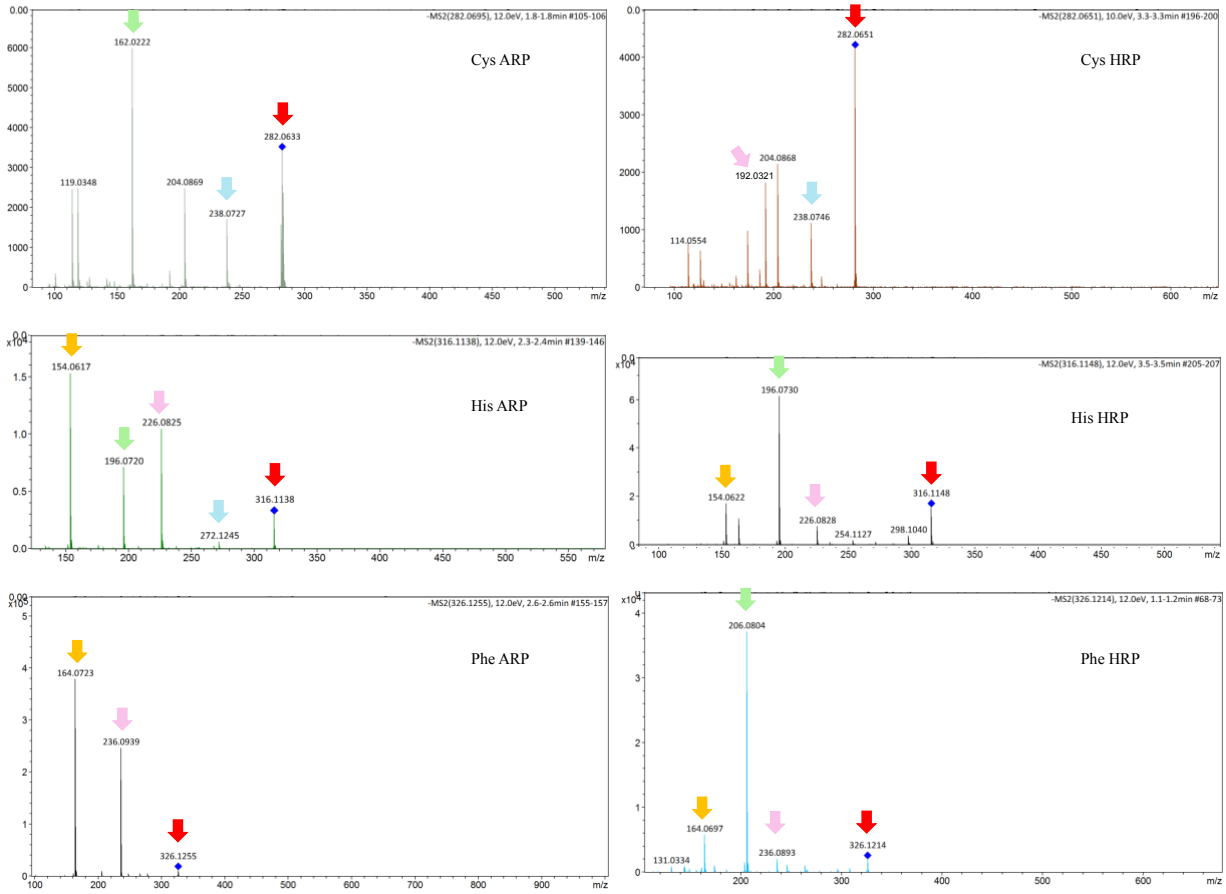

Figure 6.2 MS/MS fragmentation under ESI negative mode of mechanochemically generated ARPs and HRPs. All the mechanochemical mixtures were prepared by ball mill glucose or fructose with the amino acid at a 1:1 M ratio for 30 min at 30 Hz. Diagnostic ions are identified with arrows, where the red arrows indicate the precursor ion; light blue arrows indicate the decarboxylated ARP or HRP; pink arrows indicate the amino acid with a triose; green arrows indicate the amino acid with a diose; and orange arrows indicate the amino acid. Proposed structures are based on elemental composition.

6.2.1 Confirmation of deglycation by comparison of the MS/MS fragmentation patterns under negative ionization mode with controls

The deglycation was confirmed by comparing the MS/MS fragmentation patterns of the newly formed glycated amino acids as Heyns compounds observed in various models under negative ionization mode with standards, which provided critical insights into the chemical transformations within the Maillard reaction pathway. In the first model, where cys-ARP was milled with excess

histidine in a 1:1 ratio (Figure 6.3), it was expected to detect unreacted cys-ARP (*m/z* 282) and newly formed His-HRP (*m/z* 316) according to Figure 6.1. Comparison of the MS/MS spectra revealed that the base peak at *m/z* 282 was unreacted cys-ARP, with minimal unreacted histidine (*m/z* 154) remaining, confirming either a reaction has occurred with histidine or histidine was degraded. However, the MS/MS spectrum of *m/z* 316 was aligned with the standard his-HRP MS/MS spectrum, exhibiting a base peak at *m/z* 196, supported by literature reports (20), indicating reactions of histidine with the Amadori compound. In addition, the absence of free fructose in the reaction mixture can provide further evidence that histidine reacted with the cys-ARP, triggering interconversion into his-HRP (see Figure 6.1). The ion *m/z* 196 corresponds to a diose attached to the amino acid residue, characteristic of Schiff bases (21), indicating the formation of a mixture of his-HRP and its isomeric Schiff base in the model system. Similarly, analysis of the MS/MS spectra of *m/z* 282 revealed the presence of the ion at *m/z* 162, indicative of a Schiff base, thus affirming the coexistence of cys-ARP and its isomeric Schiff base in the model. Furthermore, the observation of the complementary four-carbon sugar fragment at *m/z* 119 affirms the molecule at *m/z* 282 as cys-ARP, as it was only observed in the standard cys-ARP MS/MS as seen in Chapter 4. The identification of unreacted cys-ARP alongside the presence of his-HRP, aligned with standard MS/MS spectra, underlines the conversion of cys-ARP into his-HRP.

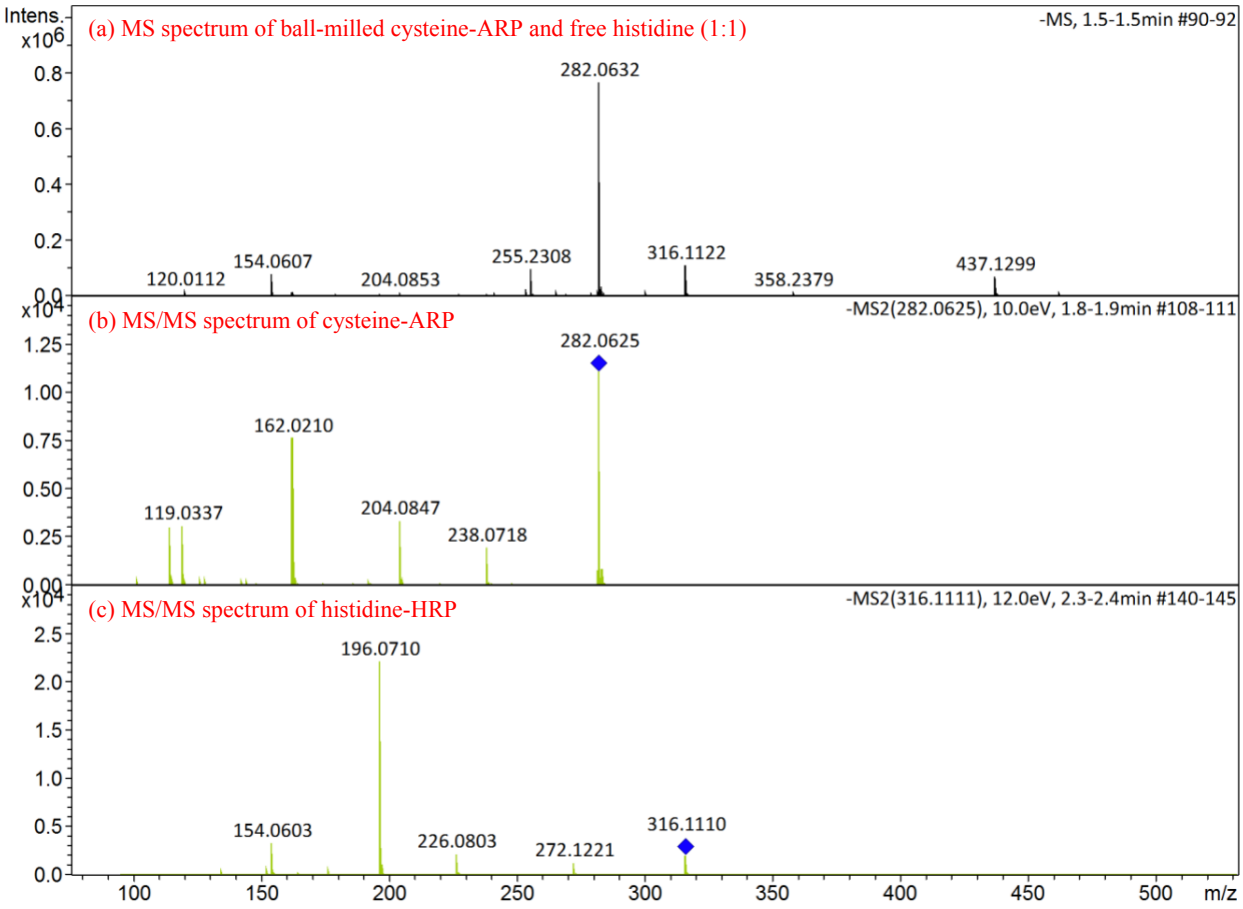

Figure 6.3 MS and MS/MS spectra of cysteine-ARP milled with free histidine (1:1). (a) MS spectrum of ball-milled cysteine-ARP + free histidine; (b) MS/MS spectrum of *m/z* 282 (cysteine-ARP); and (c) MS/MS spectrum of *m/z* 316 (histidine-HRP).

The analysis of the model his-ARP milled with free phenylalanine revealed a newly formed phe-HRP observed at *m/z* 326 in the MS spectra depicted in Figure 6.4. Building upon insight from Chapter 4, which proposes diagnostic ions for glycated amino acid isomers, the presence of the ion *m/z* 206 in the MS/MS spectra of the newly formed phe-HRP was proposed as a diagnostic ion for phe-HRP. The ion is generated through C2–C3 retroaldolization of the open form of the HRP, a phenomenon not observed in the standard phe-ARP model. However, the significant peak at *m/z* 164 in the MS spectrum of Figure 6.4, indicating the abundance of free phenylalanine, suggested that a considerable amount remained unreacted, potentially due to steric hindrance posed by the benzene ring of phenylalanine. Furthermore, the MS/MS spectra of unreacted his-ARP indicated the presence of its isomeric Schiff base, as evidenced by the ions observed at *m/z* 196 and *m/z* 272

(21). Whereas the presence and relative intensity of the ion at *m/z* 226 were indicative of unreacted his-ARP. This ion was proposed as a diagnostic ion for his-ARP due to its significantly lower relative abundance in his-HRP models. The interconversion reaction of his-ARP with phenylalanine revealed the formation of phe-HRP, supported by diagnostic ions identified in Chapter 4.

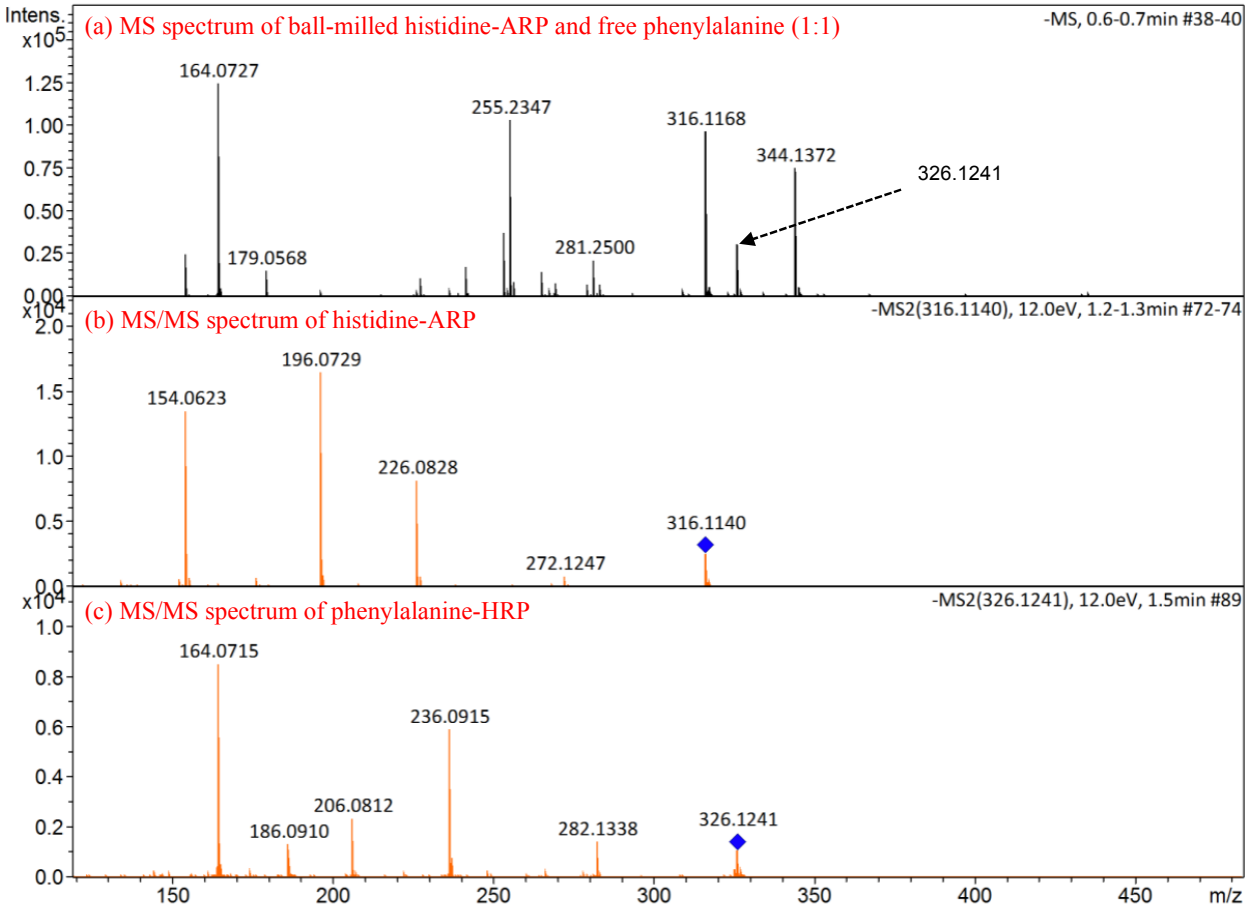

Figure 6.4 MS and MS/MS spectra of histidine-ARP milled with free phenylalanine (1:1). (a) MS spectrum of ball-milled histidine-ARP + free phenylalanine; (b) MS/MS spectrum of *m/z* 316 (histidine-ARP); and (c) MS/MS spectrum of *m/z* 326 (phenylalanine-HRP).

Interestingly, in the model system of his-ARP milled with free cysteine (Figure 6.5), the most abundant peak in the MS spectrum corresponded to cys-HRP at *m/z* 282, while the initial his-ARP peak at *m/z* 316 was relatively low. This observation strongly suggests a significant conversion of his-ARP into cys-HRP, thus affirming the interconversion process. Comparison of the formed cys-

HRP with the standard cys-HRP MS/MS spectra revealed a shared base peak at *m/z* 282. Additionally, the presence and relative intensity of the ions at *m/z* 162 and *m/z* 238 in the newly formed cys-HRP MS/MS spectrum indicates that HRP also exists in its isomeric Schiff base form, as proposed in Chapter 4 as Schiff base diagnostic ions. Meanwhile, ions at *m/z* 204 and *m/z* 114 further confirm the formation of cys-HRP. In contrast, the unreacted his-ARP MS/MS spectrum align completely with the standard his-ARP MS/MS (see Figure 6.2). The conversion of his-ARP to cys-HRP by adding exogenous cysteine was elucidated through the comparison of the MS/MS spectra to their corresponding standards, providing evidence of the transformation within the Maillard reaction pathway.

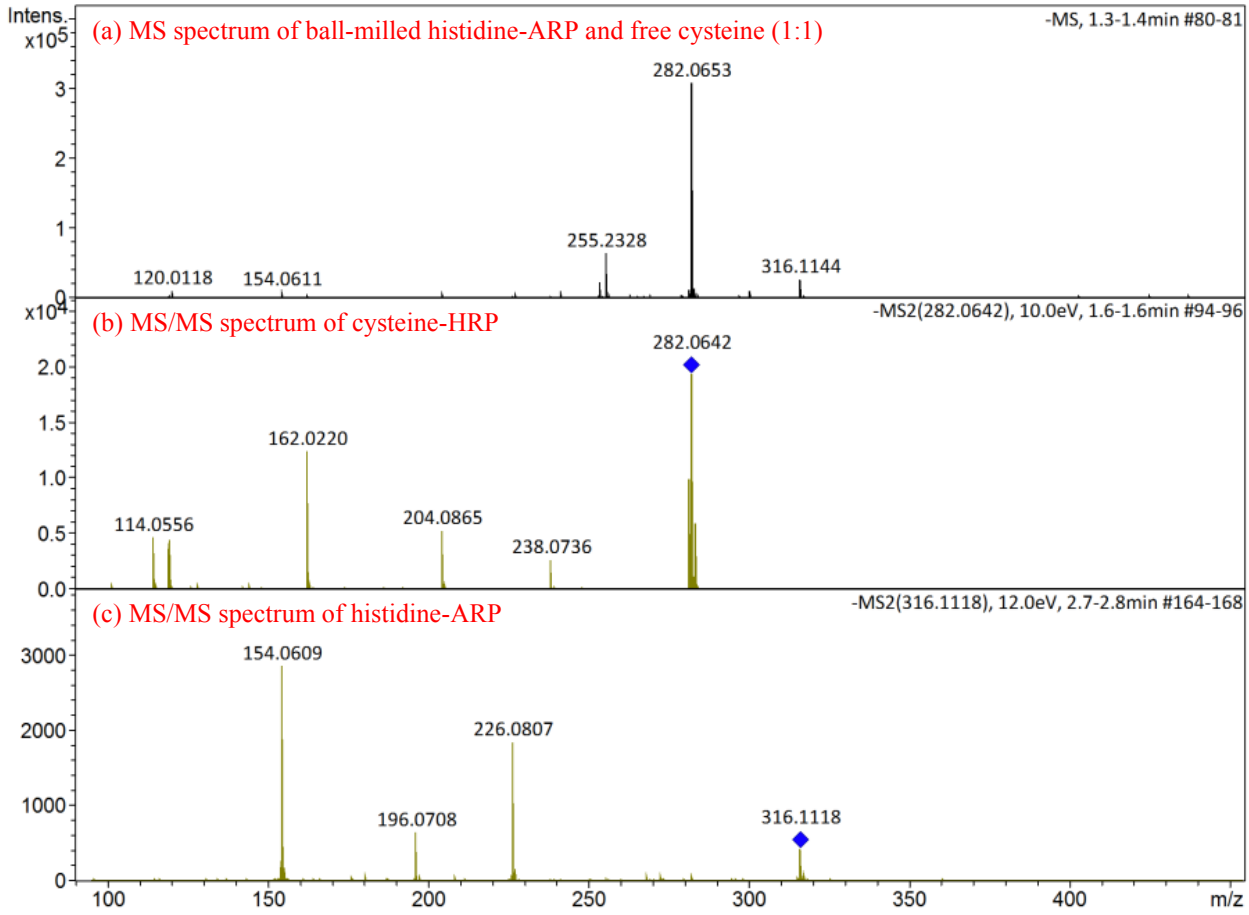

Figure 6.5 MS and MS/MS spectra of histidine-ARP milled with free cysteine (1:1). (a) MS spectrum of ball-milled histidine-ARP + free cysteine; (b) MS/MS spectrum of *m/z* 282 (cysteine-HRP); and (c) MS/MS spectrum of *m/z* 316 (histidine-ARP).

The investigation into the MS spectra of the Maillard reaction model of phe-ARP heated with free cysteine (Figure 6.6) provides valuable insights into the reaction dynamics during thermal processing. Minimal or no traces of glucose (*m/z* 179), phenylalanine (*m/z* 164), and cysteine (*m/z* 120) were observed in the MS spectra of phe-ARP heated with free cysteine in Figure 6.6, indicating complete participation or degradation of all reactants during the thermal process. In the Maillard reaction, phe-ARP can undergo interconversion with free cysteine, leading to the formation of cys-HRP. This process involves the condensation of phe-ARP with cysteine to form cys-HRP, accompanied by the release of water. Consequently, the phe-ARP precursor is consumed or degraded, and its presence is less detectable in the MS spectrum at *m/z* 326 (relative intensity: 1.7 in Figure 6.6). Similarly, the very low intensity observed for the ion at *m/z* 282 (cys-HRP relative intensity: 2.2) suggests its fast degradation under thermal conditions. Notably, the MS/MS spectrum of formed cys-HRP mirrored the standard cys-HRP MS/MS spectrum as illustrated in Figure 6.2, with a base peak of *m/z* 282. Additionally, the presence of the ion at *m/z* 162 in the formed cys-HRP MS/MS spectrum indicates the presence of isomeric Schiff base, as elucidated in Chapter 4. Furthermore, the MS/MS spectrum of unreacted phe-ARP shown in Figure 6.6 is aligned precisely with the standard phe-ARP MS/MS spectrum depicted in Figure 6.2, not only in the presence of specific fragmentation ions but also in their relative intensities. The congruence underscores the relative stability of phe-ARP under thermal conditions. Therefore, the interconversion mechanism can persist under thermal conditions when phenylalanine-ARP reacts with free cysteine, leading to the formation of cys-HRP.

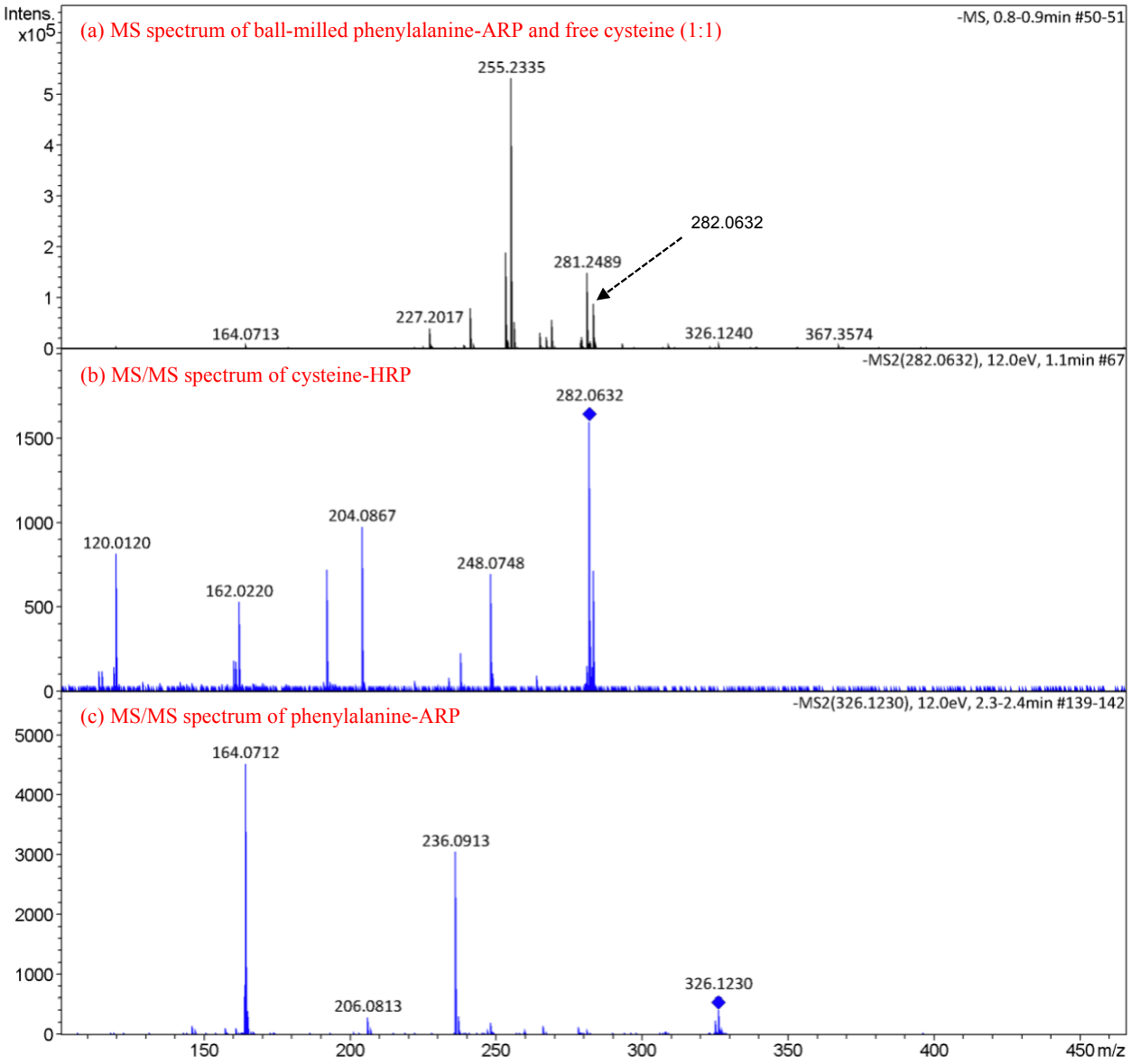

Figure 6.6 MS and MS/MS spectra of phenylalanine-ARP heated with free cysteine (1:1). (a) MS spectrum of ball-milled phenylalanine-ARP + free cysteine; (b) MS/MS spectrum of *m/z* 282 (cysteine-HRP); and (c) MS/MS spectrum of *m/z* 326 (phenylalanine-ARP).

In models containing free cysteine, originating from cys-ARP or introduced in excess to the system, the coloration of the reaction mixtures was notably lighter, suggesting that cysteine interferes with the ARP degradation pathway. This observation is consistent with findings by Zhu et al. (18), who noted decreased fluorescence and UV-VIS absorption intensities in MRPs upon adding exogenous L-cysteine. Huang et al. (17) further elucidated that l-cysteine can follow two pathways upon addition to a reaction mixture: first, interacting with reducing sugars as free amine

group providers, and second, interacting with the ARP generated during the Maillard reaction. When L-cysteine reacts with reducing sugars, it can form the relatively stable cyclic 2-threityl-thiazolidine-4- carboxylic acids (TTCA), which, upon heating, can reversibly convert to the ARP product of cysteine, potentially acid-catalyzed by other amino acids. The observed colour-inhibiting effect of l-cysteine is primarily attributed to its interaction with Amadori compounds (17), aligning with the reaction mechanism proposed by Cremer et al. (9) between an ARP and free amino acid seen in Figure 6.7. Cysteine has a multifaceted role in the formation and transformation of Maillard reaction products, as evidenced by its interference with the degradation of ARPs and the formation of Maillard reaction products.

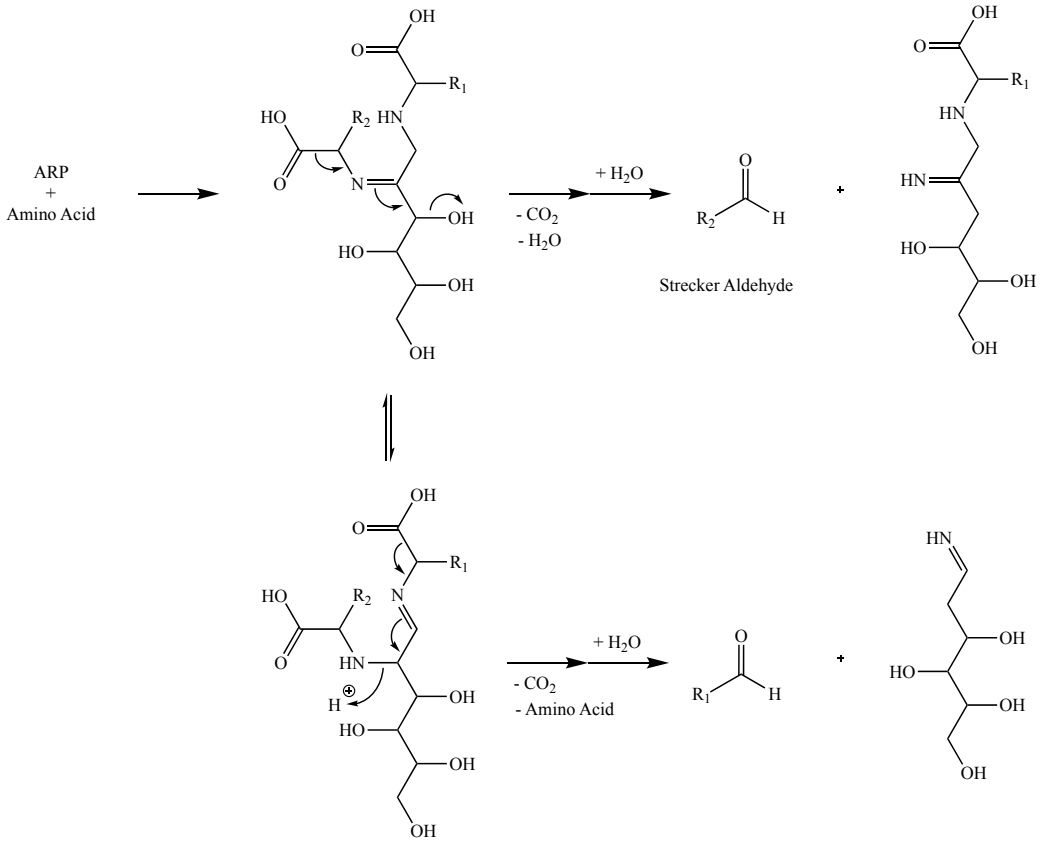

Figure 6.7 Proposed alternative reaction mechanisms of the formation of Strecker aldehydes from diamino acid sugars adapted from Cremer et al. (9). R = amino acid side chain group

6.3 Characteristic MS/MS fragmentations of diamino acid sugar derivatives

Characteristic MS/MS fragmentations of di-aminated sugar derivatives provide valuable insights into their structural elucidation and identification. Table 6.1 provides a comprehensive overview

of their MS/MS spectral data, including their significant and diagnostic ions. In Figures 6.3 to 6.6, reactions between ARPs and amino acids (1:1) are depicted, revealing that, as predicted, di-aminated sugar intermediates were present in very low yields or were absent due to their reactivity. To enhance their observation, the reactant ratio between ARPs and amino acids were adjusted to 1:2. Figures 6.8, 6.9, and 6.11 show the reaction between ARPs and amino acids adjusted to a 1:2 ratio. The elemental composition of the fragmentation ions aligned with the proposed structures of the di-aminated sugar derivatives, as summarized in Table 6.2. Similar to the ARP models described in Chapter 4, the mixture of Schiff bases and ARPs in a di-aminated sugar model sample reflects the dynamic nature of the Maillard reaction and the interplay of various factors influencing reaction kinetics and product formation. This is observed in the di-aminated sugar proceeding through imine intermediates, eventually forming a Heyns product by releasing the initial amino acid after hydrolysis.

Table 6.1 MS/MS spectral data of di-aminated sugars and their significant and diagnostic ions.

#	Model	Precursor ion $[M-H]^-$ (*m/z*)	CID voltage (eV)	Conditions (compound ratio)	Significant fragment ions in MS/MS spectra $[M-X]^-$, *m/z* (rel. int.)
1	His-ARP + Free Cys	$[M-H]^-$ 419	12	Heated (1:1)	419 (100), 375 (9.1), 341 (54.9), 329 (27.4), 299 (16.2), 264 (63.9), 251 (9.9), 221 (15.7), 220 (8.1), 189 (8.4), 186 (12.7), 174 (14.2), 154 (75)
			15	Milled (1:2)	419 (32.1), 375 (22.3), 341 (40.5), 299 (36.3), 264 (36.3), 221 (20.2), 220 (19.7), 186 (31.2), 154 (100)
			12	Milled + Heated (1:2)	419 (37), 264 (58.1), 154 (100)
2	T-Boc-Lys-ARP + Free Cys	$[M-H]^-$ 510	25	Milled (1:2)	510 (21.9), 436 (17.3), 432 (84.4), 420 (15.9), 358 (51.3), 264 (36.2), 245 (41.9), 238 (23.6), 220 (20.4), 186 (59), 171 (100)

Table 6.2 Elemental composition of characteristic ions of di-aminated sugar derivatives during MS/MS in negative ionization mode with histidine and cysteine.

#	*m/z*	MF	Error (ppm)
	Histidine-Cysteine		
1	419.1222	$C_{15}H_{23}N_4O_8S$	4.79
2	375.1311	$C_{14}H_{23}N_4O_6S$	8.74
3	341.1442	$C_{14}H_{21}N_4O_6$	7.21
4	299.08	$C_{11}H_{15}N_4O_4S$	6.52
5	264.0522	$C_9H_{14}NO_6S$	9.59
6	251.1145	$C_{11}H_{15}N_4O_3$	1.85
7	221.1034	$C_{10}H_{13}N_4O_2$	4.52
8	220.0628	$C_8H_{14}NO_4S$	9.55
9	186.0765	$C_8H_{12}NO_4$	3.66
10	174.0221	$C_6H_8NO_3S$	5.39
11	154.0618	$C_6H_8N_3O_2$	2.60
	T-Boc-Lysine-Cysteine		
1	510.2107	$C_{20}H_{36}N_3O_{10}S$	3.90
2	436.1392	$C_{16}H_{26}N_3O_9S$	0.74
3	432.2348	$C_{19}H_{34}N_3O_8$	0.78
4	420.1779	$C_{17}H_{30}N_3O_7S$	7.37
5	358.1612	$C_{15}H_{24}N_3O_7$	2.16
6	264.0541	$C_9H_{14}NO_6S$	2.39
7	245.1489	$C_{11}H_{21}N_2O_4$	7.26
8	238.1178	$C_{11}H_{16}N_3O_3$	8.04
9	220.0624	$C_8H_{14}NO_4S$	11.37
10	186.0766	$C_8H_{12}NO_4$	3.12

The reaction of his-ARP and excess cysteine, shown in Figure 6.8, involved the mechanochemically generated his-ARP being milled with two moles of cysteine, carried out in two one-mole increments. The increased reaction ratio of cysteine enhanced the intensity of its related di-aminated sugar ion observed at *m/z* 419 with an intensity count of 9230. In contrast, the 1:1 reaction of his-ARP milled with cysteine did not show the related di-aminated sugar in the MS spectrum. When the same model of his-ARP and excess cysteine at a 1:2 ratio was heated, the intensity of the ion was reduced, as seen in Figure 6.9. Nevertheless, the successful formation and subsequent analysis of the histidine-cysteine di-aminated sugar derivative elucidates an important mechanistic pathway involved in the Maillard reaction. The detection of an ion $[M-H]^-$ at *m/z* 419, as depicted in Figures 6.8 and 6.9, signifies the formation of this derivative, complemented by the elemental composition of the fragments in Table 6.2.

Further examination of the MS/MS fragmentation pathways, illustrated in Figure 6.10, revealed diagnostic ions indicative of specific chemical transformations. Notably, the formation of a 2-azaallyl anion generated through decarboxylation was observed at *m/z* 375, proposed as a diagnostic ion for Schiff bases by Xing et al. (21). Indicating the presence or formation of these intermediates within the systems under study; however, the location of decarboxylation is dependent on whether the Schiff base was present on the cysteine or histidine residue. After decarboxylation, the ion at *m/z* 341 forms $[M-H-SH-COO]^-$ due to desulfurization. The equivalent to glycated cysteine was observed in its MS/MS fragmentation pattern as *m/z* 204, as seen in Chapter 4. Furthermore, retro-aldolization reactions of the C2-C3 sugar chain of the ion at *m/z* 341 produces $[M-H-SH-COO-C_3H_6O_3]^-$ (*m/z* 251), consistent with the fragmentation pattern observed in the MS/MS spectrum of glycated cysteine, confirming the chemical transformations during the reaction between excess cysteine and his-ARP. The successive loss of formaldehyde ($-CH_2O$) from the ion at *m/z* 251 results in the fragment ion *m/z* 221. An alternate fragmentation pathway of the histidine-cysteine di-aminated sugar derivative observed at *m/z* 419 $[M-H]^-$ reveals generation of ion fragments at *m/z* 329 and *m/z* 299, attributed to retro-aldolization of the C3-C4 sugar chain and loss of formaldehyde ($-CH_2O$) in succession under collision. The fragment ion at *m/z* 299 is proposed as a diagnostic ion of the histidine-cysteine di-aminated sugar derivative. The analysis of MS/MS fragmentation pattern provides valuable insights into the structural elucidation of the histidine-cysteine di-aminated sugar derivative. The consistent fragmentation pattern observed

aligns with the expected chemical transformations, such as decarboxylation, desulfurization, and retro-aldolization reactions, confirming the formation of the derivative. However, multiple isomers of the di-aminated sugar may exist, each with potentially distinct fragmentation patterns. Further studies exploring these potential isomers are necessary to comprehensively understand the complexity of the Maillard reaction and its resulting products.

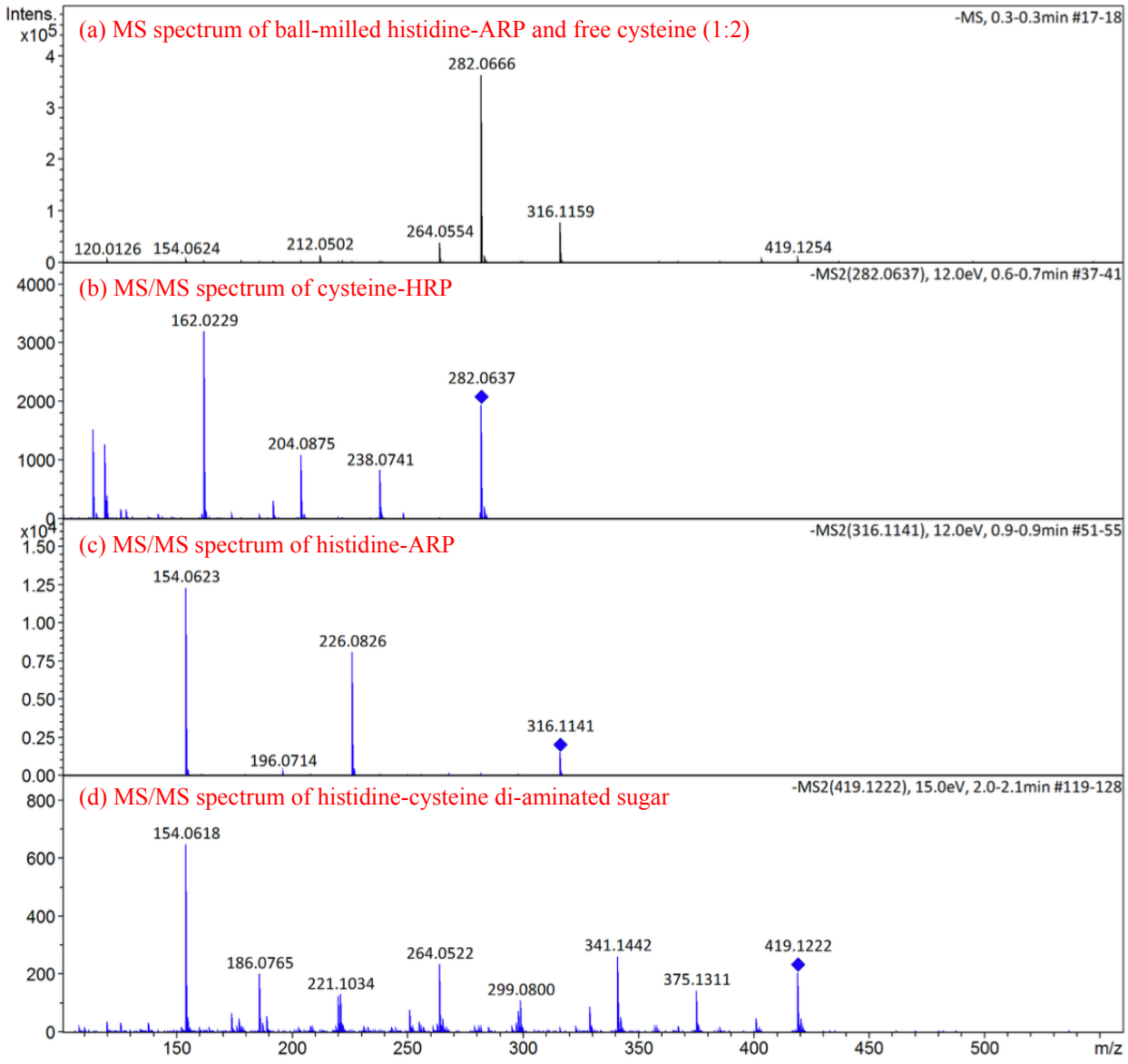

Figure 6.8 MS and MS/MS spectra of his ARP milled with free cysteine (1:2). (a) MS spectrum of ball-milled histidine-ARP + free cysteine; (b) MS/MS spectrum of *m/z* 282 (cysteine-HRP); (c) MS/MS spectrum of *m/z* 316 (histidine-ARP); and (d) MS/MS spectrum of *m/z* 419 (histidine-ARP + cysteine adduct).

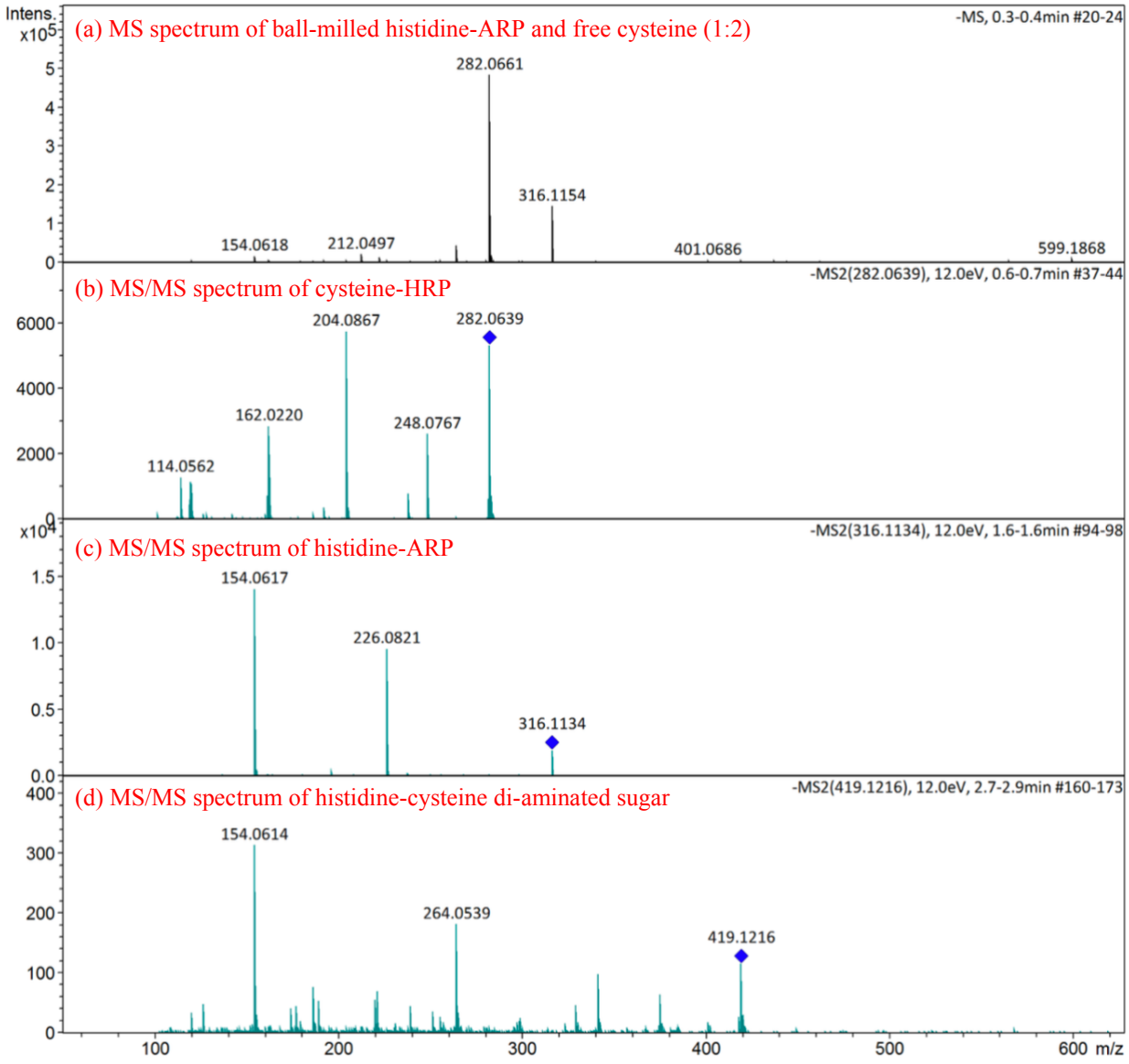

Figure 6.9 MS and MS/MS spectra of his ARP milled with free cysteine then heated (1:2). (a) MS spectrum of ball-milled histidine-ARP + free cysteine after heating; (b) MS/MS spectrum of *m/z* 282 (cysteine-HRP); (c) MS/MS spectrum of *m/z* 316 (histidine-ARP); and (d) MS/MS spectrum of *m/z* 419 (histidine-ARP + cysteine adduct).

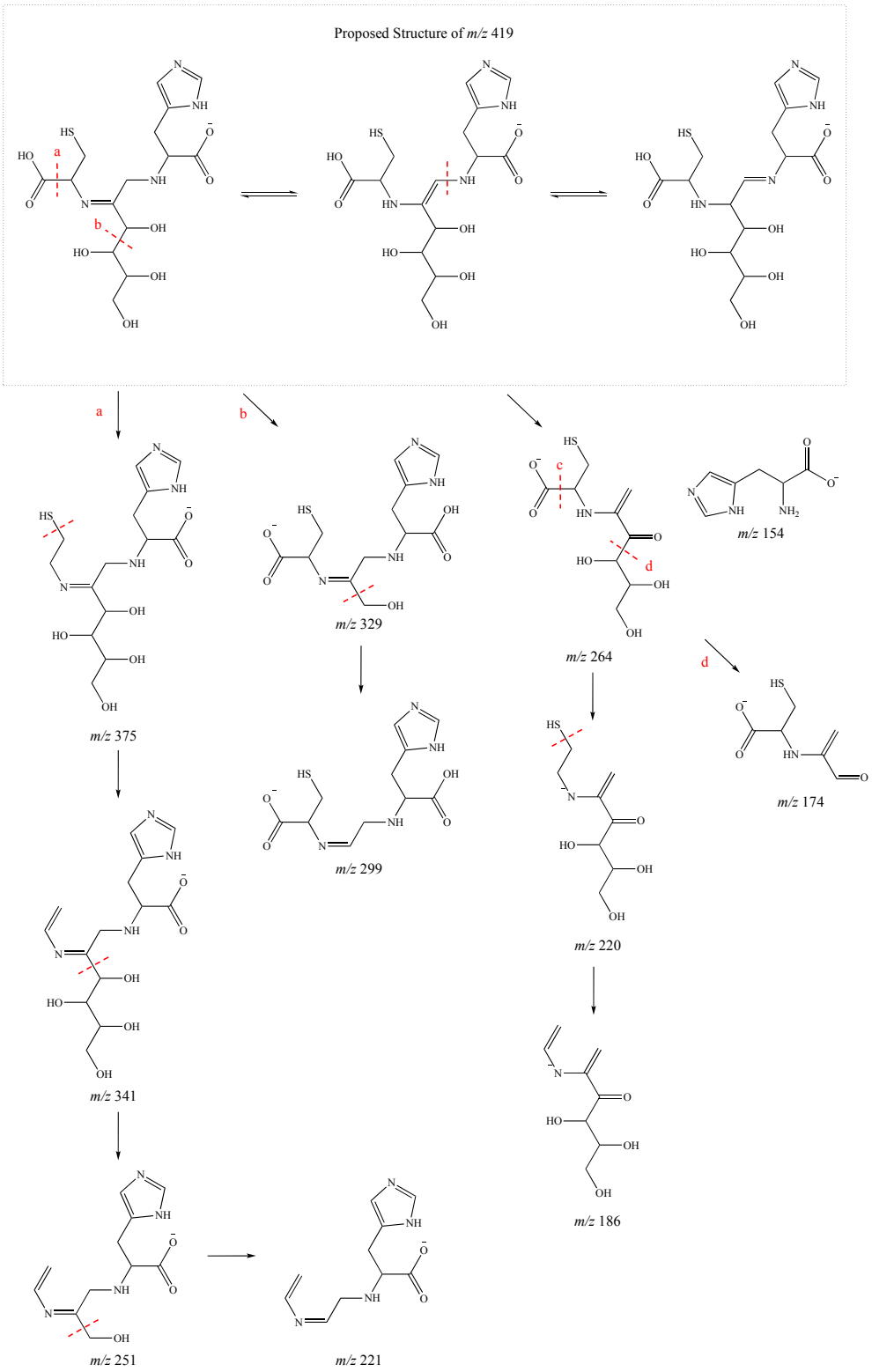

Figure 6.10 Proposed mechanism of MS/MS fragmentation of the molecular ion ([M-H]$^-$, *m/z* 419) of the histidine-cysteine di-aminated sugar derivative, consistent with the proposed structure.

The formation of a t-BOC-lysine-cysteine di-aminated sugar derivative results in detecting an ion at *m/z* 510 $[M-H]^-$ in the MS spectrum, consistent with the expected molecular weight (see Figure 6.11). The molecular ion of the t-BOC-lysine-cysteine di-aminated sugar, generated through ball milling, was subjected to MS/MS fragmentation (Figure 6.11), and the elemental composition of the observed fragments is detailed in Table 6.2.

Analogous fragmentation patterns, initiated by cysteine moiety were expected between the t-BOC-lysine-cysteine di-aminated sugar derivative and histidine-cysteine di-aminated sugar derivative MS/MS due to the shared presence of cysteine. In pathway (a) of Figure 6.12, dehydration and the subsequent loss of the tert-butyl group of the t-BOC-lysine residue generates the ion *m/z* 436. Following, the ion *m/z* 358 was formed by the decarboxylation and desulfurization of the ion at *m/z* 436 in succession. Additional retro-aldolization reaction of the C3-C4 sugar chain of the ion at *m/z* 358 results in the formation of *m/z* 238. Pathway (b) begins with the characteristic ion $[M-H]^-$ undergoing retro-aldolization of the C3-C4 sugar chain to form the ion *m/z* 420, indicative of a diose attached to the di-aminated sugar moiety. Previously, Xing and Yaylayan (21) proposed the presence of a diose attached to an amino acid residue in the MS/MS spectra as a diagnostic marker for Schiff bases. Pathway (c) involves decarboxylation and desulfurization of $[M-H]^-$ forming the ion at *m/z* 432. The histidine-cysteine di-aminated sugar derivative equivalent was seen at *m/z* 251. The analysis of MS/MS fragmentation of the t-BOC-lysine-cysteine di-aminated sugar derivative, illustrated in Figure 6.12, is consistent with the structure and provides crucial insights into the structural elucidation of t-BOC-lysine-cysteine di-aminated sugar derivative. Similar to the histidine-cysteine di-aminated sugar derivative, this analysis unveils the presence of isomeric variants within the di-aminated sugar family, emphasizing the complexity of these chemical species in Maillard reaction pathways.

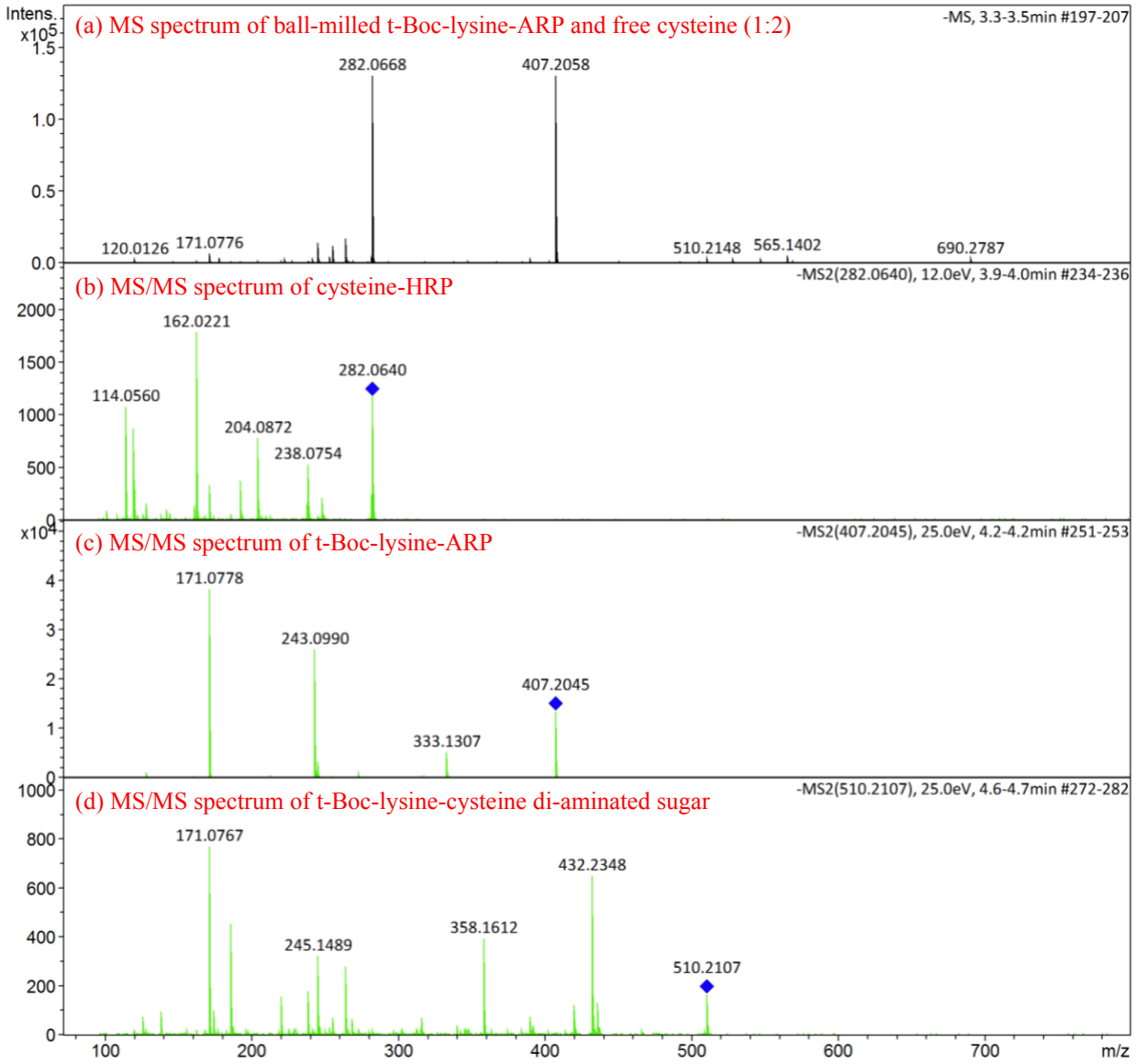

Figure 6.11 MS and MS/MS spectra of t-BOC-lysine ARP milled with free cysteine (1:2). (a) MS spectrum of ball-milled t-BOC-lysine-ARP + free cysteine; (b) MS/MS spectrum of *m/z* 282 (cysteine-HRP); (c) MS/MS spectrum of *m/z* 407 (t-BOC-lysine -ARP); and (d) MS/MS spectrum of *m/z* 510 (t-BOC-lysine -ARP + cysteine adduct).

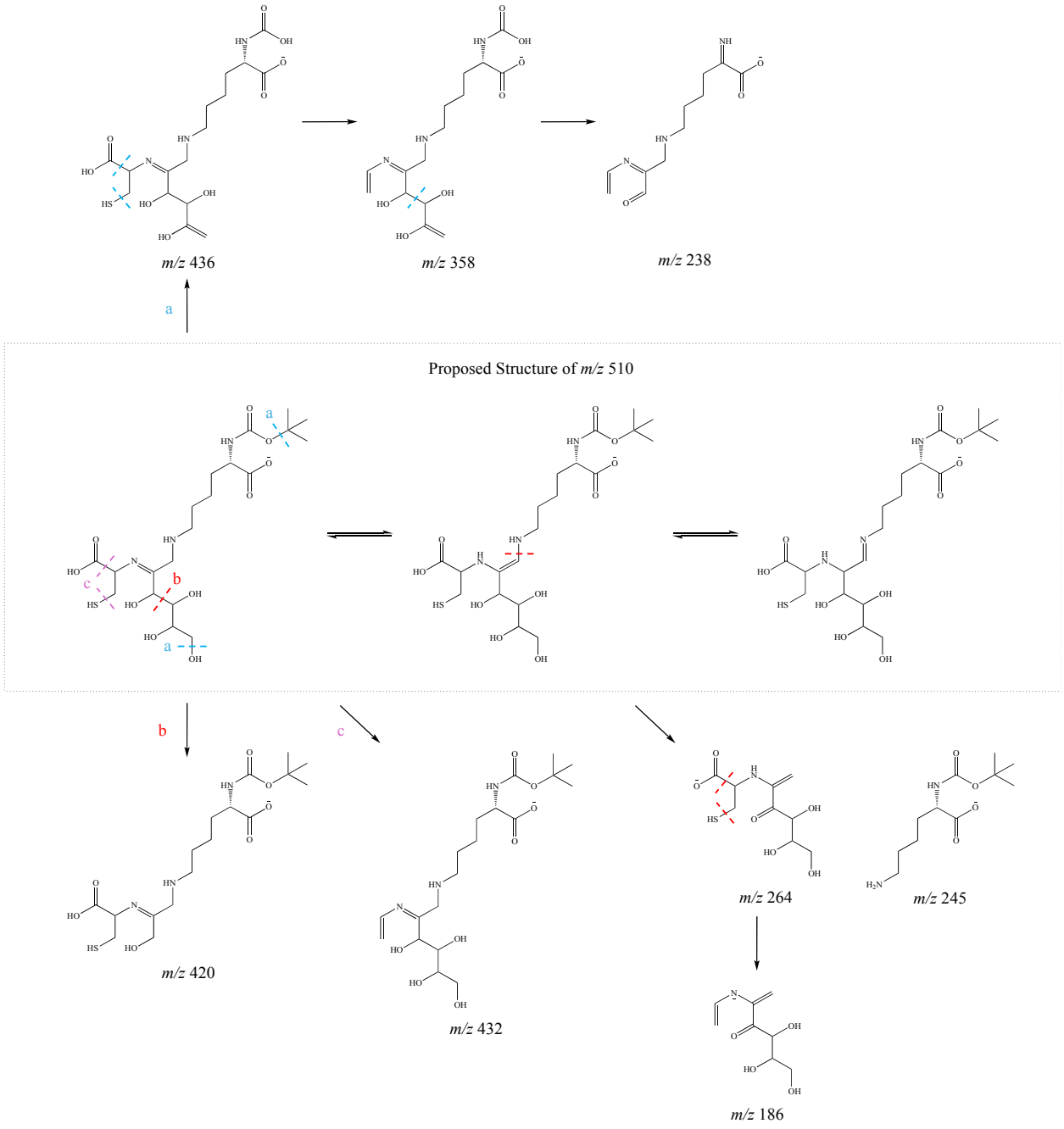

Figure 6.12 Proposed mechanism of MS/MS fragmentation of the molecular ion ([M-H]$^-$, *m/z* 510) of the t-BOC-lysine-cysteine di-aminated sugar derivative, consistent with the proposed structure.

In both experimental models, the analysis of MS/MS fragmentation revealed important insights into the cleavage of the starting glycated amino acid. Specifically, in the his-ARP + free cys model, the fragment ion corresponding to histidine was detected at *m/z* 154. Similarly, in the t-BOC-lys-ARP + free cys model, the fragment ion attributed to t-BOC-lysine was observed at *m/z* 245. In

both cases, the ion at *m/z* 264 (shown in Figures 6.9 and 6.11), representing glycated cysteine, was the complementary ion to the fragmented amino acid. The ion at *m/z* 264 then underwent further chemical transformations, forming the ion at *m/z* 186 through decarboxylation and desulfurization processes. The presence of identical fragmentation patterns across both experimental models underscores the role of cysteine in the formation of observed ions. This consistency suggests that the observed ions originate from chemical modifications of cysteine within the samples. This information is crucial for understanding the specific pathways and mechanisms involved in the fragmentation processes of the glycated amino acids under investigation.

6.4 Proposed mechanism of interconversion of ARP to HRP

Parallel to the transformation observed from glucose to fructose, the Amadori product can also undergo interconversion to the Heyns product when exposed to free amino acids (Figure 6.1). Yaylayan et al. (2) described this ARP-to-HRP conversion in the presence of free amino acid, identifying that the N-(1-deoxy-fructos-1-yl)amine is extremely unstable in heated aqueous solutions and will undergo hydrolysis, leading to the formation the HRP. As previously highlighted, Chen et al. (12) investigated the role of exogenous threonine in promoting the generation of pyrazines within the threonine-glucose ARP model using isotope labelling techniques. Their study highlighted the intricate relationship between ARPs and HRPs, revealing their dynamic interconnection (12), aligning with Yaylayan's proposed ARP-to-HRP interconversion mechanism (2). The proposed mechanism involves an aldimine condensation between an exogenous amino acid and an ARP, followed by hydrolysis, resulting in the generation of HRP alongside the endogenous amino acid. This theory was supported by their observation of HRPs derived from ^{15}N-threonine, coupled with a substantial decrease in ^{15}N-threonine content and a rapid increase of ^{14}N endogenous threonine during the initial stage of heat treatment (12).

The observation of di-amino acid derivatives and the comparison of synthesized ARP and HRP MS/MS spectra from reactions of excess amino acids mechanochemically or thermochemically reacted with ARPs to their corresponding glycated amino acid standards aid in confirming the interconversion mechanism between Amadori and Heyns products. The detection of di-aminated sugar derivatives supports the proposed mechanism where excess amino acids react with the carbonyl group of ARPs to form di-aminated sugars, facilitating the interconversion between ARPs

and HRPs. Then, comparing the MS/MS spectra of formed ARP and HRP (Figures 6.3 to 6.6) with standard ARP and HRP samples (Figure 6.2) provides insights into the transformation process. If the ARP spectra align with the standard ARP samples while the HRP spectra correspond to the excess amino acid-HRP, it indicates the successful interconversion from ARP to HRP in the presence of excess amino acids. Combining these observations, it can be confirmed that excess amino acids promote the interconversion between Amadori and Heyns products, as proposed in the mechanism. This confirmation enhances our understanding of the dynamic equilibrium between Amadori and Heyns products and validates the proposed reaction mechanism.

6.5 References

1. Xing, H.; Mossine, V. V.; Yaylayan, V. Mechanochemical Generation of N,N-Diglycated Glycine and MS/MS Characterization of its Isomeric Composition. *Food Chem*. **2022**, *397*, 133757. DOI: 10.1016/j.foodchem.2022.133757
2. Yaylayan, V. A.; Huyghues-Despointes, A.; Feather, M. S. Chemistry of Amadori Rearrangement Products: Analysis, Synthesis, Kinetics, Reactions, and Spectroscopic Properties. *Crit. Rev. Food Sci. Nutr.* **1994**, *34*(4), 321-369.
3. Zhou, T.; Huang, M.; Cui, H.; Chen, P.; Hayat, K.; Zhang, X.; Ho, C.-T. Exogenous Alanine Promoting the Reaction between Amadori Compound and Deoxyxylosone and Inhibiting the Formation of 2-Furfural during Thermal Treatment. *J. Agric. Food Chem*. **2024**, *72*(11), 5878-5886. DOI: 10.1021/acs.jafc.4c00021
4. Li, M.; Shen, M.; Lu, J.; Yang, J.; Huang, Y.; Liu, L.; Fan, H.; Xie, J.; Xie, M. Maillard Reaction Harmful Products in Dairy Products: Formation, Occurrence, Analysis, and Mitigation Strategies. *Food Res. Int*. **2022**, *151*, Article No. 110839.
5. Deng, S.; Zhai, Y.; Cui, H.; Hayat, K.; Zhang, X.; Ho, C. T. Mechanism of Pyrazine Formation Intervened by Oxidized Methionines During Thermal Degradation of the Methionine–Glucose Amadori Compound. *J. Agric. Food Chem*. **2022**, *70*(45), 14457-14467.
6. Cömert, E. D.; Gökmen, V. Kinetic Evaluation of the Reaction Between Methylglyoxal and Certain Scavenging Compounds and Determination of Their In Vitro Dicarbonyl Scavenging Activity. *Food Res. Int.* **2019**, *121*, 257-268.
7. Zhou, T.; Xia, X.; Cui, H.; Hayat, K.; Zhang, X.; Ho, C. T. Competitive Formation of 2, 3-Butanedione and Pyrazines through Intervention of Added Cysteine During Thermal Processing of Alanine-Xylose Amadori Compounds. *J. Agric. Food Chem*. **2022**, *70*(48), 15202-15212.
8. Pripis-Nicolau, L.; De Revel, G.; Bertrand, A.; Maujean, A. Formation of Flavour Components by the Reaction of Amino Acid and Carbonyl Compounds in Mild Conditions. *J. Agric. Food Chem.* **2000**, *48*(9), 3761-3766.

9. Cremer, D. R.; Vollenbroeker, M.; Eichner, K. Investigation of the Formation of Strecker Aldehydes from the Reaction of Amadori Rearrangement Products with α-Amino Acids in Low Moisture Model Systems. *Eur. Food Res. Technol*. **2000**, *211*, 400-403.
10. Westphal, G.; Kroh, L. Zum Mechanismus der „frühen Phase" der Maillard-Reaktion 2. Mitt. Folgereaktionen von N-Glycosiden. *Food/Nahrung* **1985**, *29*(8), 765-775.
11. Xia, X.; Zhou, T.; Zhang, H.; Cui, H.; Zhang, F.; Hayat, K.; Ho, C. T. Simultaneously Enhanced Formation of Pyrazines and Furans during Thermal Degradation of the Glycyl-l-glutamine Amadori Compound by Selected Exogenous Amino Acids and Appropriate Elevated Temperatures. *J. Agric. Food Chem*. **2023**, *71*(10), 4346-4357.
12. Chen, P.; Cui, H.; Zhou, T.; Feng, L.; Hayat, K.; Zhang, X.; Ho, C. T. Exogenous Threonine-Induced Conversion of Threonine-Xylose Amadori Compound to Heyns Compound for Efficiently Promoting the Formation of Pyrazines. *J. Agric. Food Chem.* **2023**, *71*(29), 11141-11149.
13. Xia, X.; Zhai, Y.; Cui, H.; Zhang, H.; Hayat, K.; Zhang, X.; Ho, C. Structural diversity and concentration dependence of pyrazine formation: Exogenous amino substrates and reaction parameters during thermal processing of l-alanyl-l-glutamine Amadori compound. *Food Chem*. **2022**, *390*, 133144. DOI: 10.1016/j.foodchem.2022.133144
14. Pan, C.; Cui, H.; Hayat, K.; Zhang, X.; Ho, C. T. Exogenous Glutamic Acid Effectively Involved in N-(1-Deoxy-D-Galulos-1-yl)-Glutamic Acid Degradation for Simultaneous Improvement of Both Milk-like and Baking Flavor. *Food Biosci*. **2022**, *47*, 101697.
15. Feng, L.; Cui, H.; Chen, P.; Hayat, K.; Zhang, X.; Ho, C. T. Promoted Formation of Pyrazines and Sulfur-Containing Volatile Compounds through Interaction of Extra-Added Glutathione or its Constituent Amino Acids and Secondary Products of Thermally Degraded N-(1-Deoxy-D-Ribulos-1-yl)-Glutathione. *J. Agric. Food Chem.* **2022**, *70*(29), 9095-9105.
16. Xu, M.; Cui, H.; Sun, F.; Jia, C.; Zhang, S. L.; Hussain, S.; Hayat, K. Preparation of N-(1-Deoxy-A-D-Xylulos-1-Yl)-Glutamic Acid via Aqueous Maillard Reaction Coupled with Vacuum Dehydration and Its Flavor Formation Through Thermal Treatment of Baking Process. *J. Food Sci*. **2019**, *84*(8), 2171-2180.
17. Huang, M.G.; Zhang, X.M.; Eric, K.; Abbas, S.; Hayat, K.; Liu, P.; Xia, S.Q.; Jia, C.S. Inhibiting the Color Formation by Gradient Temperature-Elevating Maillard Reaction of

Soybean Peptide-Xylose System Based on Interaction of L-Cysteine and Amadori Compounds. *J. Pept. Sci*. **2012**, 18: 342-349. DOI: 10.1002/psc.2406

18. Zhu, J.; Xia, X.; Zhang, F.; Song, S.; Cui, H.; Hayat, K.; Ho, C. T. Taste Characteristic and the Mechanism of Light-Colored Maillard Reaction Products Derived from Gluten Hydrolysate. *Food Biosci*. **2023**, *52*, 102394.
19. Hou, L.; Xie, J.; Zhao, J.; Zhao, M.; Fan, M.; Xiao, Q.; Liang, J.; Chen, F. Roles of Different Initial Maillard Intermediates and Pathways in Meat Flavor Formation for Cysteine-Xylose-Glycine Model Reaction Systems. *Food Chem*. **2017**, *232*, 135-144. DOI: 10.1016/j.foodchem.2017.03.133.
20. Li, K.; Wang, J.; Zhuang, Y.; Yuan, G.; Li, Y.; Zhu, X. Glucose-Histidine Heyns Compound: Preparation, Characterization and Fragrance Enhancement. *Carbohydr. Res.* **2023**, *532*, 108922. DOI: 10.1016/j.carres.2023.108922
21. Xing, H.; Yaylayan, V. Mechanochemical Generation of Schiff Bases and Amadori Products and Utilization of Diagnostic MS/MS Fragmentation Patterns in Negative Ionization Mode for their Analysis. *Carbohydr. Res*. **2020**, *495*, 108091. DOI: 10.1016/j.carres.2020.108091
22. Szwergold, B. S. Carnosine and Anserine Act as Effective Transglycating Agents in Decomposition of Aldose-Derived Schiff Bases. *Biochem. Biophys. Res. Comm*. **2005**, *336*, 36-41.
23. Emel'yanov, V. V. Glycation, Antiglycation, and Deglycation: Their Role in Aging Mechanisms and Geroprotective Effects. *Adv. Gerentology* **2017**, *7*(1), 1-9.
24. Filipp, L.; Bausch, F.; Neuhaus, L.S.; Flade, J.; Henle, T. Metabolization of the Amadori Product N-ε-Fructosyllysine by Probiotic Bacteria. *J. Agric. Food Chem*. **2024**, *75* (5), 2718-2726. DOI: 10.1021/acs.jafc.3c07927

Chapter 7. General Conclusions

The Maillard reaction is a complex chemical reaction network between sugars and amino acids, pivotal in food processing, contributing to flavour and aroma development. Despite significant attention devoted to exploring initial Maillard reaction intermediates, such as Amadori and Heyns products, there remains a notable gap in our understanding of their subsequent reactions with free amino acids or sugars. This study aimed to address this gap by exploring the formation of novel flavour-active compounds during the thermal processing of food, focusing on the interactions between excess sugars and amino acids relative to initial Maillard reaction adducts, potentially leading to the creation of unique flavour compounds.

Utilizing mechanochemistry to selectively generate Amadori and Heyns compounds through ball milling of amino acids and glucose or fructose, this study investigated ARPs and their subsequent reactions with free amino acids and sugars. The findings revealed that milling ARPs with excess amino acids or reducing sugars accelerated the formation of di-aminated sugars or diglycated amino acids. Additionally, the conversion between ARPs and HRPs in the presence of free amino acids was explored, contributing to a comprehensive understanding of this pivotal aspect of food chemistry. High-resolution mass spectrometry was employed to detect their structures, while subsequent use of ESI-qTOF-MS/MS revealed diagnostic MS/MS fragmentation patterns consistent with the proposed structures. Additionally, comprehensive MS/MS fragmentation analysis elucidated the structural characteristics of di-aminated sugar and diglycated amino acid derivatives and provided insight into their formation mechanisms.

By exploring the dynamics of thermal deglycation in the context of the Maillard reaction, particularly in the presence of free amino acids, this study demonstrated a novel approach for addressing glycation-induced damage in food systems and physiological processes, providing insights into potential strategies for improving food quality and promoting human health. Moreover, the interconversion of Schiff bases between Amadori and Heyns products in di-aminated sugars with amino acids or proteins presents prospects for non-enzymatic deglycation of amino acids, particularly proteins, while enabling the formation of volatile flavours from Heyns degradation products without the addition of fructose, thereby mitigating potential health consequences associated with its use. Such an approach holds promise in reducing the harmful

effects of glycation and preserving the optimal functionality of proteins. The study positively contributed to the knowledge of the Maillard reaction for analyzing and identifying important non-volatile MR intermediates and Amadori products in complex food matrices, thus contributing to future advancements in food science.